



Master Thesis

**Rheological characterisation of polymer melts on an
injection moulding machine using a new slit die
measurement system**

Submitted by

Ramesh Kumar Selvasankar



Institute of Plastics Processing

Stv. Vorstand: Ass. Prof. Dr. Walter Friesenbichler

University of Leoben

Austria

Leoben, 23.09.2008

Affidavit

I declare in lieu of oath, that I wrote this thesis and performed the associated research myself, using only literature cited in this volume.

Date

Signature

Acknowledgements

Foremost, my grateful acknowledgement is to Em.Univ.Prof.Dr.-Ing.Günter R. Langecker, for having provided me this opportunity to perform this work at the institute and for his detailed and constructive comments.

I am deeply indebted to Ass.Prof.Dipl.-Ing.Dr.mont. Walter Friesenbichler, my advisor, for his active guidance, constant encouragement, valuable discussions and advice.

I express my deep and sincere gratitude to my supervisor Dipl.-Ing. Ivica Duretek, for his help, guidance, encouragement, sound advice, good teaching, good company, and lots of ideas, through out the course of my work.

I would like to express my sincere thanks to Dipl.-Ing. Stephan Schuschnigg, for helping me to solve the critical problems I faced in Visual basic and for his support in writing the program.

I wish to thank Dipl.-Ing. Rajganesh Jegadeesan, for his support and ideas.

I would like to thank Anja Germuth, for helping me to carry out the measurements on the injection moulding machine.

I am grateful to all the staffs and colleagues at the institute of plastics processing, for assisting and helping me in many different ways.

I am indebted to my many student colleagues for providing a stimulating and fun environment. I am especially grateful to Michael Kipperer, Christof Kucher, Simon Stadelmann, Wolfgang Kienzl and many others.

Lastly, and most importantly, I wish to thank my parents, family and friends, for their emotional support and love. To them I dedicate this thesis.

Abstract

Determination of the polymer melts behaviour under the conditions of temperature and shear rate are very important for the accurate flow simulation. The reliability of the simulation results mainly dependent on the rheological characteristics of the polymers. The rheological characterisation is usually carried out in conventional capillary rheometer, where the measurable shear rate range is between $10^2 - 10^5 \text{ s}^{-1}$. But the shear rates experienced by the melt during the injection moulding of parts with very small dimensions (micro sized) may exceed 10^6 s^{-1} , which is out of range of conventional capillary rheometer to characterise. For the rheological characterisation of polymer melts by high shear rates under real life scenario, a new injection moulding machine rheometer with interchangeable slit die inserts have been developed at the Institute of Plastics Processing, as a part of the EU-Collective Research Projects (Pro4Plast) "New product development guidance systems (PGDS) for complex injection moulded plastic parts by enhanced injection moulding simulation and material data measurement applicable by SMEs".

During the injection process the pressure loss and the increase in the melt temperature along the flow length were measured. By varying the volume flow rate, different shear rates have been achieved. With this technique, a Polypropylene material type HG313MO has been characterised at 3 temperatures. The measured wall temperature was found to be 80°C higher than the set temperature due to shear heating and hence there was an increase in the melt temperature, at very high flow rates. This temperature increase has been corrected during the viscosity calculation. For calculating the materials rheological data a calculation program has been written in Excel-VBA. Also the viscosity measurements have been performed in the conventional high pressure capillary rheometer and cone and plate rheometer. The rheological data produced by the injection moulding machine rheometer and commercial high pressure capillary rheometer has been compared.

Key words: rheology, viscosity, injection moulding, slit die, high pressure capillary rheometer, shear heating

Kurzfassung

Die Bestimmung des Fließverhaltens von Polymerschmelzen bei verschiedenen Temperaturen und Schergeschwindigkeiten ist für die genaue Strömungssimulation sehr wichtig. Die Zuverlässigkeit der Simulation für die praktische Anwendung hängt wesentlich von den rheologischen Eigenschaften des Polymers ab. Die rheologische Charakterisierung erfolgt üblicherweise durch Messungen mit dem Standard-Kapillarrheometer, bei welchem der Schergeschwindigkeitsbereich zwischen 10^2 s^{-1} bis 10^5 s^{-1} liegt. Bei der Produktion von Bauteilen mit sehr kleinen Abmessungen (Mikro-Teile) können Schergeschwindigkeiten von ca. 10^6 s^{-1} erreicht werden. Für die rheologische Charakterisierung der Polymere unter praxisrelevanten Schergeschwindigkeiten und Bedingungen wurde am Institut für Kunststoffverarbeitung im Rahmen des EU- Collective Research Projectes (Pro4Plast) „New product development guidance system (PDGS) for complex injection moulded plastic parts by enhanced injection moulding simulation and material data measurement applicable by SMEs“ ein Spritzgießrheometer mit austauschbaren Schlitzdüsen gebaut.

Während des Einspritzvorgangs werden der Druckverlust und die Temperaturerhöhung der Schmelze entlang der Düse gemessen. Durch die Variation des Volumendurchsatzes werden verschiedene Schergeschwindigkeiten erreicht. Mit dieser Methode wurde das Polypropylen der Type HG313MO bei 3 Temperaturen charakterisiert. Bei hohen Schergeschwindigkeiten wurde infolge der Dissipationserwärmung eine Wandtemperaturerhöhung von bis zu 80°C gemessen, was auch eine Erhöhung der Schmelztemperatur zur Folge hat. Diese wurde bei der Berechnung der Viskosität durch eine Temperaturkorrektur berücksichtigt. Für die rheologische Auswertung wurde ein Excel-VBA Programm geschrieben. Die Viskositätsmessungen wurden auch am Hochdruckkapillarrheometer und am Rotationsschwindungrheometer durchgeführt. Die mit den verschiedenen Messmethoden ermittelten Viskositätsdaten wurden miteinander verglichen.

Schlagwörter: Rheologie, Viskosität, Spritzgießen, Schlitzdüse, Hochdruckkapillarrheometer, Dissipationserwärmung

Contents

1	INTRODUCTION AND OBJECTIVES	1
2	THEORETICAL BACKGROUND.....	3
3	RHEOLOGICAL MEASUREMENT ON INJECTION MOULDING MACHINE (IMM).....	5
3.1	RHEOLOGICAL INJECTION MOULD	5
3.2	WORKING METHODOLOGY	8
3.3	VISCOSITY CALCULATION	10
4	VISCOSITY MODELS	14
4.1	POWER LAW OR OSTWALD-DE WAELE MODEL.....	15
4.2	CROSS MODEL.....	16
4.3	CARREAU MODEL	17
4.4	MODIFIED CARREAU MODEL.....	18
5	TEMPERATURE DEPENDENCE OF VISCOSITY.....	19
6	VISCOUS DISSIPATION.....	22
6.1	HEAT GENERATION CALCULATION BY AGASSANT METHOD.....	24
7	NUMERICAL OPTIMISATION ALGORITHM	31
7.1	NELDER MEAD SIMPLEX METHOD	31
7.2	PROCEDURE FOR OPTIMISING A FUNCTION	32
7.2.1	Initial Triangle.....	32
7.2.2	Midpoint of the good side.....	32
7.2.3	Reflection.....	32
7.2.4	Expansion.....	33
7.2.5	Contraction.....	34
7.2.6	Shrinking	35
7.2.7	Logical Decisions.....	35
7.2.8	Termination.....	35
8	RHEOLOGICAL DATA CALCULATION PROGRAM – RHEOSOFT.....	37
8.1	MEASURED DATA	38
8.2	BASIC DATA FOR VISCOSITY CALCULATION	40
8.2.1	Equilibrium pressure calculation.....	40
8.2.2	Wall temperature and melt temperature determination	44
8.2.3	Volumetric flow rate.....	45
8.2.4	Temperature Corrected Viscosity.....	47
8.2.5	Viscosity approximation.....	51

Contents

9	EXPERIMENTAL	56
9.1	MATERIAL.....	56
9.2	EQUIPMENT.....	56
9.3	MATERIAL DATA MEASUREMENT	57
9.3.1	High Pressure Capillary Rheometer	57
9.3.2	Cone and Plate Rheometer.....	60
9.3.3	Pressure-Volume-Temperature (pvT) Diagram.....	61
9.3.4	Specific Heat Capacity.....	62
9.3.5	Thermal Conductivity	62
9.4	INJECTION MOULDING MACHINE RHEOMETER (IMMR).....	63
10	RESULTS AND DISCUSSIONS	67
10.1	PRESSURE – SPECIFIC VOLUME – TEMPERATURE.....	67
10.2	THERMAL CONDUCTIVITY.....	68
10.3	SPECIFIC HEAT CAPACITY	69
10.4	VISCOSITY	70
10.4.1	Conventional Rheometer Data	70
10.4.2	Injection Moulding Machine Rheometer (IMMR).....	74
10.5	COMPARISON BETWEEN COMMERCIAL RHEOMETER AND IMMR.....	77
11	CONCLUSION	81
12	LITERATURE	83
13	NOMENCLATURE	85
14	APPENDIX	87

1 Introduction and Objectives

Injection moulding is a material processing field in which lot of new developments are arising. The importance for injection moulding of micro-sized parts with dimensions in the micrometer range is growing very fast. As micro-moulding attracts more and more attention, using computer simulation tool to solve difficult moulding issues becomes an inevitable part. The simulation of injection moulding process provides support in deciding the part, mould and the process design. The reliability of filling simulation results depends mainly on the following factors: input material data, process parameters and numerical model. In particular, among the process parameters the rheological data of the polymers have the most influence on simulation of the filling phase.

These rheological data used in the current flow simulation packages are mostly obtained from capillary rheometer at shear rate range between 10 and 10,000 s^{-1} . But during filling micro-sized parts, shear rates can exceed 100,000 s^{-1} and in some injection moulding cases the shear rates raise up to 10^7 s^{-1} , and this is well outside the range of the commercial rheometers. Consequently, very little is known on the rheology of polymer melts in the higher shear rate range and this range is of great importance in injection moulding [1-5,9].

The material data obtained from the capillary rheometer are extrapolated to high shear rates with conventional simulation software, which may induce inaccuracy in flow predictions. So the macroscopically measured viscosities may not be suitable for modelling melt flowing through micro scale dimensions. Another aspect in conventional simulation software is that capillary rheometer take the viscosity measurements under isothermal conditions (constant temperature), but very high shear rates generate rise in temperature of the melt which cannot be neglected [4,9].

The main objective of this work is to determine the polymer melt viscosity at high shear rates under processing conditions. As a part of the EU-Collective Research Projects "New product development guidance system (PDGS) for complex injection moulded plastic parts by enhanced injection moulding simulation and material data measurement applicable by SME, Acronym Pro4Plast, Contact No.: COLL-CT-2006-030205, a new rheological measurement technique called injection moulding machine rheometer (IMMR) has been developed at the Institute of Plastics Processing in Leoben. This system consists of an injection moulding machine with a special rheological injection mould, with a slit die insert. By measuring the pressure drop, volumetric flow rate and wall temperature, the material's viscosity data can be obtained.

1. Introduction and Objectives

In this work, this new measurement method has been used to measure the rheological properties of a polypropylene at high shear rates and the results have been compared with conventional rheometer data. As a part of this work, for deriving the material's flow constants, a special program has been developed using Microsoft Excel 2002 and Visual Basic 6.0.

2 Theoretical Background

A thorough understanding of the rheological properties of polymers in the conditions which exist during the processing stage is very important both to control the quality of the final moulded part and the auto regulation of the machine, in order to ensure an optimal production. But the rheological characterisation of the polymer melts is complicated because there are many factors that influence their flow properties. Examples of the main factors that affect the flow behaviour (Figure 1) may include: processing temperature, rate of flow or shearing, pressure etc

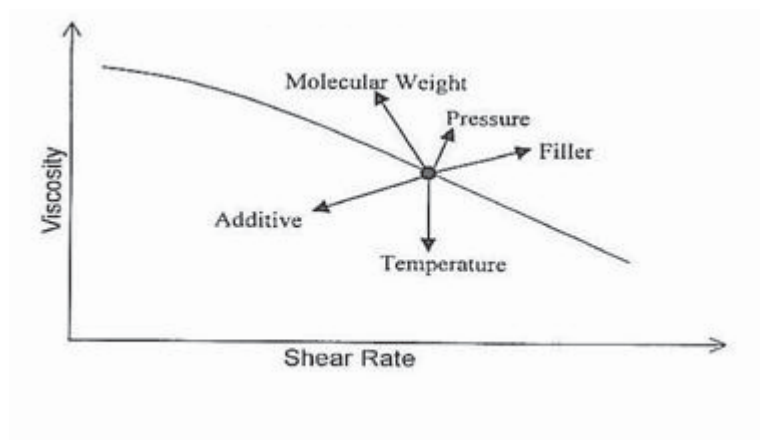


Figure 1: Factors influencing the viscosity of polymer melts [6]

The mathematical model describing quantitatively the relationship between shear stress and shear rate during flow of the polymeric fluids is called the constitutive equation. For a general flow of polymer fluids, the following rheological equation is extensively accepted:

$$\tau = \eta(\dot{\gamma}, T, p) \cdot \dot{\gamma} \quad (1)$$

Where

τ - Shear stress

η - Viscosity

$\dot{\gamma}$ - Shear rate

T - Temperature

p - Pressure

2. Theoretical Background

An outstanding characteristic of the polymer melt is their non-Newtonian behaviour whereby the viscosity decreases as the shear rate increases. This non-Newtonian behaviour is of tremendous practical importance in the processing and fabrication of plastics. The decreased viscosity makes the polymer easier to process and to inject the melt through small channels during the filling process. At the same time, the energy required by the injection moulding machine is reduced by the same phenomenon. For injection moulding processes, the shear rate is usually in the range of 10^3 s^{-1} to 10^6 s^{-1} . In the high shear rate range the viscosity is usually extrapolated from the measured viscosity data at lower shear rates. However the polymer viscosity at very high shear rate is not linear. A very little is known on the rheology of polymer melts at very high shear rate up to 10^6 s^{-1} or more [1-3,5].

The measurement of viscosity using an injection moulding machine offers a much higher pressure to achieve extreme high shear rates, but unavoidably, the performance of shearing itself would generate the heat within the melt and thus it might increase the temperature of the melt sufficient enough to reduce the viscosity. The recorded rise in the temperature of the plastic melts at higher shear rate range is about $50\text{-}70^\circ\text{C}$ [1,3,4], which is large enough to cause a significant reduction in the viscosity. Therefore it is important to consider these temperature increases in the flow for the viscosity calculation and they cannot be neglected.

3 Rheological Measurement on Injection Moulding Machine (IMM)

Rheological data measured using an injection moulding machine rheometer generates a more realistic melting mechanism, and therefore it should lead to more realistic process simulation results for temperature sensitive polymers. Obtaining shear viscosity data at the pressures, temperatures, and shear rates associated with the injection moulding process is most commonly accomplished using conventional capillary rheometer. These conventional laboratory instruments offer outstanding precision, but their 'melting mechanism' is purely conductive heat transfer. This is unlike injection moulding, where both conductive heat transfer and viscous heating during plasticizing and injection can play an important role (i.e. shear history). Injection moulding based rheometers also offers a wealth of other advantages. They are especially useful when working with materials where shearing is critical. They offer advantages in terms of test time, and these rheometers can be easily automated.

The measurement principle of this rheometer is very similar to the conventional high pressure capillary rheometer. Instead of cylinder here the injection unit of the injection moulding machine is used to plasticize and melt the polymer. Instead of piston, the screw injects the melt into the die system at a specified injection speed or specified volumetric flow rate. The pressure loss and the melt temperature along the flow channel are recorded by the pressure transducers and thermocouples respectively. Using these measured parameters the viscosity is calculated.

3.1 Rheological Injection Mould

In order to measure precisely the flow behaviour at higher shear rate range, a special injection mould with interchangeable conical slit die inserts with varying slit heights has been developed at the Institute of Plastics Processing, University of Leoben, Austria. The schematic 2D and 3D representation of the mould is shown in *Figure 2a* and *Figure 2b* respectively. The rheological injection mould is very similar to a normal injection mould, but without sprue, runner system, cooling circuit and can be easily mounted on the injection moulding machine.

3. Rheological Measurement on Injection Moulding Machine (IMM)

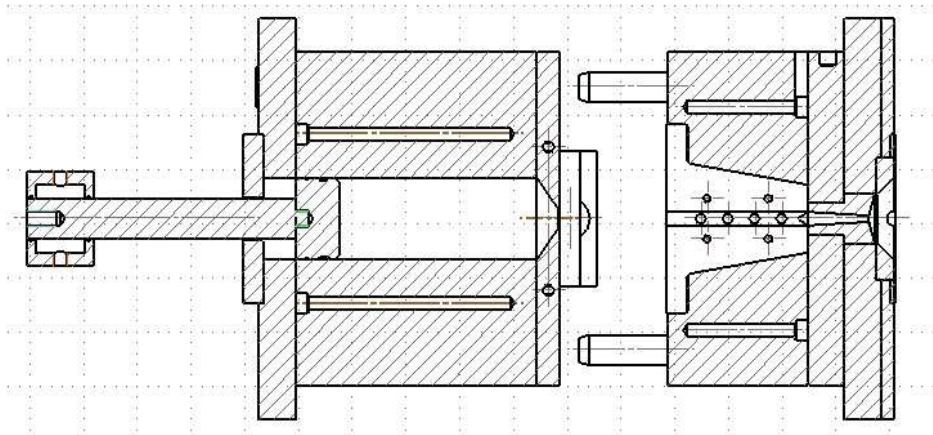


Figure 2a: 2D view of rheological injection mould with slit die

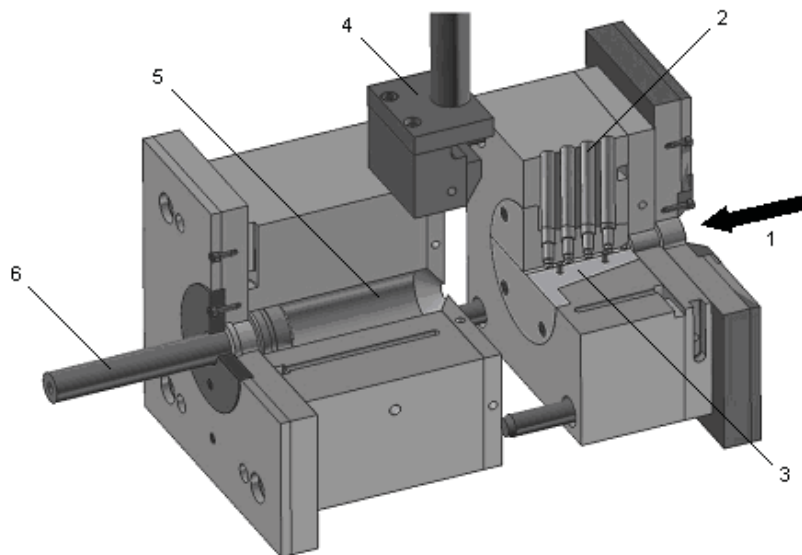


Figure 2b: 3D view of rheological injection mould with slit die; 1- injection side, 2- bores for pressure & temperature sensors, 3- interchangeable slit die insert, 4- stripper blade, 5- volumetric flow rate measurement cylinder, 6- piston with stroke sensor

The mould consists of two halves. One half, which has the provision for attaching the slit die insert (Figure 3) is mounted on the injection unit side. In order to achieve a wide range of shear rates three dies with different slit heights (1 mm, 0.5 mm and 0.35 mm) are used. These slit dies are separable into two parts at its axial symmetry and have an entrance angle of 60°. The total length of the flow channel is 105.5 mm and the width is 10 mm.

3. Rheological Measurement on Injection Moulding Machine (IMM)

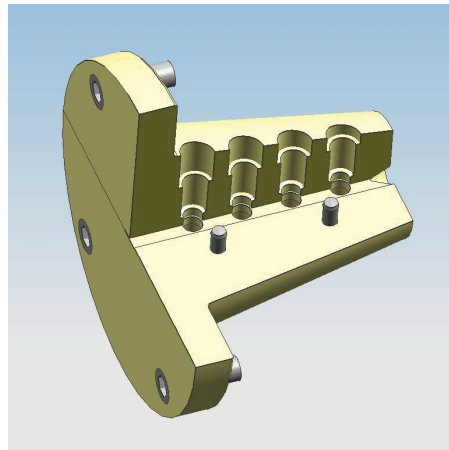


Figure 3: Sectional 3D representation of conical slit die insert

The major reason for using such a high L/H ratio die is to achieve a fully developed flow, and second to avoid the entrance effects as measured positions on the die wall are far away from the entrance. The flow path consists of four bores 20 mm apart from each other, with diameters 14 mm on the top and bottom side, to accommodate pressure transducers and temperature sensors. The holes are deep enough for the sensors to have a direct contact with the flowing melt. The pressure sensors are flush type sensors, which has direct contact with the melt. Two types of temperature sensors can be used. The first one is the infrared sensors, which can measure directly the melt temperature. The other one is a special kind of sensors with three thermocouples (Figure 4) positioned in such a way that each thermocouple measures the temperature 1, 1.5 and 3 mm away from the flow channel wall. These three temperatures are extrapolated and the wall temperature is calculated. The wall temperature (WT) is measured both near the entrance and near the exit, in order to find the wall temperature increases along flow length due to shear heating.

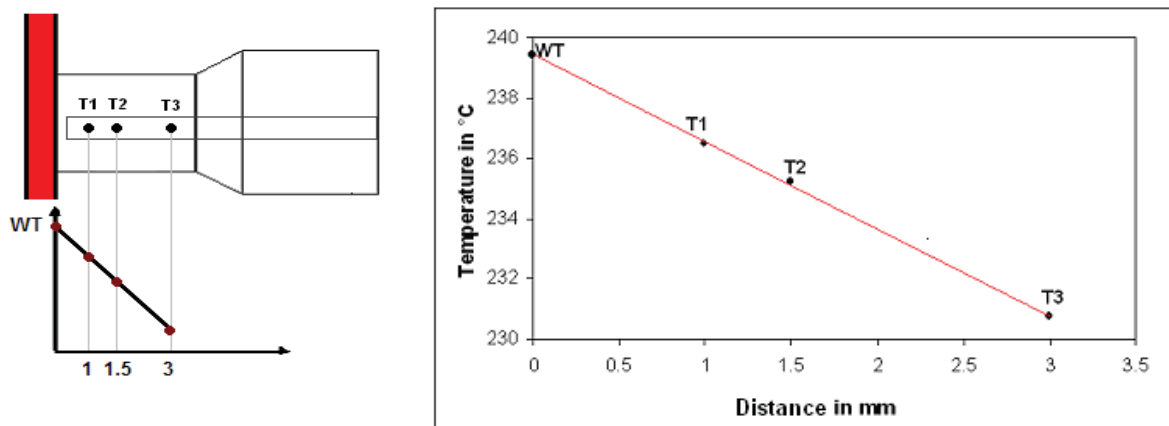


Figure 4: Wall temperature measurement

3. Rheological Measurement on Injection Moulding Machine (IMM)

The other half of the mould, mounted on the ejection side, consists of a cylinder and a piston system to measure the volumetric flow rate. This system is used in order to eliminate the leakage flow problems at the back flow valve of the plastification unit. For calculating the volume flow rate, the displacement rate of the piston is needed and this is measured using a stroke sensor. The forward and backward motion of the piston is attained by the movement of the ejection system. The cylinder has a maximum storage capacity of 424.115 cm³. A pneumatically operated stripper blade is attached on the top to wipe the melt flowing out of the cylinder during ejection of the melt from the cylinder.

The heating of the mould is done using four cartridge heaters as well as four heater plates covering the movable mould half, which are regulated directly by the injection moulding machine.

3.2 Working Methodology

The main parameters to be measured for calculating the viscosity are pressure loss along the flow length, temperature of the polymer melt and volumetric flow rate. To acquire these physical parameters, the rheological injection mould with the die inset is heated to the required measurement temperature. Before starting the measurement the mould must be at stable temperature. The barrel zones of the injection unit have to be brought to the required temperatures.

According to the required volumetric flow rate the plastic material has to be plasticized. Before injecting the melt into the die, the piston in the flow rate measurement cylinder is positioned in such a way, that the available free volume inside the cylinder is approximately zero. Both the mould halves have to be closed and the measurement can be started. The melt is injected into the die at the specified injection velocity. The pressure transducers and the temperature sensors, placed on the flow path, record the change in pressure and the wall temperature. These signals are recorded by a data acquisition system. There is no packing phase since there is no closed end in the flow channel, and the melt is injected at a constant velocity. The melt exit the flow channel and enters into the cylinder making the piston to move in the backward direction. The displacement of the piston is recorded by a stroke sensor which is connected to the data acquisition system. Once the hub volume is empty, the measurement can be stopped and all the measured values are saved. The mould halves can be then opened and the melt accumulated in the cylinder is pushed out by the forward motion of the piston. The melt flowing out is wiped out by the stripper blade. Simultaneously the plastification of the melt for the next

3. Rheological Measurement on Injection Moulding Machine (IMM)

measurement can be done. The process is repeated for different flow rates or injection speeds for different melt temperatures.

These measured data cannot be used as such for calculation, since the physical parameters measured are over a time period and has hundreds of measured values; only the equilibrium pressure is required for calculation. The first step in calculating the viscosity is to find the equilibrium pressure range and accordingly the wall temperature in the equilibrium range. The pressure and temperature (average of wall temperature near entrance and exit of the die) profiles for Polypropylene HG313MO at 210°C over time measured at flow rate 10 cm³/s are shown in Figure 5.

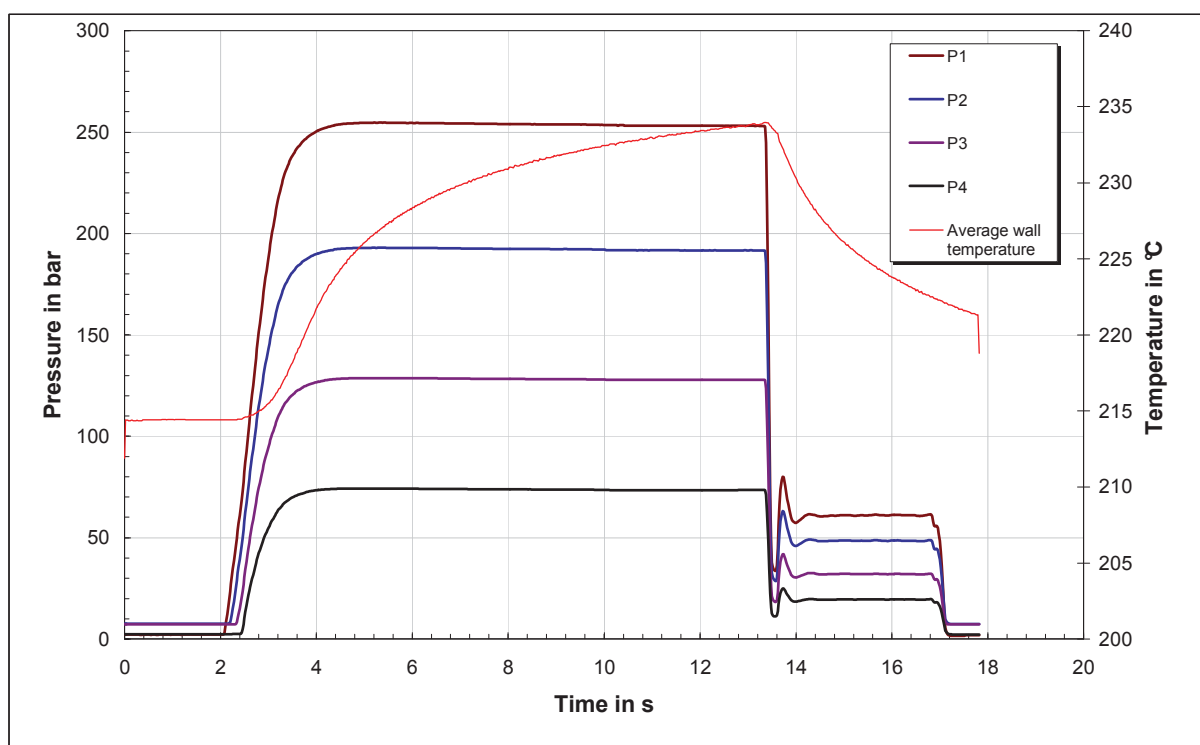


Figure 5: Pressure and temperature vs. injection time profile

The pressures are very low (zero) until the melt reaches the sensors positions. Once it attains the position, the pressures (P1, P2, P3 and P4) start increasing gradually (depends on the injection speed) and after a certain period the pressure is constant. For the calculation, the equilibrium pressure is important and the time period (t_1 and t_2), where the equilibrium pressure lies, has to be manipulated and the average of the pressures in this time zone has to be used for further calculations. The other important factor is the pressure gradients along the flow length. The pressures measured at different positions along the die length must be linear; it means that the pressures are reasonably constant in the flow channel with a fixed cross-section.

3. Rheological Measurement on Injection Moulding Machine (IMM)

The steel temperature measured increases once the injection phase starts and in the equilibrium pressure range, the averages of the temperatures (T1, T2 and T3) are calculated. These average temperature values are then extrapolated towards the wall and the temperature at the flow channel wall is determined. This wall temperature measured near the entrance and the exit are then used for calculating the average melt temperature in the die. The injection speed can be determined from the piston position profile over time. The slope of the piston velocity curve is constant during the injection phase since the flow rate does not vary in the course of the injection stroke. This slope gives the injection speed which is used for calculating the accurate flow rate through the slit die. From these values the viscosity can be determined.

3.3 Viscosity Calculation

From the amount of melt exiting the slit die per unit time and the required pressure across the flow length one can calculate the melt viscosity at a particular shear rate.

The first step is to calculate the shear rate and shear stress. The apparent shear rate can be calculated by using equation (2).

$$\dot{\gamma}_{app} = \frac{6 \cdot Q}{B \cdot H^2} \quad (2)$$

Where:

Q - Volumetric flow rate

B - Breadth of the slit

H - Height of the slit

$\dot{\gamma}_{app}$ - Apparent shear rate

The volumetric flow rate is calculated (equation 3) from the rate of displacement of the piston in the cylinder, which is obtained from the stroke length vs. time curve and the cross sectional area of the cylinder.

$$Q = \tilde{v} \cdot A \quad (3)$$

Where:

\tilde{v} - Piston velocity

A - Area of cross section of the piston/cylinder

The corrected apparent shear rate can be calculated using the shape factor “ F_p ” for pressure flows. This shape factor assumes values smaller than 1 and represents the

3. Rheological Measurement on Injection Moulding Machine (IMM)

reducing effect of the flights on the flow rate between the walls of the flow channel due to wall adhesion. This can be calculated from the following relation [7]:

$$F_p = \frac{12 \cdot \eta}{B \cdot H^2} \cdot \frac{L}{\Delta P} \cdot \int_0^B \int_0^H v_x(y,z) dy \cdot dz \quad (4)$$

The shape factor depends only on the H/B ratio. When the value of H/B becomes very small, the factor approaches unity [8].

The corrected wall shear rate can be written as:

$$\dot{\gamma}_{app,cor} = \frac{6 \cdot Q}{B \cdot H^2} \cdot \frac{1}{F_p} \quad (5)$$

The wall shear stress can be determined using the equation (6).

$$\tau_w = \frac{\Delta P \cdot H}{2 \cdot \Delta L} \quad (6)$$

Where:

ΔL - Length of the slit

ΔP - Pressure drop along the slit length ΔL

τ_w - Wall shear stress in Pa

The above equation is applicable when the ratio of width to thickness of the flow channel is greater than 10. If the ratio is less than 10, then the wall shear stress (equation 6) becomes

$$\tau_w = \frac{F_{shear}}{A} = \frac{\Delta P}{2 \cdot \Delta L} \left(\frac{B \cdot H}{(B + H)} \right) \quad (7)$$

Where

F_{shear} - Shear force

A - Cross sectional area of the slit

The pressure drop can be determined by taking the difference of two pressures measured along the flow length and the corresponding length is considered for the shear stress calculation (Figure 6).

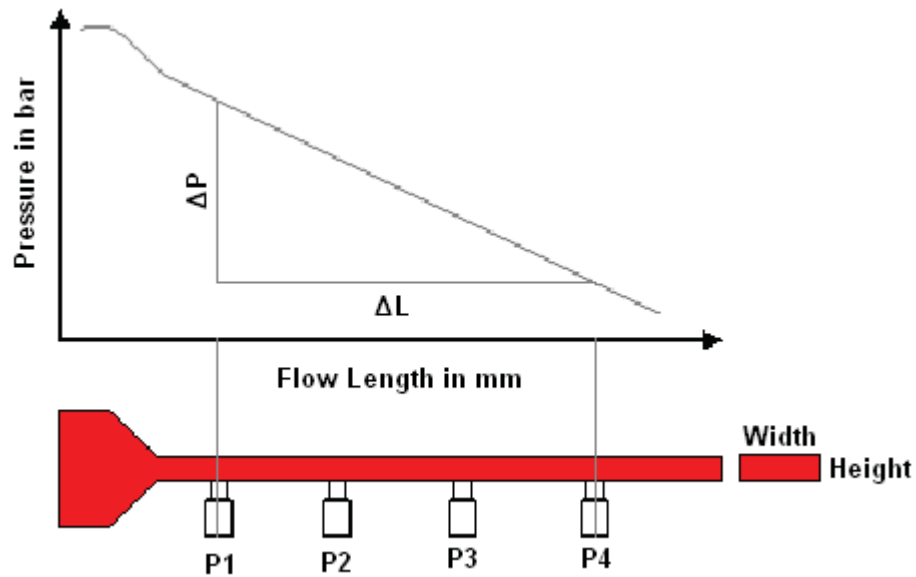


Figure 6: Pressure distribution along the flow length of the slit die

The true shear rate is obtained from the apparent shear rate by applying the correction for the non-Newtonian behaviour of the melt according to Weissenberg-Rabinowitsch. This correction is based on the assumption that polymer flow does not slide along the wall. In real, polymer melts exhibit a non-parabolic velocity profile, due to the shear thinning behaviour of polymer melts due to molecular disentanglement. This correction takes into account the non-parabolic velocity profile of the non-Newtonian fluids. The Weissenberg Rabinowitsch equation corrects the rate of shear at the wall for non-Newtonian fluids, which is given in equation (8).

$$\dot{\gamma}_w = \frac{\dot{\gamma}_{app}}{3}(2+m) \quad (8)$$

Where:

$\dot{\gamma}_w$ - True shear rate

m - Slope of the flow curve

The exponent m can be expressed by equation (9).

$$m = \frac{d \lg \dot{\gamma}_{app}}{d \lg \tau_w} \quad (9)$$

The exponent is determined by plotting a double log plot of the apparent shear rate in the Y-axis and the wall shear stress in the X-axis (Figure 7) and the points are approximated by polynomial second order or third order equation. The first derivative of this equation gives the value of m.

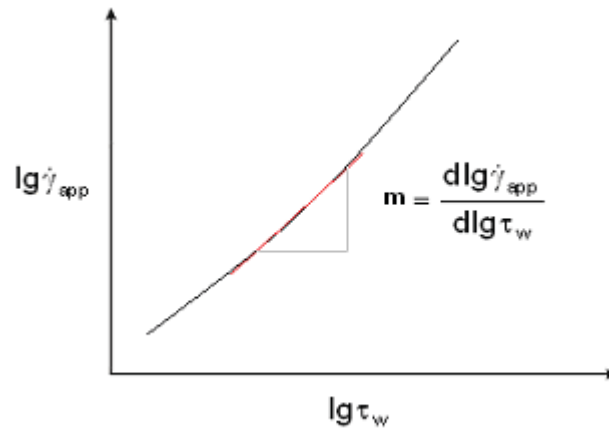


Figure 7: Weissenberg-Rabinowitsch correction

After correction, the true viscosity of the polymer melt can be obtained by dividing the wall shear stress by true shear rate (equation 10).

$$\eta_w = \frac{\tau_w}{\dot{\gamma}_w} \quad (10)$$

Where:

η_w - True viscosity

The above calculated viscosity is without temperature correction and the actual melt temperature is not considered. But in general, at very high shear the wall temperature raises up to 90°C and considerably the melt temperature also increases due shear heating, which can highly influence the viscosity of the melt. So this rise in temperature should be corrected iteratively and the temperature corrected viscosity can be obtained. For this purpose the Cameron number is used. By Agassant method [9,13] the average melt temperature inside the flow channel is calculated and with this melt temperature the temperature corrections can be done. The infrared temperature sensors can be implemented in the rheological injection mould to check the calculated average melt temperature experimentally.

4 Viscosity Models

The mathematical model describing quantitatively the relation between shear stress and the shear strain during flow of the polymeric fluids is called the constitutive equation. Because of the molecular chain structure and viscoelasticity of the polymeric materials are quite complicated, although various forms of constitutive equations have been proposed. For a general flow of polymeric fluids, the following rheological equation is extensively accepted:

$$\tau = \eta(T, \dot{\gamma}, P) \cdot \dot{\gamma} \quad (11)$$

Where:

τ - Shear stress

η - Shear viscosity

$\dot{\gamma}$ - Shear rate

T - Temperature

P - Pressure

For a given polymer, viscosity is mainly a function of temperature, shear rate and pressure. If the flow is steady shear flow, then the stress and strain are called as shear stress and shear rate, respectively.

It can be seen from the equation (11) that constitutive equations corresponds to various fluids and flow conditions can be derived if different viscosity expressions are substituted into equation (11). On the other hand the viscosity of polymer fluids is a measure of the flow property. Consequently, setting up a viscosity model for description of the relation between fluid viscosity and relevant parameters, including molecular structure parameters and processing parameters, to predict the flow properties of the resin under various conditions, is one of the targets that rheologists and polymer processing engineers have been working for.

A number of viscosity models have been published, such as the well known Ostwald-de Waele model, Cross model and Carreau model, and so on. These viscosity models are used to represent the flow properties of polymer melts in simulation of injection molding. Though numbers of well known models are available, it is important to choose a model, which is both accurate over the whole processing range and for which data can be readily obtained [11].

It should be noted that some materials, in particular liquid crystal polymers and some engineering blends, do display different characteristics. The aim of the viscosity

4. Viscosity Models

model is to match the observed behaviour of the material as closely as possible. Mathematical interpretation of the viscosity models are described in the following sections.

4.1 Power Law or Ostwald-de Waele Model

It is well known that most of the polymers are shear thinning or pseudo plastic and their apparent viscosity is usually a decreasing function of the shear rate. The power law model proposed by Ostwald and de Waele is a simple model that accurately represents the shear thinning region in the viscosity versus the strain rate curve but neglects the Newtonian plateau present at very low shear rates. The power law model can be written as follows:

$$\eta(\dot{\gamma}) = k \cdot \dot{\gamma}^{n-1} \quad (12)$$

Where

k - Consistency index

n - Power Law index

The consistency index may include the temperature dependence of the viscosity and the power law index represents the shear thinning behaviour of the polymer melt. It should be noted that the limits of this model are

$\eta \rightarrow 0$ As $\dot{\gamma} \rightarrow \infty$ and

$\eta \rightarrow \infty$ As $\dot{\gamma} \rightarrow 0$

This is a major draw back of the power-law model as it predicts an infinite value for the viscosity as the shear rate tends to zero. Most molten polymers, on the contrary, show a finite and constant (Newtonian) viscosity at very low shear rates [13]. The two extremes of power law index behaviour are:

- Newtonian behaviour if $n = 1$
- Plastic behaviour if $n = 0$

4. Viscosity Models

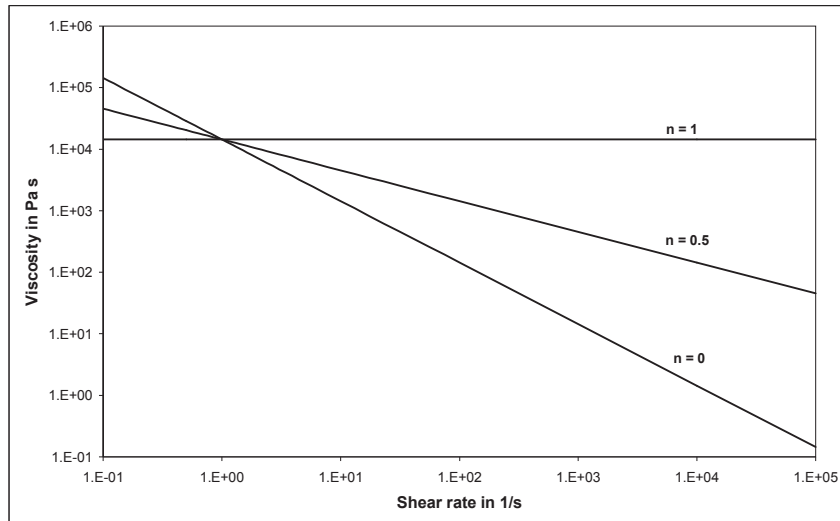


Figure 8: Viscosity described by power law

The relation between viscosity and shear rate is usually represented on log-log scale (Figure 8); the power law behaviour is then given by a straight line of slope $n-1$.

4.2 Cross Model

The rheological model based on Cross model is one of the most commonly used models for the viscosity approximation. Most of the rheometer packages and simulation software use this model. It can be used to extract some meaningful numbers from the full viscosity versus shear rate profile as shown in Figure 9.

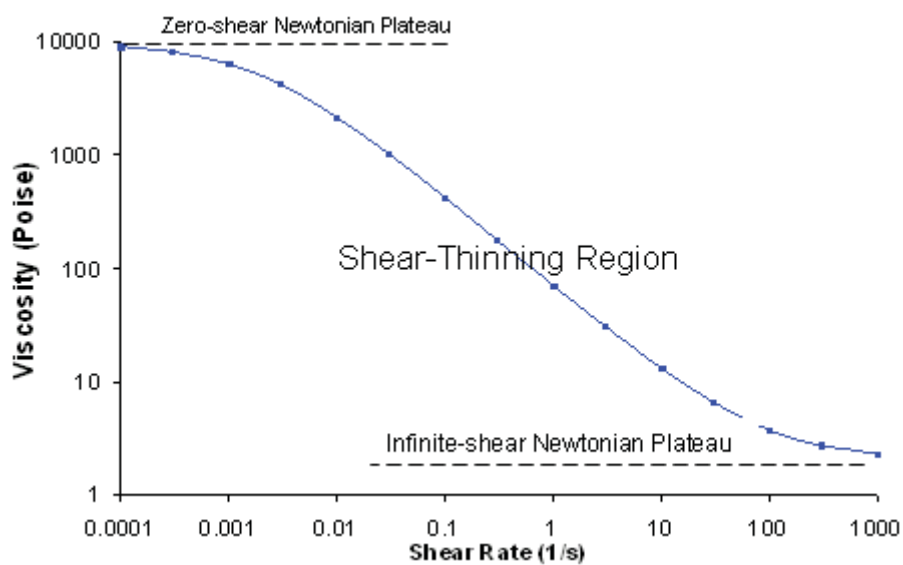


Figure 9: Complete viscosity profile of polymer melts [14]

4. Viscosity Models

The Cross model has the form:

$$\eta(\dot{\gamma}) = \frac{A}{1 + (B\dot{\gamma})^C} \quad (13)$$

Where

A - Zero shear viscosity

B - Cross time constant (or consistency)

C - Slope of power law region

The zero shear viscosity is the magnitude of the viscosity at the lower Newtonian plateau. The reciprocal of B gives us the critical shear rate that proves a useful indicator of the onset shear rate of shear thinning. The constant C is dimensionless and is a measure of the dependence of the viscosity on shear rate in the shear thinning region. A value of zero indicates Newtonian behaviour and with C tending to unity for increasing shear thinning behaviour.

4.3 Carreau Model

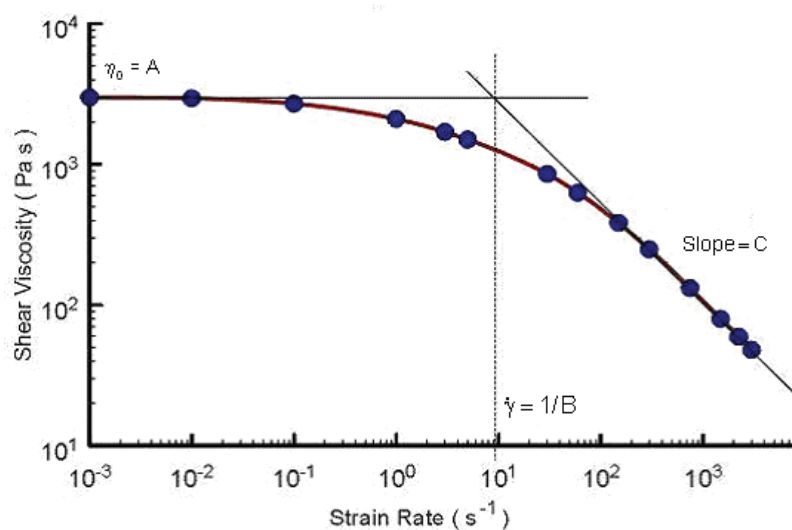


Figure 10: Carreau model [15]

The Carreau model is more realistic than power law model because it fits the data very well at both high and low shear rates. Due to the mathematical complexities it is not possible to obtain analytical solutions with Carreau model, but it is excellent for numerical simulation of flow processes.

4. Viscosity Models

The Carreau model has the form:

$$\eta(\dot{\gamma}) = \frac{A}{(1 + B\dot{\gamma})^C} \quad (14)$$

Where

A - Viscosity at zero shear rate

B - Time constant calculated from the reciprocal of the strain rate at which the zero shear rate component and the power law component of the flow curve intersect.

C - Slope of the power law component

4.4 Modified Carreau Model

The modified Carreau model is given by the following relation [26]:

$$\eta(\dot{\gamma}) = D + \frac{A}{(1 + B \cdot \dot{\gamma})^C} \quad (15)$$

Where:

A - Zero shear viscosity

B - Relaxation time

C - Transition range

D - Infinite shear viscosity

A slight variation of the Carreau model is the Modified Carreau model. With this model it is possible to estimate the viscosity of polymers by infinite high shear rates (second Newtonian plateau).

5 Temperature Dependence of Viscosity

The effect of temperature on the material properties, especially on viscosity is large, and can often mask non-Newtonian effects in flow. The viscosity of most polymers change greatly with temperature (Figure 11). Viscosity is known to have an exponential dependence on temperature, which can be expressed by the Arrhenius expression equation (24). This type of equation is usually suitable for describing the variation of viscosity with temperature, for polymer fluids at temperature far above the glass transition temperature T_g or the melting point.

$$\eta = \eta_0 \exp \frac{E}{R} \left(\frac{1}{T} - \frac{1}{T_0} \right) \quad (16)$$

Where

η_0 - Zero-shear viscosity

E - Activation energy

R - Universal gas constant (8.314×10^{-3} kJ/mol.K)

T - Melt temperature in Kelvin

T_0 - Reference temperature in Kelvin

The activation energy for flow increases as the size of side groups increases and as the chain becomes more rigid. The value of the activation energy depends strongly on whether the viscosities at various temperatures are evaluated at constant shear rates or at constant shear stress. If E is evaluated at a constant shear stress, it is found that E is essentially a constant independent of what value is chosen for shear stress. However, if E is evaluated at a constant shear rate, the activation energy generally decreases with increasing shear rate.

5. Temperature Dependence of Viscosity

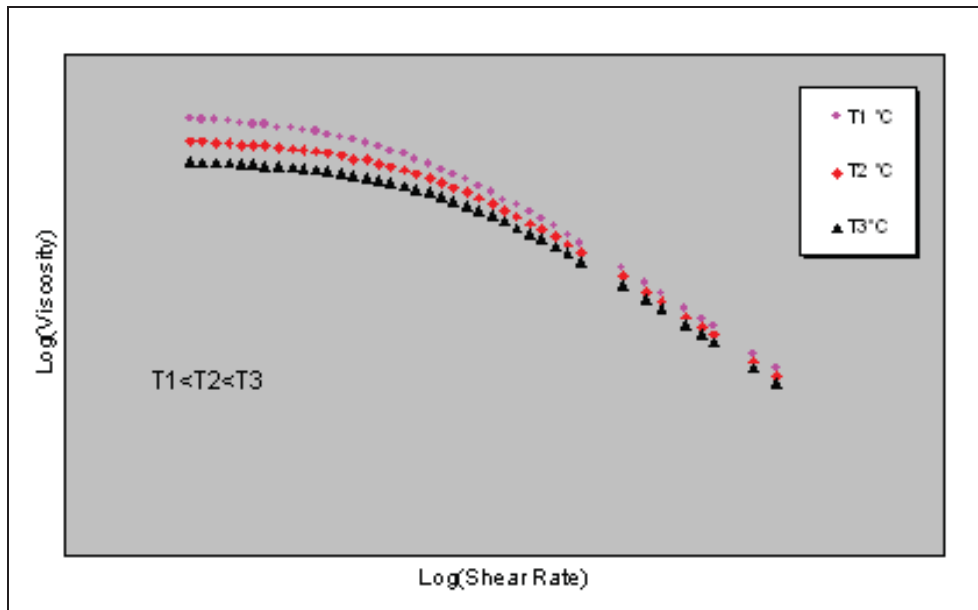


Figure 11: Temperature dependence of polymer melt viscosity

For amorphous thermoplastic materials, however, the glass transition regions are close to their fluid states. Free volume effects predominate and the dependence of viscosity on temperature is better described by the familiar WLF (Williams-Landel-Ferry) (equation 17), where c_1 and c_2 are the material constants.

$$\log(\eta) = \log(\eta_0) - \frac{c_1(T - T_0)}{c_2 + (T - T_0)} \quad (17)$$

Where

T -Melt temperature

T_0 - Reference melt temperature

c_1 -Constant

c_2 -Constant

As stated before the rheological properties of the polymer melt are highly dependent on temperature and shear. In order to obtain the clear picture of this behaviour, experiments must be carried out over a range of temperatures and shear rates. These data can be brought onto a single master curve by means of the “Time-Temperature- superposition” principle, which greatly simplifies the description of the effect of temperature.

There is a need to compare the behaviour of one polymer with other polymers. Several schemes have been developed for doing this by superposition principle in which one curve is shifted relative to another curve. The superimposed curves form a single curve, which is called the master curve. The display of data on a single curve of material behaviour that covers a much border range of shear rate (or frequency) than can be measured at a single temperature.

5. Temperature Dependence of Viscosity

The concept of superposition is that all the relaxation processes of a material have the same dependence on temperature. The temperature is assumed to be affected by the relaxation modulus by changing the relaxation time by a factor a_T . This factor can be empirically determined as a shift factor [12]. For example, in case of shear viscosity function, temperature independent representations can be prepared by plotting $\eta(\dot{\gamma})/a_T$ versus $\dot{\gamma} \cdot a_T$ on a double logarithmic plot. The shift factor can be determined by examining the amount of shifting necessary to bring data measured at different temperatures and shear rates onto one curve. The factors are determined usually by an iterative procedure.

For the practical calculation of the a_T factor of semi-crystalline polymers, equation (18), called “Arrhenius-Equation” can be used.

$$a_T = \exp \frac{E}{R} \left(\frac{1}{T} - \frac{1}{T_0} \right) \quad (18)$$

For amorphous polymers the a_T factor can be calculated using the WLF-equation (19).

$$a_T = - \frac{c_1(T - T_0)}{c_2 + (T - T_0)} \quad (19)$$

Using the shift factor and the viscosity models, the dependence of the viscosity on temperature and shear rate can be expressed.

6 Viscous Dissipation

Temperature variations can be caused by temperatures external to the fluid, for example a hot tube wall or they can be caused by self-heating due to viscous dissipation, since the molten polymers are highly viscous, but have low thermal conductivity. Therefore it is inefficient for the molten polymer to transfer the heat by conduction across the thickness of the flow channel.

The measurement of viscosity using an injection moulding machine offers a much higher pressure to achieve extreme high shear rates, but unavoidably, the performance of shearing itself would generate the heat within the melt and thus it might increase the temperature of the melt sufficient enough to reduce the viscosity. Therefore it is often most important to consider the temperature variations in flow.

In order to describe the heat generation, let us consider the flow of a Newtonian polymer in a flow channel of length L with a constant wall temperature equal to T_0 , the initial temperature of the polymer. The evolution of the temperature profile in the polymer along the flow length is shown in Figure 12.

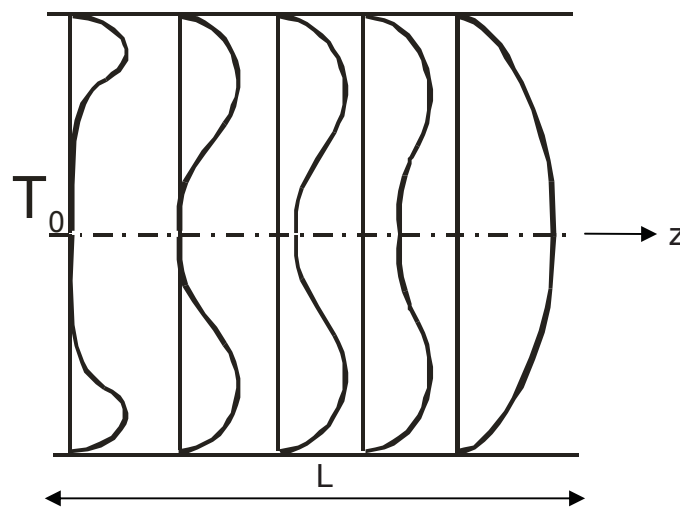


Figure 12: Temperature along flow length [13]

Near the entrance, the maximum temperature is obtained close to the wall, since the shear forces are maximum at the wall. But progressively, due to the heat conduction towards the centre, the temperature profile evolves towards an equilibrium profile with the temperature maximum at the centre. In general three different zones can be described [13]:

- Near the entrance of the tube, the temperature rise is small and the heat transferred by conduction through the channel wall is negligible. The heat dissipated is used to heat the polymer, as if the liquid was thermally isolated from the surroundings. This is the *adiabatic* regime.

6. Viscous Dissipation

- The temperature, short downstream from the entrance, is such that the conduction cannot be any longer neglected. This dissipation power is distributed into internal heat and heat, transferred by conduction to the surroundings. This is known as the *transition* regime.
- Further downstream, the temperature rise attains a limiting value and all the dissipated power is transferred by conduction to the surroundings. In this case the heat transferred by conduction is equal to the dissipated power. So there is no increase in the bulk temperature along the flow length. This is called the *equilibrium* regime.

For defining the thermal regime (adiabatic, equilibrium or transition regime) encountered by the polymer melt flowing through a rectangular flow channel of length L and of thickness H , the Cameron Number (Ca) can be used, which is given by the ratio of the heat conduction along the direction perpendicular to flow to the heat convection along the axial direction of flow. The Cameron number can be calculated using equation (20).

$$Ca = \frac{\lambda \cdot L}{\rho \cdot C_p \cdot \bar{v} \cdot H^2} \quad (20)$$

Where:

λ - Thermal conductivity of the polymer at average melt temperature

L - Axial characteristic dimension of the flow geometry

H - Transverse characteristic dimension of the flow geometry

\bar{v} - Average velocity of the polymer flow inside the flow channel

ρ - Density at average melt temperature

C_p - Heat capacity at average melt temperature

The different thermal regime experienced by the polymer melt inside the flow channel can be described according to the Cameron number, which is given in Table 1.

Table 1: Thermal regime by Cameron number [13]

$Ca < 10^{-2}$	Adiabatic regime
$Ca = 1$	Equilibrium regime
$10^{-2} < Ca < 1$	Transition regime

6.1 Heat Generation Calculation by Agassant Method

The average temperature increase of the polymer melt inside the flow channel can be calculated according to Agassant [13]. The average melt temperature can be determined considering a rectangular slit geometry without change in the flow cross sectional area. In order to derive a mathematical solution the Power law model, which describes the shear thinning behaviour of the polymer melts, is considered. Due to the mathematical complexities, the Cross and Carreau model are not used. Also the melt temperature increases strongly at very high shear rates and these shear rate range can be normally approximated by Power law model.

The derivation is carried out using the die geometry (H, L, B), the temperature invariable material constants – density (ρ), thermal conductivity (λ), specific heat capacity (C_p) at constant pressure and the viscosity data (k and n by Power Law). The variables received are pressure loss (Δp) or average velocity (\bar{v}) [10].

In the earlier study done by Rois [10] and Schuschnigg [9], equations for calculating the rise in the melt temperature inside a slit die has been derived for three different cases; they are - first for the fully developed temperature profile, second for the transition region and third for the adiabatic condition. The following derivations have been extracted from Schuschnigg's [9] work.

The energy equation in a Cartesian coordinate system can be written as:

$$\rho c_p v(y) \frac{\partial T}{\partial z} = - \frac{\partial}{\partial y} q_y + \tau_{xy} \frac{\partial v_x}{\partial y} \quad (21)$$

By using Power Law relation equation (22),

$$\tau = k \cdot \dot{\gamma}^n \quad (22)$$

the viscosity can be given by equation (23).

$$\eta = \frac{\tau}{\dot{\gamma}} = k \cdot \dot{\gamma}^{n-1} \quad (23)$$

The shear rate arises from the pressure loss along the die length.

$$\dot{\gamma} = \left(\frac{\Delta p}{kL} \right)^{\frac{1}{n}} \cdot y^{\frac{1}{n}} = \frac{1+2n}{n} \cdot \bar{v} \cdot \left(\frac{H}{2} \right)^{\frac{1+n}{n}} \cdot y^{\frac{1}{n}} \quad (24)$$

The wall shear rate can be given by the following relation:

$$\dot{\gamma}\left(y = \frac{H}{2}\right) = \dot{\gamma}_w = \left(\frac{\Delta p H}{2kL}\right)^{\frac{1}{n}} \quad (25)$$

The average shear rate over the slit height can be calculated as:

$$\bar{\dot{\gamma}} = \frac{2}{H} \int_0^{\frac{H}{2}} \dot{\gamma} \cdot dy = \left(\frac{\Delta p}{kL}\right)^{\frac{1}{n}} \left(\frac{H}{2}\right)^{\frac{1}{n}} \frac{n}{1+n} \quad (26)$$

The velocity profile along the height of the slit can be defined by the shear rate.

$$-\frac{dv_x}{dy} = \dot{\gamma}(y) = \left(\frac{\Delta p}{kL}\right)^{\frac{1}{n}} \cdot y^{\frac{1}{n}} \quad (27)$$

$$v_x(y) = \left(\frac{\Delta p}{kL}\right)^{\frac{1}{n}} \frac{n}{1+n} \left(\frac{H}{2}\right)^{\frac{1+n}{n}} \left[1 - \left(\frac{2}{H}y\right)^{\frac{1+n}{n}}\right] = \frac{1+2n}{1+n} \bar{v} \left[1 - \left(\frac{2}{H}y\right)^{\frac{1+n}{n}}\right] \quad (28)$$

Integrating the flow velocity over the flow channel cross sectional area the volumetric flow rate in the die can be calculated.

$$\dot{V} = 2 \int_0^{\frac{H}{2}} B \cdot v_x(y) dy = 2B \left(\frac{\Delta p}{kL}\right)^{\frac{1}{n}} \frac{n}{1+2n} \left(\frac{H}{2}\right)^{\frac{1+2n}{n}} \quad (29)$$

The average flow velocity is calculated by the following relation:

$$\bar{v} = \frac{\dot{V}}{BH} = \left(\frac{\Delta p}{kL}\right)^{\frac{1}{n}} \frac{n}{1+2n} \left(\frac{H}{2}\right)^{\frac{1+n}{n}} \quad (30)$$

For calculating the average shear stress in the slit, the equation (31) is used:

$$\bar{\tau} = \frac{2}{H} \int_0^{\frac{H}{2}} \tau(y) \cdot dy = \frac{\Delta p H}{4L} \quad (31)$$

6. Viscous Dissipation

6.1.1 Heat Generation Calculation in case of Wall temperature = Initial melt temperature ($T_w = T_0$)

6.1.1.1 Completely developed flow $Ca \geq 1$

In a completely developed flow, the heat generated due to shearing on the wall is completely transferred to surroundings, so that there is no rise in the temperature along the flow length. There is a temperature profile only along the height of the slit.

When the equilibrium condition is reached, the contribution of the convection terms in the energy equation (equation 21) is zero, i.e.:

$$\rho c_p v(y) \frac{\partial T}{\partial Z} = 0 \quad (32)$$

The heat conduction becomes:

$$q_y = -\lambda \frac{\partial T}{\partial y} \quad (33)$$

Substituting these terms in the energy equation (21), we get

$$\frac{d}{dy} \left(-\lambda \frac{dT(y)}{dy} \right) = \tau_{xy} \cdot \dot{\gamma} = k \cdot \dot{\gamma}^{1+n} \quad (34)$$

On integrating the above equation over the slit height from the centre

$$\frac{dT(y)}{dy} = -\frac{k}{\lambda} \bar{v}^{1+n} \left(\frac{1+2n}{n} \right)^n \left(\frac{H}{2} \right)^{\frac{(1+n)^2}{n}} y^{\frac{1+2n}{n}} + C_1 \quad (35)$$

Applying the boundary conditions, i.e. the temperature gradient at the centre is zero, C_1 is determined as:

$$\frac{dT(y=0)}{dy} = 0 \quad \text{and} \quad C_1 = 0 \quad (36)$$

Integration of equation (35) gives equation (37).

$$T(y) = -\frac{k}{\lambda} \bar{v}^{1+n} \left(\frac{1+2n}{n} \right)^n \frac{n}{1+3n} \left(\frac{H}{2} \right)^{\frac{(1+n)^2}{n}} y^{\frac{1+3n}{n}} + C_2 \quad (37)$$

Substituting the boundary conditions, the integration constant value can be achieved.

$$T\left(y = \frac{H}{2}\right) = T_w \rightarrow C_2 = T_w + \frac{k}{\lambda} \bar{v}^{1+n} \left(\frac{1+2n}{n} \right)^n \frac{n}{1+3n} \left(\frac{H}{2} \right)^{\frac{(1+n)^2}{n}} \left(\frac{H}{2} \right)^{\frac{1+3n}{n}} \quad (38)$$

6. Viscous Dissipation

After considering the boundary conditions, the temperature distribution along the slit height is given as:

$$T(y) = T_w + \frac{k}{\lambda} \bar{v}^{1+n} \left(\frac{1+2n}{n} \right)^n \frac{n}{1+3n} \left(\frac{H}{2} \right)^{1-n} \left[1 - \left(\frac{2}{H} y \right)^{\frac{1+3n}{n}} \right] \quad (39)$$

Substituting the average velocity (equation 30) in the above equation, the temperature at the middle of the slit height ($y=0$) can be determined by:

$$T(y=0) = T_w + \frac{k}{\lambda} \frac{1}{n} \left(\frac{\Delta p}{L} \right)^{\frac{1+n}{n}} \frac{n}{1+2n} \frac{n}{1+3n} \left(\frac{H}{2} \right)^{\frac{1-3n}{n}} \quad (40)$$

For Newtonian flow ($n=1$), the following relation can be used:

$$T(y) = T_w + \frac{\eta}{\lambda} \bar{v}^2 \frac{3}{4} \left[1 - \left(\frac{2}{H} y \right)^4 \right] \quad (41)$$

In practical situations, the equilibrium regime is rarely attained.

6.1.1.2 Transition region $1 > Ca > 10^{-2}$

In the case of the transition regime, a part of the dissipated energy is transferred to the walls by conduction. So the heat loss at the walls can not be neglected in this case. The shearing generates energy which increases the melt temperature. Another part of energy is transferred by conduction normal to the flow direction.

The derivation is carried out by considering the integral form of energy balance equation over a volume element, which is given by equation (42).

$$\rho c_p v(y) 2B dy \frac{d\bar{T}}{dz} = 2B \int_0^{\frac{H}{2}} \tau_{xy}(y) \cdot \dot{\gamma}(y) dy - 2Bq dy \quad (42)$$

The heat flux at the wall is given the below relation.

$$q = -\lambda \left. \frac{dT}{dy} \right|_{\frac{H}{2}} = k \bar{v}^{1+n} \left(\frac{1+2n}{n} \right)^n \left(\frac{H}{2} \right)^{-n} \quad (43)$$

In order to integrate equation (42), an expression for q with respect to \bar{T} must be derived. Considering the relation (44),

6. Viscous Dissipation

$$\bar{T} = \frac{2B}{\dot{V}} \int_0^{\frac{H}{2}} T(y) \cdot v(y) dy = T_w + \frac{k}{\lambda} \bar{v}^{1+n} \left(\frac{H}{2}\right)^{1-n} \left[\left(\frac{1+2n}{n}\right)^n \left(\frac{2n(1+3n)}{(1+4n)(2+5n)}\right) \right] \quad (44)$$

the heat flux q is given as:

$$q = (\bar{T} - T_w) \frac{\lambda}{\left[\left(\frac{1+2n}{n}\right)^n \frac{2n(1+3n)}{(1+4n)(2+5n)} \right]} \left(\frac{1+2n}{n}\right)^n \left(\frac{H}{2}\right)^{-1} \quad (45)$$

With these relations a differential equation is formed.

$$\rho c_p \bar{v} \frac{H}{2} d\bar{T} = \left[k \bar{v}^{1+n} \left(\frac{1+2n}{n}\right)^n \left(\frac{H}{2}\right)^{-n} - (\bar{T} - T_w) \frac{\lambda}{\left[\left(\frac{1+2n}{n}\right)^n \frac{2n(1+3n)}{(1+4n)(2+5n)} \right]} \left(\frac{1+2n}{n}\right)^n \left(\frac{H}{2}\right)^{-1} \right] \cdot dz \quad (46)$$

Reducing the above equation gives:

$$\begin{aligned} \frac{\rho c_p \bar{v} H^2}{\lambda L} \frac{L}{4} \left[\left(\frac{1+2n}{n}\right)^n \frac{2n(1+3n)}{(1+4n)(2+5n)} \right] \left(\frac{n}{1+2n}\right)^n d\bar{T} &= \\ = \left[\frac{k \bar{v}^{1+n}}{\lambda} \left(\frac{H}{2}\right)^{1-n} \left[\left(\frac{1+2n}{n}\right)^n \frac{2n(1+3n)}{(1+4n)(2+5n)} \right] - (\bar{T} - T_w) \right] \cdot dz & \end{aligned} \quad (47)$$

Rearranging equation (47), gives:

$$\begin{aligned} \frac{d\bar{T}}{(\bar{T} - T_w) - \frac{k \bar{v}^{1+n}}{\lambda} \left(\frac{H}{2}\right)^{1-n} \left[\left(\frac{1+2n}{n}\right)^n \frac{2n(1+3n)}{(1+4n)(2+5n)} \right]} &= \\ = -Ca \frac{4}{\left[\left(\frac{1+2n}{n}\right)^n \frac{2n(1+3n)}{(1+4n)(2+5n)} \right] \left(\frac{n}{1+2n}\right)^n L} dz & \end{aligned} \quad (48)$$

The Cameron number, which is defined by equation (20) appears in this result and integrating the above equation leads to equation (49)

$$\ln \left[(\bar{T} - T_w) - \frac{k\bar{v}^{1+n}}{\lambda} \left(\frac{H}{2} \right)^{1-n} \left[\left(\frac{1+2n}{n} \right)^n \frac{2n(1+3n)}{(1+4n)(2+5n)} \right] \right] C_1 =$$

$$= -Ca \frac{4}{\left[\left(\frac{1+2n}{n} \right)^n \frac{2n(1+3n)}{(1+4n)(2+5n)} \right] \left(\frac{n}{1+2n} \right)^n \frac{z}{L}} \quad (49)$$

Calculating the integration constant C_1 , including the boundary condition $T(z=0) = T_w$ and rearranging the equation, we get the following equation for the determination of the melt temperature increase over the slit height along the flow length.

$$\bar{T}(z) = T_w + \frac{k\bar{v}^{1+n}}{\lambda} \left(\frac{H}{2} \right)^{1-n} \left[\left(\frac{1+2n}{n} \right)^n \frac{2n(1+3n)}{(1+4n)(2+5n)} \right]^* \cdot \left[1 - \exp \left(-Ca \frac{4}{\left[\left(\frac{1+2n}{n} \right)^n \frac{2n(1+3n)}{(1+4n)(2+5n)} \right] \left(\frac{n}{1+2n} \right)^n \frac{z}{L}} \right) \right] \quad (50)$$

6.1.1.3 Adiabatic regime $Ca < 10^{-2}$

The adiabatic regime is observed at the beginning of the flow. The entire shear heat built-up in the polymer melt is not transmitted to the wall of the flow channel. So in this case the walls are perfectly isolated.

The heat conduction term is equal to zero.

$$\lambda \frac{\partial^2 T}{\partial y^2} = 0 \quad (51)$$

The integral form of energy balance equation over a volume element can be written as:

$$\rho c_p v(y) 2B dy \frac{d\bar{T}}{dz} = 2B \int_0^{\frac{H}{2}} \tau_{xy}(y) \cdot \dot{\gamma}(y) dy - 2B q dy \quad (52)$$

After substituting the values for each term equation (53) follows.

$$\rho c_p \frac{1+2n}{1+n} \bar{v} \left[1 - \left(\frac{2}{H} y \right)^{\frac{1+n}{n}} \right] dy d\bar{T} = \left(\int k \bar{v}^{1+n} \left(\frac{1+2n}{n} \right)^{1+n} \left(\frac{H}{2} \right)^{-\frac{(1+n)^2}{n}} y^{\frac{1+n}{n}} dy \right) dz \quad (53)$$

Integrating the above equation and rearranging the equation, gives:

6. Viscous Dissipation

$$\rho c_p \bar{v} \frac{H}{2} d\bar{T} = k \bar{v}^{1+n} \left(\frac{1+2n}{n} \right)^n \left(\frac{H}{2} \right)^{-n} dz \quad (54)$$

Simplifying this equation, leads to equation (55).

$$d\bar{T} = \frac{k \bar{v}^n}{\rho c_p} \left(\frac{1+2n}{n} \right)^n \left(\frac{H}{2} \right)^{-1-n} dz \quad (55)$$

With the boundary conditions

$$d\bar{T}(z=0) = T_w \quad (56)$$

the value for the integration constant is obtained as:

$$C_1 = T_w \quad (57)$$

The adiabatic temperature increase along the die length is calculated from the following equation:

$$\bar{T}(z) = T_w + \frac{k \bar{v}^n}{\rho c_p} \left(\frac{1+2n}{n} \right)^n \left(\frac{H}{2} \right)^{-(1+n)} z \quad (58)$$

Substituting the expression for the average velocity in the above equation, a simplified equation is obtained.

$$\bar{T}(z) = T_w + \frac{\Delta p}{\rho c_p} \frac{z}{L} \quad (59)$$

7 Numerical Optimisation Algorithm

7.1 Nelder Mead Simplex Method

A simplex method for finding a local minimum of a function of several variables has been devised by Nelder and Mead. For two variables, the simplex is a triangle, and the method is a pattern search that compares functional values at the three vertices of a triangle. The worst vertex, where the function value is the largest, is rejected and replaced with a new vertex. The simplest step is to replace the worst point with a point reflected through the centroid of the remaining points. If this point is better than the best current point, then we can try stretching exponentially out along this line. On the other hand, if this new point is not much better than the previous value, then we are stepping across a valley, so we shrink the simplex towards the best point. A new triangle is formed and the search is continued. The process generates a sequence of triangles (which might have different shapes), for which the function values at the vertices get smaller and smaller. The size of the triangle is reduced and the coordinates of the minimum point are found.

The algorithm is stated using the term simplex (a generalised triangle in N dimensions) and will find the minimum of a function of N variables. It is effective and computationally compact [16].

In Nelder mead method simplex transformations are controlled by four parameters [17,18], α for reflection, β for contraction, γ for expansion and δ for shrinkage.

They should satisfy the following constraints

$$\alpha > 0, \quad 0 < \beta < 1, \quad \gamma > 1, \quad \gamma > \alpha, \quad 0 < \delta < 1 \quad (60)$$

The standard values, used in most implementations, are

$$\alpha = 1, \quad \beta = \frac{1}{2}, \quad \gamma = 2, \quad \delta = \frac{1}{2} \quad (61)$$

7.2 Procedure for optimising a function

Let $f(x, y)$ be the function, having two variables, which is to be minimized [15].

7.2.1 Initial Triangle

To start, a triangle (Figure 13) is formed with given three vertices (starting points).

$$V_k = (x_k, y_k) \quad (62)$$

Where $k = 1, 2, 3$

The function $f(x, y)$ is then evaluated at each three points:

$$Z_k = f(x_k, y_k) \quad (63)$$

The subscripts are then reordered so that $Z_1 < Z_2 < Z_3$ and accordingly the three vertices can be specified as best, good and worst vertex.

Best vertex $B = (x_1, y_1)$

Good vertex $G = (x_2, y_2)$

Worst vertex $W = (x_3, y_3)$

7.2.2 Midpoint of the good side

The construction process uses the midpoint (M) of the line segment joining B and G . It is found by taking the average of the coordinates.

$$M = \frac{B + G}{2} = \left(\frac{x_1 + x_2}{2}, \frac{y_1 + y_2}{2} \right) \quad (64)$$

7.2.3 Reflection

The function decreases as the vertex moves along the side of the triangle from W to B , and it decreases as the vertex moves along the side from W to G . Hence it is feasible that $f(x, y)$ takes smaller values at points that lie away from worst vertex W on the opposite side of the line between B and G . A test point R is obtained by 'reflecting' the triangle through the side BG . To determine the point R , first the midpoint M of the side BG is found using the equation (64). A line segment is created between the points W and M . Let the distance be D . The last segment is extended a distance D through M to locate the point R (Figure 13).

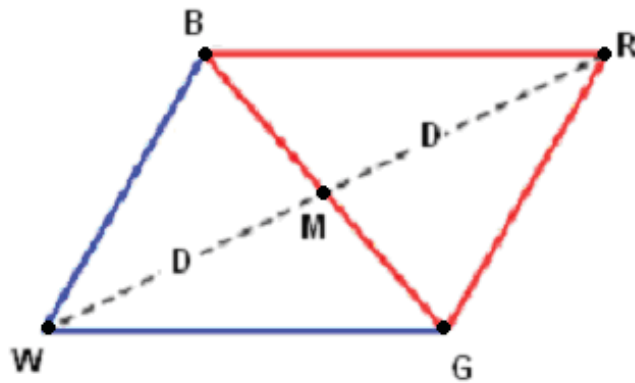


Figure 13: Triangle BGW and midpoint M and reflected point R

The vector formula for R is

$$R = M + (M - W) = 2M - W \quad (65)$$

The function value at R is then calculated. According to the comparison between the values at R and W, expansion or contraction is done.

7.2.4 Expansion

If the function value at R is smaller than the function value at W, then the movement of the vertex is in the correct direction towards the minimum. Perhaps the minimum might be a bit farther from the point R. So the extension of the line segment (Figure 14) through M and R to the point E is performed. This forms an expanded triangle BGE (Figure 14). The point E is found by moving an additional distance D along the line joining M and R. The vector formula to find the point E is given by equation (66).

$$E = R + (R - M) = 2R - M \quad (66)$$

The function value at E is calculated and if the value is less than the function value at R, then a better vertex is found.

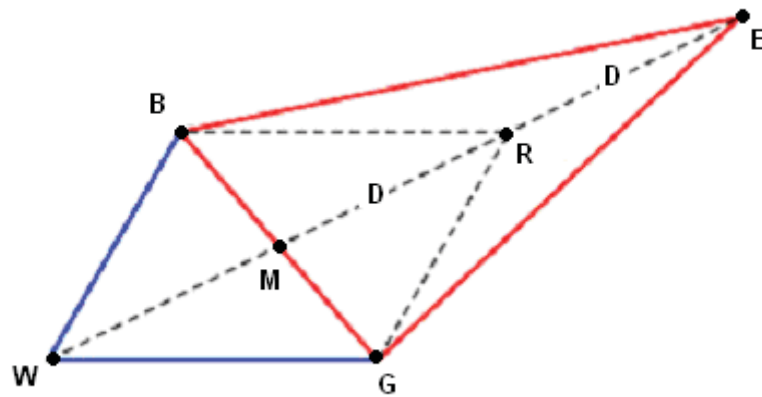


Figure 14: Triangle BWG and extended point R

7.2.5 Contraction

If the function values at R and W are the same, another point must be tested. Perhaps the function is smaller at M, but the point W cannot be replaced by M, since a triangle is a must. In this case two midpoints C_1 and C_2 respectively of the line segments WM and MR have to be considered (Figure 15).

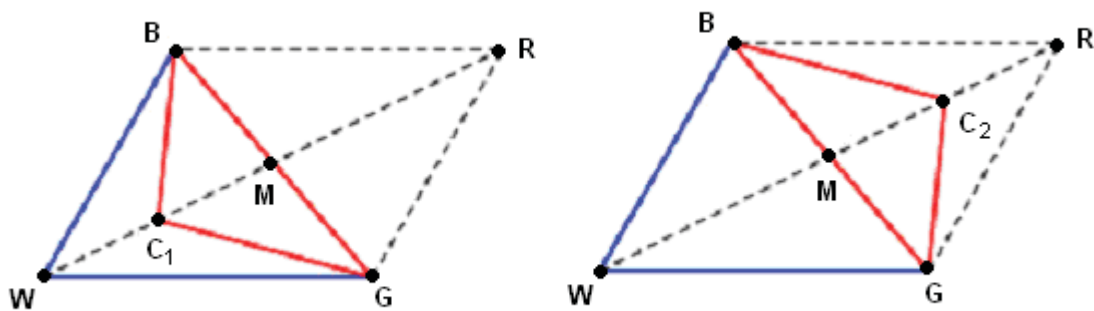


Figure 15: Contraction point C_1 and C_2

The function values at these two points are found and the point with smaller function value is taken as C and this point is used for further calculation. The vector formula to find C is given by equation (67)

$$C = \frac{(W+M)}{2} \text{ (or) } \frac{(M+R)}{2} \quad (67)$$

With this C value a new triangle BGC is formed. The choice between C_1 and C_2 might seem inappropriate for the two dimensional case, but it is important in higher dimensions.

7.2.6 Shrinking

If the function value at C is not less than the value at W, the points G and W must be shrunk towards B (Figure 16). The point G is replaced by M and W is replaced with S, which is the midpoint of the line segment joining B and W.

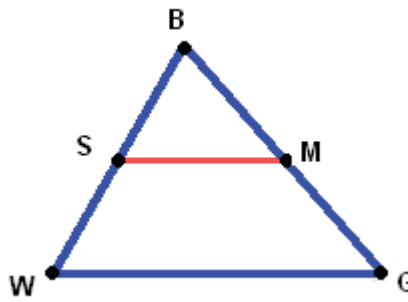


Figure 16: Shrinking the triangle BWG towards B

7.2.7 Logical Decisions

In each step, a new vertex is found, which replaces W. As soon as it is found, further investigation is not needed, and the iteration step is completed. The logical details for two dimensional cases are explained in Table 2.

7.2.8 Termination

The Nelder-Mead algorithm must terminate in a finite number of steps or iterations. Quite generally, the termination test is composed of three different parts:

- 1. *domain* convergence or termination test. It becomes *true* when the working simplex is sufficiently *small* in some sense (some or all vertices are close enough).
- 2. *function value* convergence test. It becomes *true* when (some or all) function values are *close* enough in some sense.

8 Rheological Data Calculation Program – RheoSoft

Injection moulding machine rheometer is a simple and fast way to measure the flow behaviour of a polymer melt at high shear rates [19,20]. But the analysis of the measured data is complicated, since the measured files have too many data and calculation of the viscosity values manually will be time consuming. In order to simplify the calculation process and time a program has been created using Microsoft Excel 2002 and Visual Basic.

RheoSoft is a program developed in this master thesis to calculate the material's rheological data and also to calculate the viscosities with temperature-correction for the measurements, done on the injection moulding machine rheometer in easier, simpler and faster way. The program is written in Visual Basic 6.0 and it works in Microsoft Excel 2000 and higher versions. The program performs complex data analysis and outputs the calculated values and graphic results to the Excel worksheets. Also the program can generate the end report with all the measured data and viscosity data as a word document. Excel Visual Basic is a useful and convenient tool for evaluating huge data. Also data entry is greatly simplified and custom reports can be generated with ease.

The program has been developed in two levels:

- Standard data evaluation
- Scientific data evaluation, including melt temperature correction

The differences between these two versions are:

1. Pressure transducer: In the standard version only two pressure transducers (mounted 60 mm apart from each other) can be used, but in the highly scientific version four pressure transducers (with a gap of 20 mm between each sensor) can be used.
2. Temperature sensor: Only one infrared temperature sensors (IR sensor), to measure directly the melt temperature in the channel and a thermocouple to measure the wall temperature near the entrance of the die can be used. But in the scientific version two IR-sensors and two thermocouples to measure the wall temperature near the entrance and near the exit can be used. In scientific version the wall temperature increase along the flow length can be easily determined.

8. Rheological Data Calculation Program – RheoSoft

3. Temperature correction: The viscosity values calculated from the standard program are without temperature correction, which is carried out in the scientific version.

The program is an “add-in” for Microsoft Excel and can be easily installed in Excel. On installing the add-in, a menu called P4P-RheoSoft is created in the Tools menu and also an icon is created on the command bar of the Excel window. Clicking either the menu or the icon and the RheoSoft dialogue box with multiple tabs opens (Figure 17).

The screenshot shows the P4P-RheoSoft V.1.0 dialog box. The window title is "P4P- Rheo Soft V.1.0". The interface has a tabbed structure with the following tabs: "IMPORT MATERIAL", "VISCOSITY RHEOLOGICAL MOULD", "VISCOSITY MODELS SENSORS", "IMM", and "TEMPERATURE". The "VISCOSITY RHEOLOGICAL MOULD" tab is selected. The "MATERIAL SPECIFICATIONS" section contains two input fields: "Material name" with the value "PP" and "Charge number" with the value "HG313MO". The "MATERIAL DATA" section is divided into three sub-sections: "pVT" with four input fields (k_1(ccmbar/g) = 31280, k_2(ccmbar/g°C) = 1.3014, k_3 (bar) = 1623.2, k_4 (bar) = 27345); "Thermal conductivity" with two input fields (A = 0, Lambda/B (W/mK) = 0.177); and "Specific heat capacity" with two input fields (a (J/gK°C) = 0.0025, b (J/gK) = 2.0959). At the bottom of the dialog are three buttons: "OK", "NEW", and "CLOSE".

Figure 17: RheoSoft „add-in“ dialogue box

8.1 Measured data

During the injection of the polymer melt through the slit die at a specified flow rate, the following parameters are recorded by the data acquisition system:

- Melt pressure at four different positions along the total length of the flow channel

8. Rheological Data Calculation Program – RheoSoft

- Melt temperature, using two IR-sensors. Calculated wall temperature, using two heat flux sensors along the length of the die, each of them measuring three steel temperatures at different distances from the wall.
- The axial position of the piston in the volumetric flow rate measurement cylinder

All these sensors measure the signals and send it to an analog-digital convertor (Spider8 by Hottwinger Baldwin Messtechnik, Germany). Using the data acquisition software (Catman easy developed by Hottwinger Baldwin Messtechnik, Germany), the signals are measured at a particular frequency. These measured signals are converted to digital values using the calibration values. Next they are saved as excel files.

Figure 18 shows the values from all the measurement sensors, plotted over the time scale.

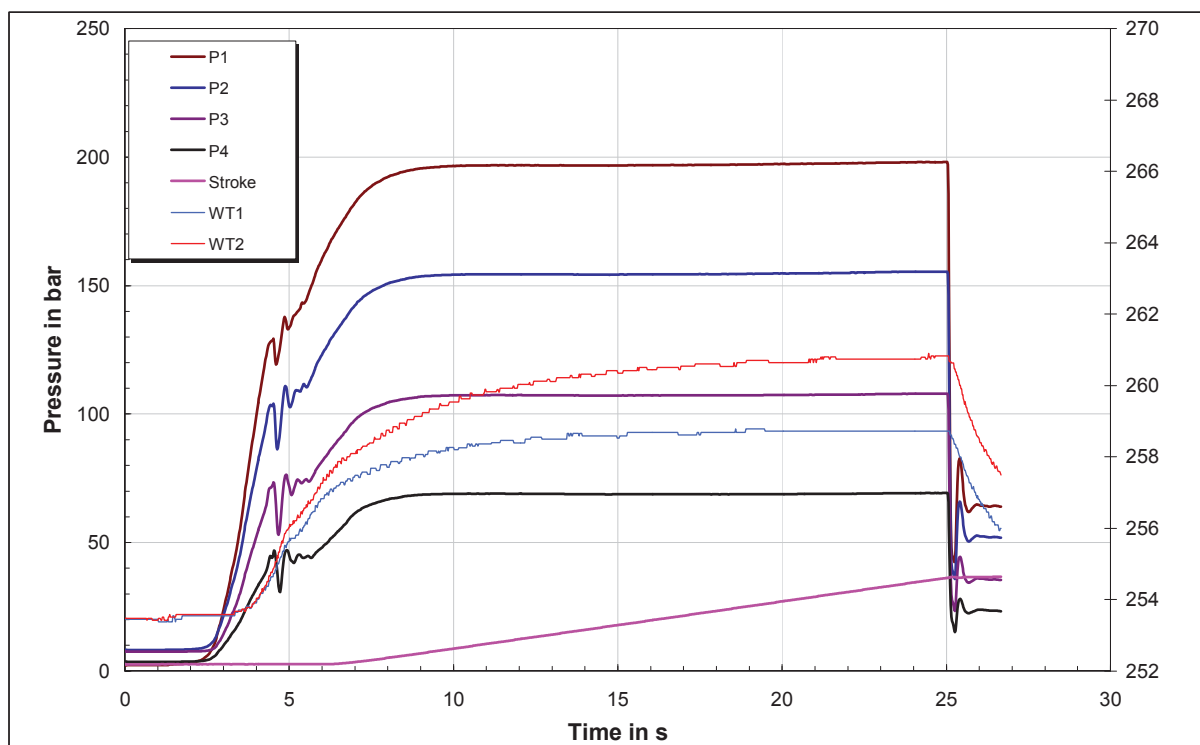


Figure 18: Measured data from the injection moulding machine rheometer for PP HG313MO at 250°C at flow rate of 5 cm³/s, P1-P4: measured pressures; WT1: wall temperature near entrance of the die; WT2: wall temperature near exit of the die; Stroke: Displacement of the piston in the volume flow rate measurement cylinder

8.2 Basic data for viscosity calculation

For calculating the basic data (equilibrium pressure, temperature and volumetric flow rate) for each measurement, additional data are required, and these data has to be given by the user in the RheoSoft dialogue box. The required additional data from the user are:

1. Die Specifications:

- Slit height,
- Length,
- Width,

2. Pressure sensors and their position,

3. Temperature sensors,

4. Stroke sensor,

5. Screw diameter,

6. Diameter of the piston,

7. Thermal data (heat conductivity, pVT-data and specific heat capacity)

The other additional data, which has to be given by the user, are

- Material specifications,
- Machine specifications,
- Temperatures in mould and machine,

which are used only for documentation purpose. In the scientific version the temperature correction can be performed and if there is no need for temperature correction, then the option of temperature correction can be set to “no” and viscosity values are determined without temperature correction.

After putting in all these required data, the calculation of the basic data can be performed for each measurement one after the other. For this, first the measured data has to be imported into the excel sheet. The calibrated values are imported in the order of time, pressures, temperatures and stroke.

8.2.1 Equilibrium pressure calculation

The pressure measured is not constant through out the cycle time (Figure 19). From the plot it is clear that the recording of the measured data starts before the injection phase and the pressure is low until the injection of the melt begins. Once the melt is

8. Rheological Data Calculation Program – RheoSoft

injected and it reaches the sensor the pressure starts increasing and at a certain time range it is constant. When the injection phase is finished the pressure decreases rapidly to the initial value. This equilibrium pressure range has to be determined, and in this time range the temperature has to be calculated.

For finding this equilibrium pressure range, only the pressure values recorded during the injection phase (working range) by either P1 or P2 position sensor is considered.

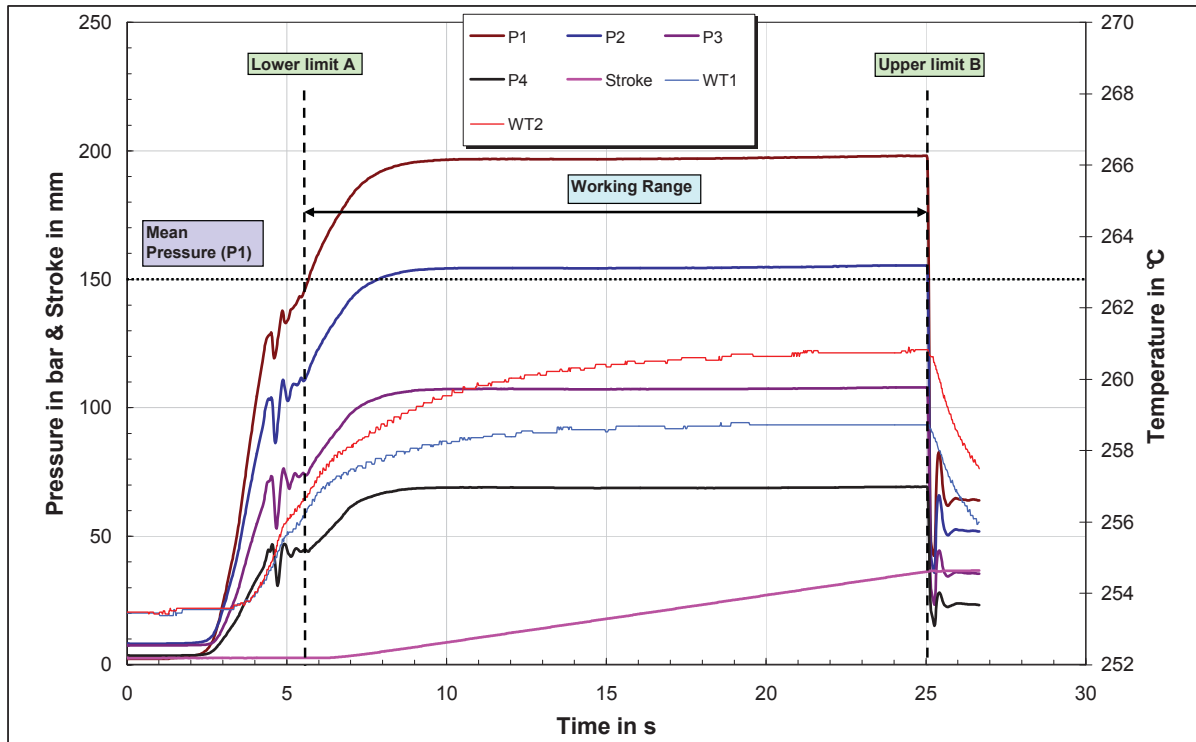


Figure 19: Pressure, temperature and stroke profile with working range

This working range is determined by calculating the mean of the pressures measured and the time range, where the pressure values, higher than the mean pressure, are considered and the rest are eliminated. This reduces the number of data and makes the calculation faster and easier. The equilibrium pressure range lies in the working range, and for finding this range the standard deviation of the pressure is considered.

The standard deviation (S.D) for the pressure values is calculated using the following relation:

$$S.D = \sqrt{\frac{1}{N} \sum_{i=1}^N (p_i - \bar{p})^2} \quad (68)$$

Where:

p_i - Pressure value at time t_i (i= Lower limit to Upper limit)

\bar{p} - Mean of pressure values in the selected range

N - Total number of measured values in the selected range

For calculating the mean pressure the following equation is used.

$$\bar{p} = \frac{1}{N} \sum_{i=1}^N p_i \quad (69)$$

The tolerance value given by the user is used as the reference value. The time limits of the working range are considered as the starting value, and the calculated standard deviation value in the time range is compared with the reference value. If the deviation is less than the tolerance value then this time range is considered as the equilibrium range. If the value is higher, then the time limits are reduced and checked for the minimum. The process is repeated until the minimum is attained or the difference of the time limits is equal to 2 seconds. If this stage is case, then either tolerance value is changed and the procedure is repeated or the range is selected manually.

The tolerance value can be set to a very minimum value (e.g. 0.1 bar) for the measurement performed at very low injection speeds. Because the measurement times at low injection speeds are high and the equilibrium pressure can be easily determined. But in the case of high injection speeds, the total injection time is two seconds or less. To find the equilibrium range with 0.1 bar tolerance is not possible.

The algorithm used in RheoSoft to determine the equilibrium pressure is given in Figure 20 as a flow diagram.

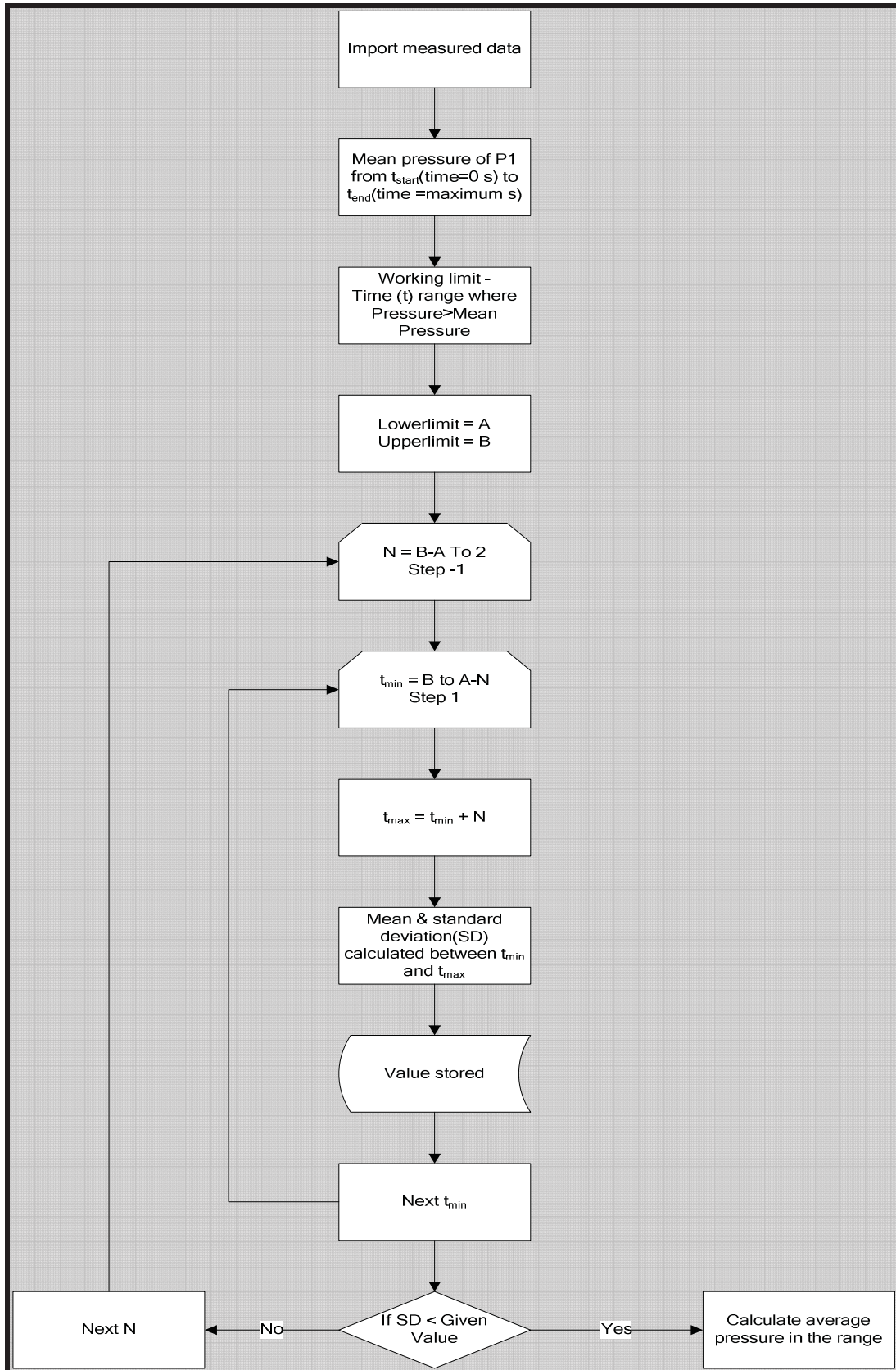


Figure 20: Algorithm to find equilibrium pressure range

The pressure loss along the flow length is plotted and points are approximated by linear regression. Figure 21 shows the pressure loss along the flow length for PP HG313MO measured at 250°C at two different volumetric flow rates. If the linearity of the pressure profile along the length of the die is acceptable, then the average of all the pressures and temperatures in the selected range is determined.

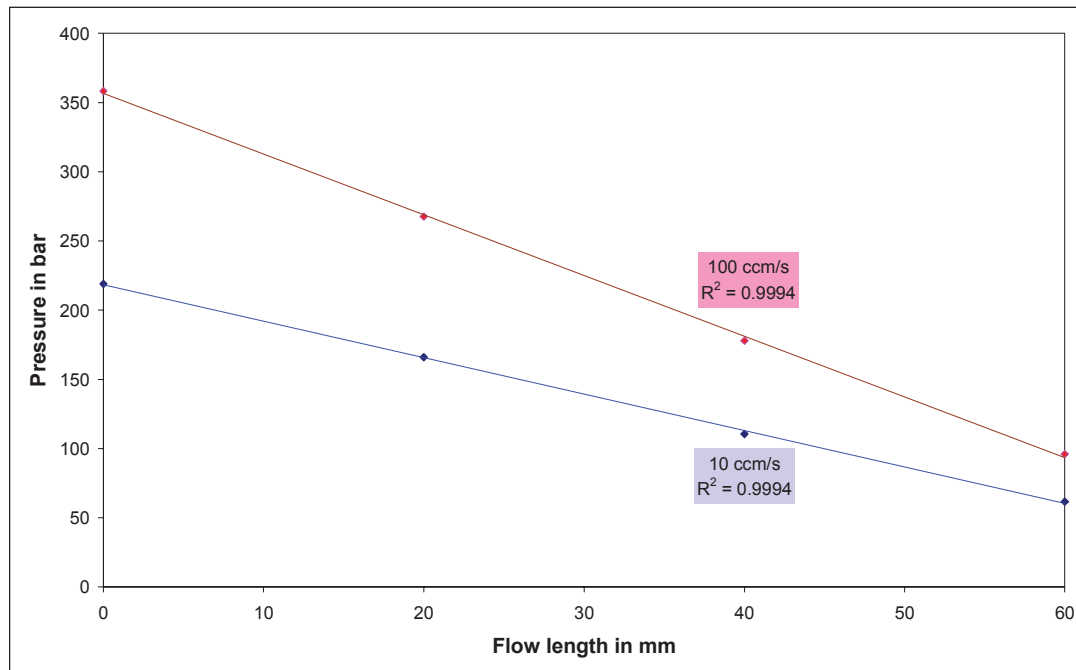


Figure 21: Pressure distribution along the axial distance of the slit die

8.2.2 Wall temperature and melt temperature determination

As mentioned in section 3.1 the wall temperature is measured near the entrance and near the exit of the flow channel using a heat flux sensor, designed by Institute of Plastics Processing, University of Leoben, Austria (Figure 4) with three thermocouples placed at different distance away from the wall. From the three measured values, the wall temperature (WT1, WT2) is calculated either by linear or by exponential or polynomial (second order) extrapolation.

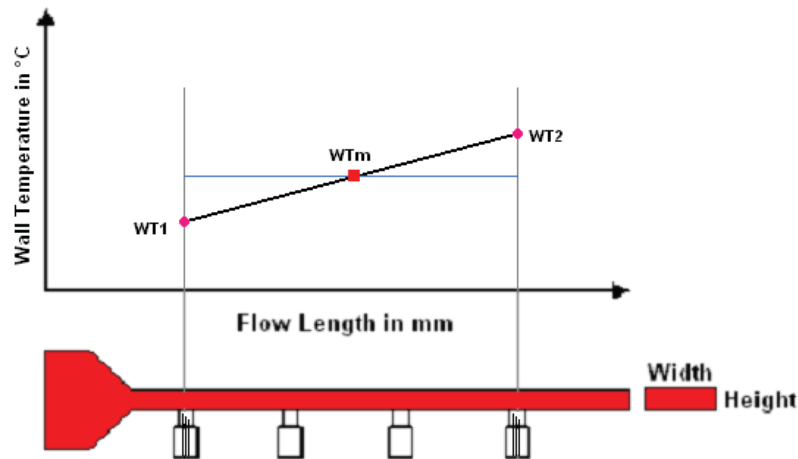


Figure 22: Average wall temperature along the flow length

The temperatures at the wall along the slit die are not isothermal during the injection phase. The wall temperature at the exit side is relatively higher than the temperature near the entrance due to shear heating (Figure 22). The average of these two wall temperatures gives the average wall temperature (WT_m) at the middle of the flow length.

This average wall temperature is further used for calculating the melt temperature. To calculate the melt temperature first the Cameron Number is calculated using equation (28). The thermal material data (thermal conductivity, specific heat capacity, ρvT) are needed in order to calculate the Cameron number and the melt temperature. As reference temperature for the thermal data WT_m is chosen as starting value.

8.2.3 Volumetric flow rate

The accurate volumetric flow rate is calculated from the displacement of the piston in the volumetric flow rate measurement cylinder. The displacement of the piston is recorded throughout the complete cycle time of a measurement. From the plot of displacement over time (Figure 23) the injection time range can be easily determined. This range is considered for calculating the volumetric flow rate.

With the working range, the velocity of the piston movement is calculated and with the piston velocity and piston dimension the accurate volumetric flow rate is calculated (equation 70).

$$Q = \frac{1}{4} \cdot d_c^2 \cdot \pi \cdot \tilde{v} \quad (70)$$

Where

d_c - Diameter of the piston

\tilde{v} - Piston velocity

Q - Volumetric flow rate

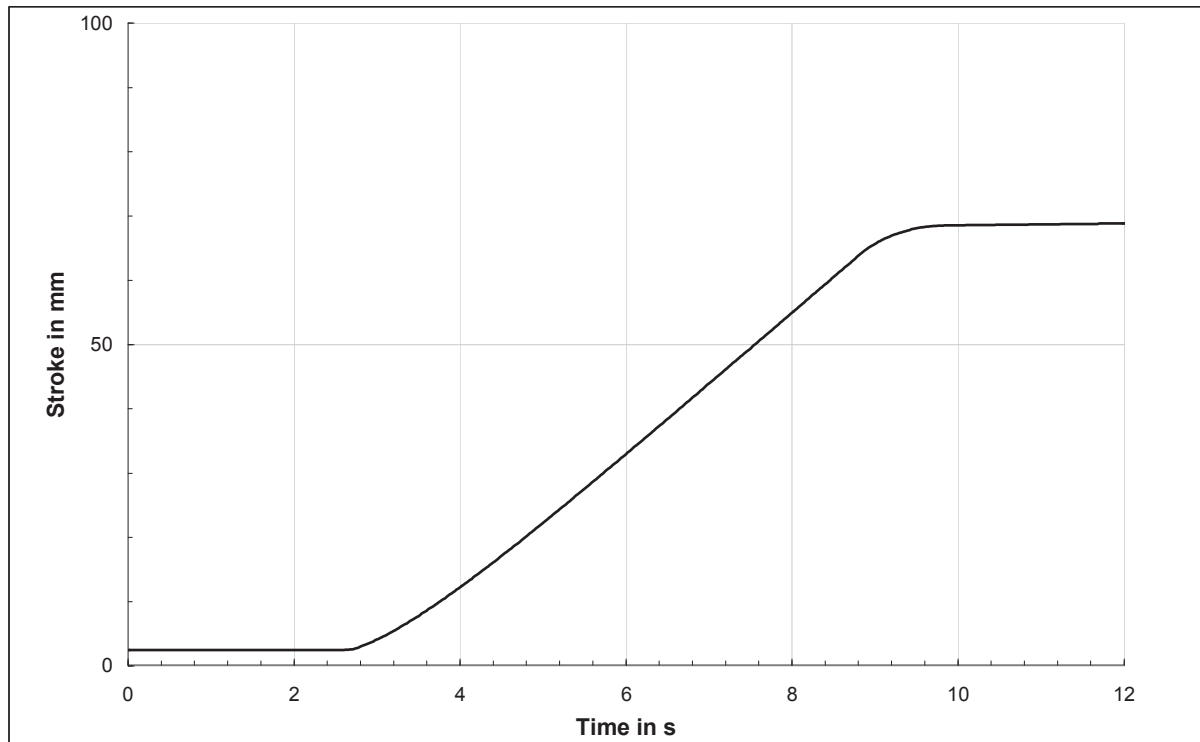


Figure 23: Position of the piston over time scale for PP HG313MO at 230°C with a volumetric flow rate of 30 cm³/s

The measured points in the working range are approximated by linear regression (equation 71).

$$s = \tilde{v} \cdot t + b \quad (71)$$

Where

s - Displacement

t - Time

b - Intercept

The slope of working range is the piston velocity and this slope is calculated using the following relationship:

$$\tilde{V} = \frac{N \cdot \sum_{i=1}^N t_i \cdot s_i - \sum_{i=1}^N t_i \cdot \sum_{i=1}^N s_i}{N \cdot \sum_{i=1}^N t_i^2 - \left(\sum_{i=1}^N t_i \right)^2} \quad (72)$$

Where

N - Total number of measured values in the equilibrium pressure range

i - Measured point in the range

If the stroke sensor is not used, then the flow rate, set on the injection moulding machine during each measurement, is used for the shear rate calculation. If the setting is done in injection speed, then the flow rate is calculated from the screw dimension and the injection speed.

$$Q = v' \cdot A_s \quad (73)$$

Where

v' - Injection speed

A_s - Cross sectional area of the screw

Having all the basic data, the apparent and true viscosity are determined as described in section 3.3.

8.2.4 Temperature Corrected Viscosity

In order to calculate the temperature corrected viscosity accurately, viscosity data over a wide range of shear rate for a minimum of three different melt temperatures are necessary. The mathematical approximation is carried out using the rheological models –Power Law (equation 12) and Cross (equation 13).

The steps involved in calculating the temperature corrected viscosity are represented in the following flow diagram (Figure 24). Each step in the calculation procedures is detailed below [9]:

Step 1 (Yellow in Figure 24):

In the first step the average pressure and temperature for different flow rates, measured at three different melt temperatures, are calculated from the measurements made on the IMMR. From these basic data the apparent viscosity values are calculated. Also the viscosity values at lower shear rate range, measured using a rotational rheometer and capillary rheometer, are imported for all the melt

temperatures. At the end of this step, the viscosity values for a wide range of shear rate, for different melt temperatures are collected.

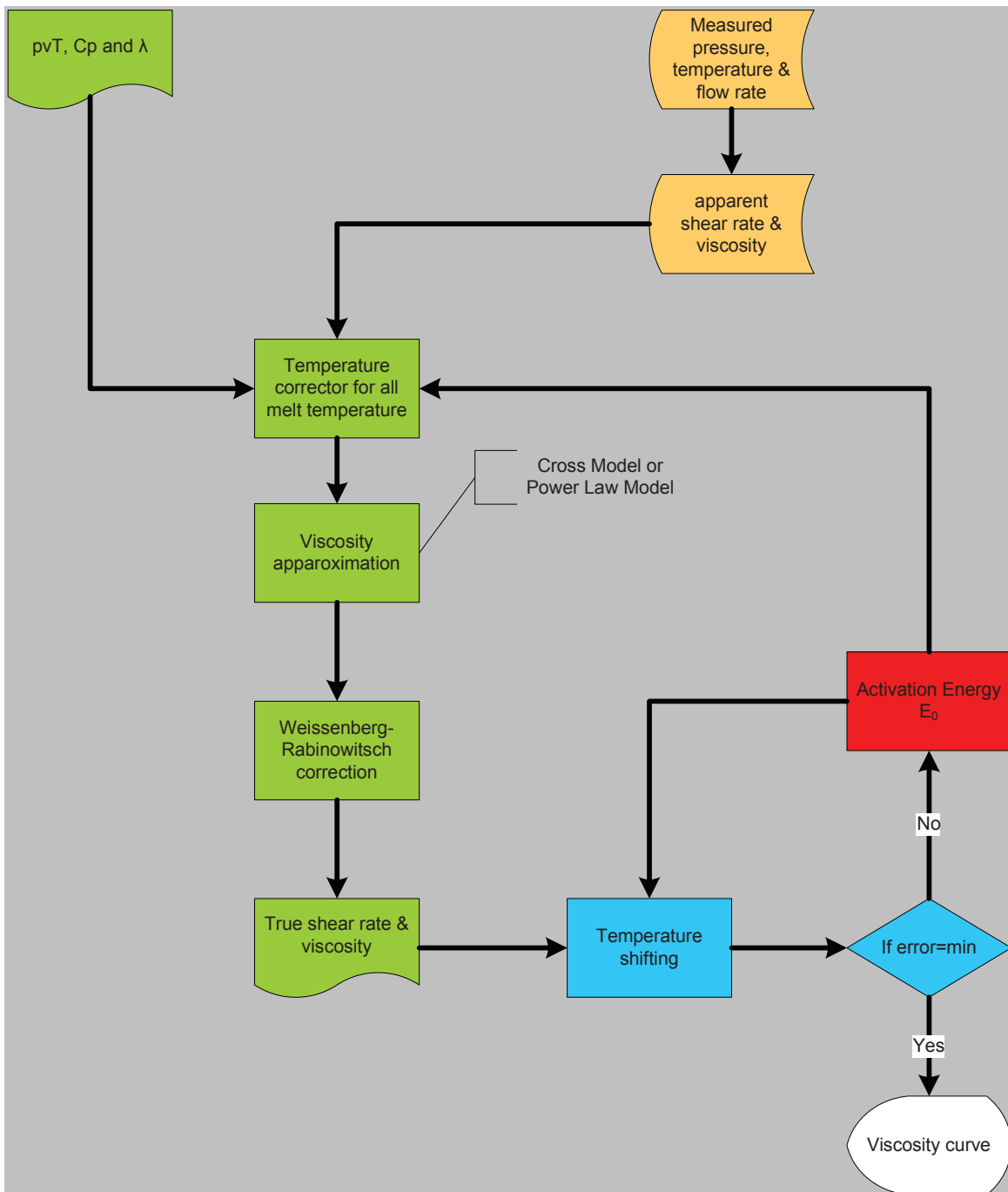


Figure 24: Procedure followed for Temperature correction [9]

Step 2 (Green in Figure 24):

In the second step, for all the collected viscosity values the temperature shifting is done using the Arrhenius equation. For this temperature shifting, initially the average melt temperature in the flow channel (average over the total flow channel volume) is calculated. Cameron number (equation 28) is used to decide the appropriate model

8. Rheological Data Calculation Program – RheoSoft

for calculating the temperature increase by Agassant method (see 6.1). For this calculation the material's thermal conductivity in the melt temperature range, pvT-data and specific heat capacity in the melt temperature range are considered.

The thermal conductivity is specified as a single value, because the heat conductivity can be taken as constant in the melt temperature range. For more accuracy it is calculated from the coefficients of linear approximation for the heat conductivity measured in the melt temperature range. As initial value for the melt temperature the mean wall temperature WTm can be chosen.

$$\lambda = A \cdot T + B \quad (74)$$

Where

λ - Thermal conductivity

T - Melt temperature

A, B - Linear approximation coefficients

The density of the material at melt temperature is calculated from the pvT data, which is approximated by Menges equation for the melt temperature range. As initial value for T the mean wall temperature WTm is chosen.

$$\frac{1}{\rho(T,p)} = v(T,p) = \frac{K1}{p+K4} + \frac{K2}{p+K3} \cdot T \quad (75)$$

Where

ρ - Density

v - Specific volume

p - Pressure

T - Melt temperature

K1, K2, K3, K4 - Approximation coefficients

The specific heat capacity value is also calculated from the linear approximation coefficients, for the melt temperature range. Similar to the calculation of thermal conductivity and pvT-data, for the melt temperature we choose WTm.

$$c_p = a_{c_p} \cdot T + b_{c_p} \quad (76)$$

Where

C_p - Specific heat capacity

T - Melt temperature

a_{c_p}, b_{c_p} - Linear approximation coefficients

If the calculated Ca is greater than 1 ($Ca > 1$), then the calculated mean wall temperature is considered as the average melt temperature.

In case $1 > Ca > 0.01$ then the equation (50) is used to calculate the increase in the melt temperature in the flow channel (see section 6.1.1.2).

For the adiabatic case where $Ca < 0.01$, the increase in melt temperature is determined using equation (58) (see section 6.1.1.3).

For calculation of the average melt temperature the viscosity values in the shear thinning region of the apparent viscosity curve is approximated using the Power law model. The Power law model constants K and n are determined analytically [9]. The calculated average melt temperature is used for the temperature correction of the apparent values. The activation energy for the temperature correction is initially determined using Arrhenius model for the viscosities measured on rotational rheometer (zero shear viscosity) and the capillary rheometer. With this activation energy the temperature corrected viscosity and shear rate are obtained using the following relations:

$$\dot{\gamma}_{app,T} = a_T \cdot \dot{\gamma}_{app} \quad (77)$$

$$\eta_{app,T} = \frac{\eta_{app}}{a_T} \quad (78)$$

The temperature corrected apparent viscosity values are approximated using Cross model. By carrying out the Weissenberg-Rabinowitsch correction, the temperature corrected true viscosity values are determined.

Step 3 (Blue in Figure 24):

In step 3 the calculated true viscosity values for all the melt temperatures are shifted to the reference temperature using Arrhenius equation. And all the true values are approximated using Cross model. The non-Newtonian region of the viscosity curves are approximated using Power law model and these constant values will be used in the second loop for the accurate calculation of the temperature increase, by returning to step 2.

From these values, the total error for the temperature correction is calculated using the following equation [9]:

$$e = \sum \left(\frac{\frac{\eta_{T_i}(\dot{\gamma}_i)}{a_T} - \eta_{T_0}(\dot{\gamma}_i)}{\eta_{T_0}(\dot{\gamma}_i)} \right)^2 = \sum \left(\frac{\frac{\eta_{T_i}(\dot{\gamma}_i)}{a_T} - \frac{A_{T_0}}{1 + (B_{T_0} \cdot \dot{\gamma} \cdot a_T)^{C_{T_0}}}}{\frac{A_{T_0}}{1 + (B_{T_0} \cdot \dot{\gamma} \cdot a_T)^{C_{T_0}}}} \right)^2 \quad (79)$$

This error is reduced to minimum iteratively, by changing the activation energy value. The final value is used for calculating the temperature corrected viscosity in step 2 in the second loop.

Step 4 (Red in Figure 24):

The calculated activation energy in step 3 is transferred to the temperature correction in step 2 and the new temperature corrected true values are determined, for which again the temperature shifting is performed. This process is done in a cyclic manner for 4 cycles, in order to obtain more accurate values.

Step 5 (White in Figure 24):

Once the temperature correction and temperature shifting are performed, the temperature corrected true viscosity values and the Cross approximated viscosity values are graphically displayed.

After completing the temperature correction, the approximation for these temperature corrected values using other viscosity model can be performed.

8.2.5 Viscosity approximation

A viscosity function (or model) is required for modeling an injection moulding process. Number of well known models is available, but it is important to choose a model, which is both accurate over the processing range and for which data can be readily obtained. The aim of the viscosity model is to match the observed behaviour of the material as closely as possible.

In RheoSoft there are different models available and the required model is chosen for carrying out the approximation. This approximation is done for the whole viscosity curve; say zero shear viscosity to the high shear rate ranges measured using the IMMR and the capillary rheometer, for all the measured melt temperatures. For the approximation the Nelder Mead simplex method is used. The parameters to be calculated depend on the chosen model, and the function to be minimized is given in equation (80).

$$e = \sum \left(\frac{\frac{\eta_{T_i} - \eta_{T_0}}{a_T}}{\eta_{T_0}} \right)^2 \quad (80)$$

Where

e - Error

η_{T_i} - Measured viscosity at melt temperature T_i in Pas

η_{T_0} - Calculated viscosity by a specified model with reference melt temperature T_0 in Pas

a_T - Temperature shift factor

The function value e is reduced to minimum by changing the coefficients in the viscosity model iteratively.

The different models available in RheoSoft and their respective equations are shown in Table 3.

Table 3: Mathematical equations for the viscosity models and the temperature shift factor [26]

Viscosity model	Equation
Power Law Model	$\eta = a_T^n \cdot k \cdot \dot{\gamma}^{(n-1)}$
Carreau Model	$\eta = \frac{A \cdot a_T}{(1 + B \cdot a_T \cdot \dot{\gamma})^C}$
Cross Model	$\eta = \frac{A \cdot a_T}{(1 + (B \cdot \dot{\gamma} \cdot a_T)^C)}$
Modified Carreau Model	$\eta(\dot{\gamma}) = a_T \cdot D + \frac{A}{(1 + a_T \cdot B \cdot \dot{\gamma})^C}$
Arrhenius equation	$a_T = \exp \left[\frac{E}{R} \left(\frac{1}{T} - \frac{1}{T_0} \right) \right]$
WLF-equation	$\lg a_T = - \frac{C_1(T - T_0)}{C_2 + (T - T_0)}$

The complete procedure involved in calculating the viscosity without temperature correction is represented in the following flow diagrams (Figure 25 and Figure 26).

8. Rheological Data Calculation Program – RheoSoft

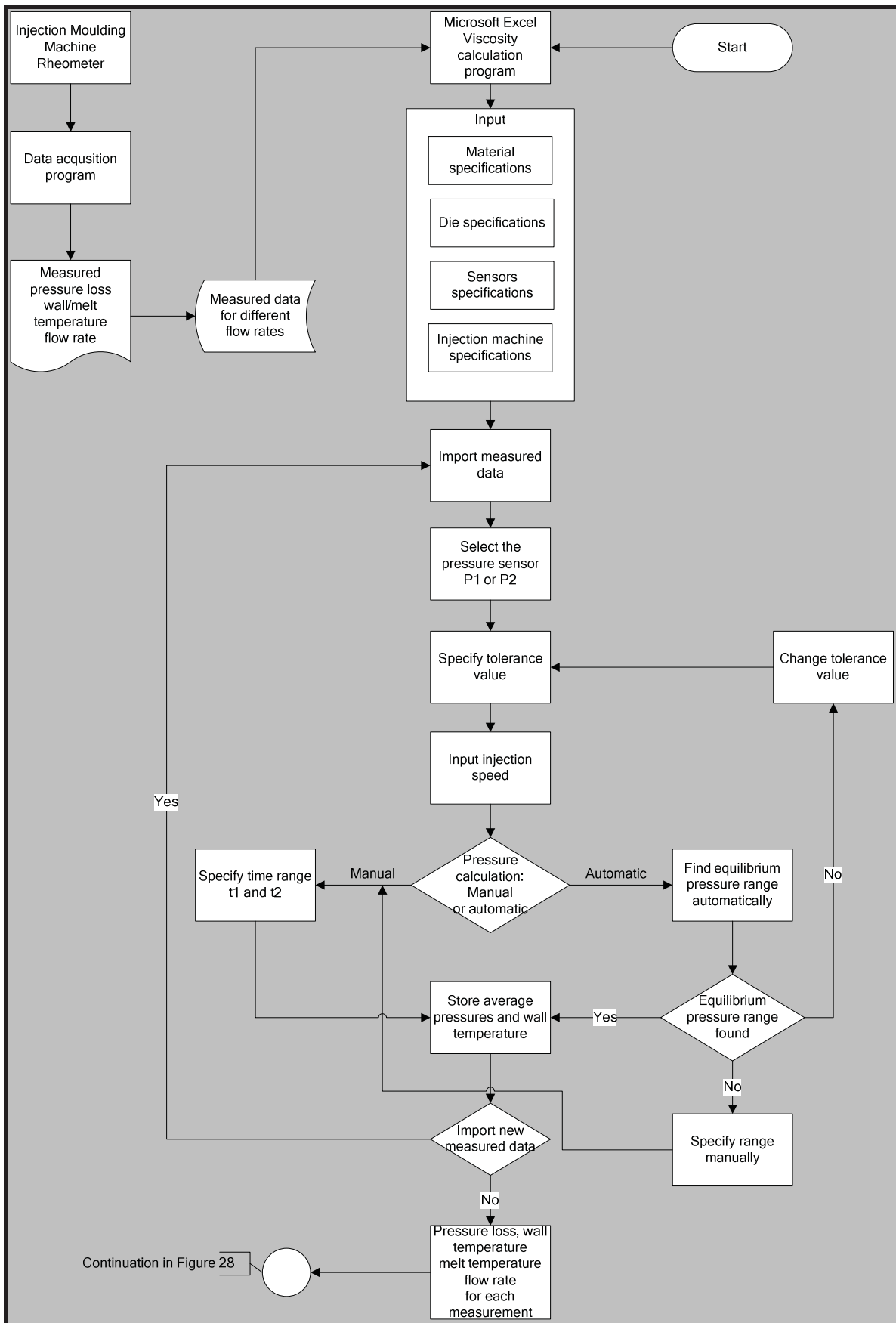


Figure 25: Flow diagram – Steps in calculating the viscosity data using RheoSoft

8. Rheological Data Calculation Program – RheoSoft

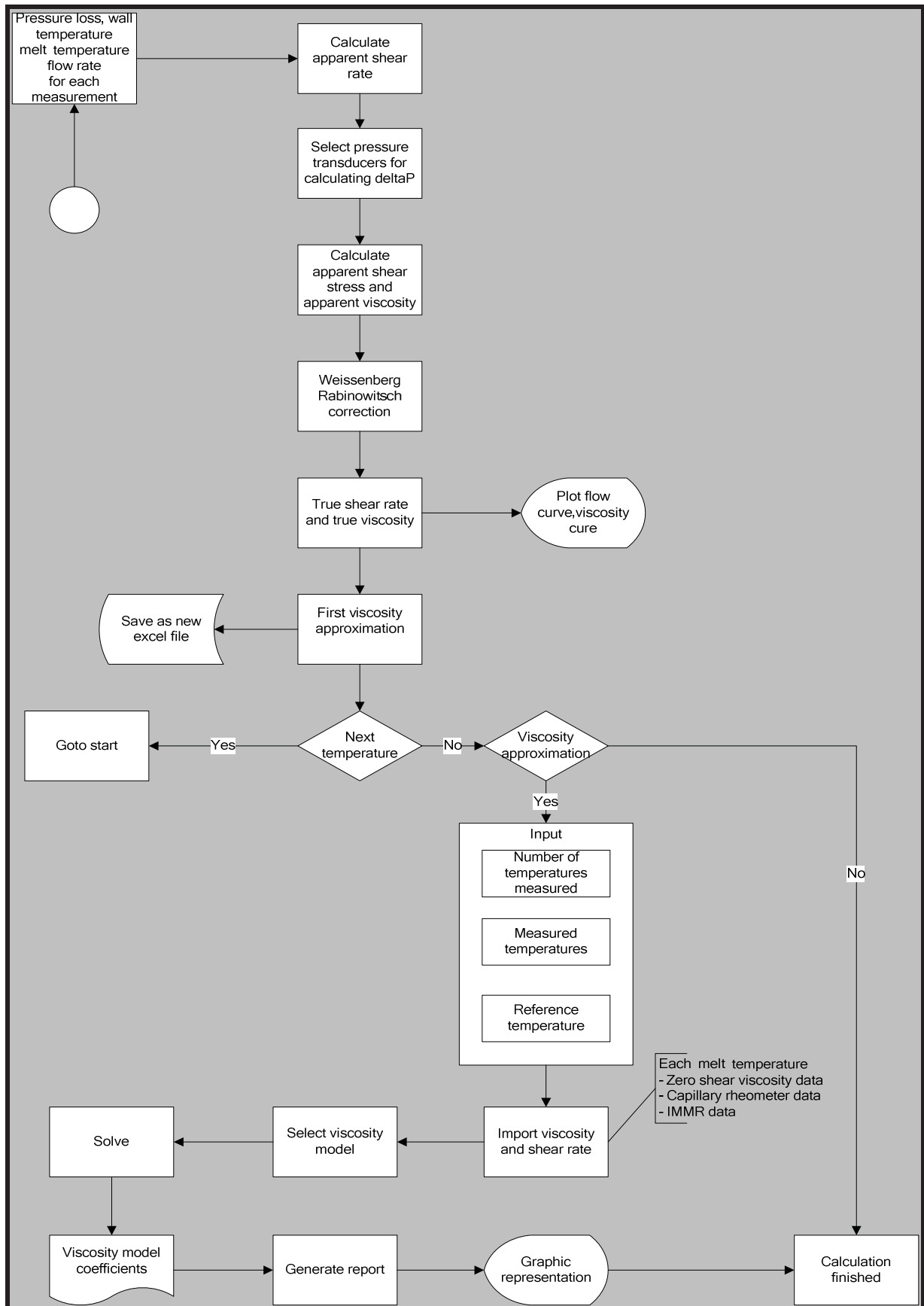


Figure 26: Flow diagram – Steps in calculating the viscosity data using RheoSoft

9 Experimental

9.1 Material

The material used for the experimental work was an injection grade polypropylene HG313MO, which is a homopolymer, manufactured by Borealis AG, Austria [21]. This grade is designed for high-speed injection moulding and contains nucleating, antistatic and slip additives. Its high flowability makes it especially suitable for products with long flow length. This polymer is a CR (controlled rheology) grade with narrow molecular weight distribution. The DSC curve shows the melting point peak at 166°C.

9.2 Equipment

The equipments used for the measurement are given in the table below.

Table 4: Used equipments

Instrument	Type	Manufacturer
High Pressure Capillary Rheometer	Rheograph 2002	Göttfert Werkstoff- Prüfmaschine GmbH, Buchen, Germany
Injection Moulding Machine	VC 940/130 Electric	ENGEL AUSTRIA GmbH, Schwertberg, Austria
Rheological Injection Mould	---	Developed by Institute of Plastics Processing, University of Leoben, Austria within EC-Project, "Pro4Plast"
Pressure Transducers	MDA 462-1/2 UNF	Dynisco Europe GmbH, Heilbronn, Germany
Thermocouples	Type K	THERMOCOAX GmbH, Stapelfeld, Germany
Contactless Magnetostrictive Linear Position Transducer	IK4-A	GEFRAN SPA, Italy
Data Acquisition System	SPIDER 8	Hottwinger Baldwin Messtechnik GmbH, Darmstadt, Germany
Calibration System for Temperature Sensors	Profical II	Gräff GmbH, Troisdorf, Germany
Dead Weight Tester	CPB 5000 HP	WIKA Alexander Wiegand GmbH & Co.KG, Klingenberg, Germany

9.3 Material Data Measurement

The viscosity measurements on the cone and plate rheometer and on the high pressure capillary rheometer and thermal properties measurements were done for the same material, by Kipperer Michael [22]. All these material data are taken from his work.

9.3.1 High Pressure Capillary Rheometer

The rheological measurements were carried out using a high pressure capillary rheometer, type RHEOGRAPH 2002, manufactured by Göttfert Werkstoff-Prüfmaschinen GmbH – Rheological testing devices, Buchen, Germany.

The RHEOGRAPH 2002 allows the routine analysis of the flow and viscosity of thermoplastics and rubbers at shear rate from 10^1 s^{-1} to 10^5 s^{-1} . The maximum force is 20 kN, so this instrument can measure pressure up to 1200 bar. The transducer range must be selected depending on the measurement pressure range in order to avoid errors caused by the transducer at low pressure and to avoid the damage of the transducer membrane at high pressures. The maximum velocity of the piston is 20 mm/s.

The measurements are carried out using a 15mm diameter cylinder and round capillary die. The measurements are performed using three dies of varying L/D ratios. The test parameters and all information for documenting were given in the WinRHEO software. The whole system is heated to the required temperature. The heating system is controlled by three separate Pt100-type thermocouples. Once the isothermal condition is obtained, the measurement cylinder is filled with the test material and compressed with a tamper, to avoid air entrapment. Once the material is filled the measurement can be started. The piston was attached to the machine. The measurement was started.

The pre-heating time or the melting time runs when the measurement is started. When this pre-heating time is finished, the piston starts moving automatically at the specified velocity or flow rate. The melt pressure is measured using a pressure transducer placed near the entrance of the die. When the pressure is steady the program stores the pressure automatically and switch on to the next flow rate and continues until the cylinder is empty or all the flow rates are measured. With these pressure values, flow rates and die geometry the viscosity can be determined.

9. Experimental

9.3.1.1 Capillary Die

Capillary die (Figure 27) system was used in this work to measure the melt viscosity. A set of capillary dies with a diameter of 0.5 mm and an angle of entrance of 180° was selected. The lengths to diameter ratio (L/D) of the dies were 10, 20 and 30 respectively.

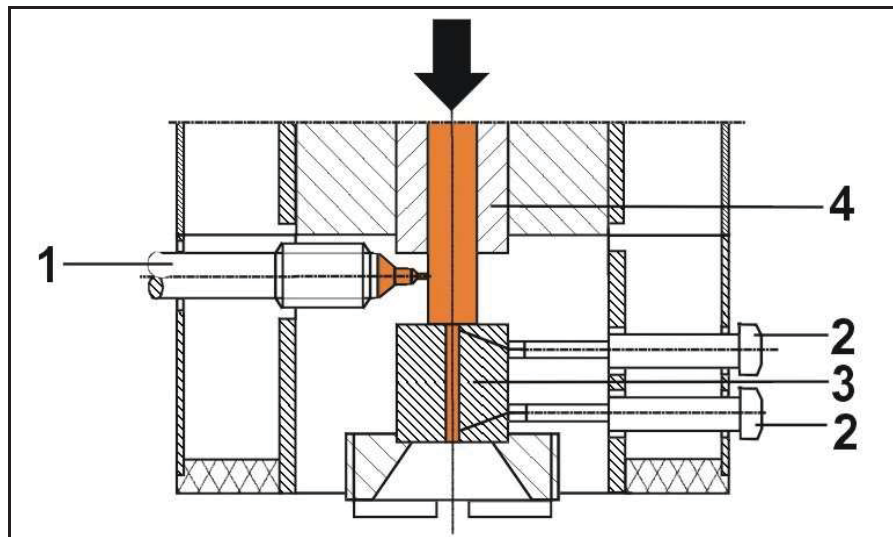


Figure 27: Schematic of high pressure capillary rheometer with round die; 1-Melt pressure transducer, 2-Temperature sensor, 3-Capillary die, 4-Exchangeable barrel

The temperature near to the die wall during the measurement was measured using two 1 mm diameter J-type thermocouples.

The measurements were carried out for three different melt temperatures (210°C, 230°C and 250°C). With the measured pressure, piston velocity, temperature and die geometries the viscosity was determined. From the piston velocity the volumetric flow rate was determined, using the following equation:

$$Q = \frac{\pi \cdot D_p^2}{4} \cdot v_p \quad (81)$$

Where

D_p - Diameter of the piston

v_p - Piston velocity

The apparent shear rate was determined by:

$$\dot{\gamma}_{app} = \frac{4 \cdot Q}{\pi \cdot R^3} \quad (82)$$

Where

R - Radius of the capillary

From the pressure drop values, the apparent shear stress values were calculated using the following relation:

$$\tau_{app} = \frac{P \cdot R}{2 \cdot L} \quad (83)$$

Where

P - Measured pressure

Using the apparent shear stress and apparent shear rate values the apparent viscosity was determined.

$$\eta_{app} = \frac{\tau_{app}}{\dot{\gamma}_{app}} \quad (84)$$

Two corrections are commonly applied for the capillary die measurement in order to obtain the correct viscosity [23]. They are the Bagley correction and Weissenberg-Rabinowitsch correction.

Depending on the location of the pressure transducer, Bagley correction is performed. If pressure loss is measured directly along the flow length (slit die) no correction is necessary. If the pressure is measured in the cylinder, at the entrance of the capillary, then Bagley correction must be done. The change in the cross section from large diameter cylinder to the small one of the capillary causes deviations from an ideal fully developed flow. Due to these changes in cross section additional pressure losses occur. To eliminate this pressure loss at the entrance, Bagley correction is done. These additional pressure losses can be eliminated by measuring the pressure drop at constant shear rate for several capillary lengths and extrapolating to zero length as shown in Figure 28.

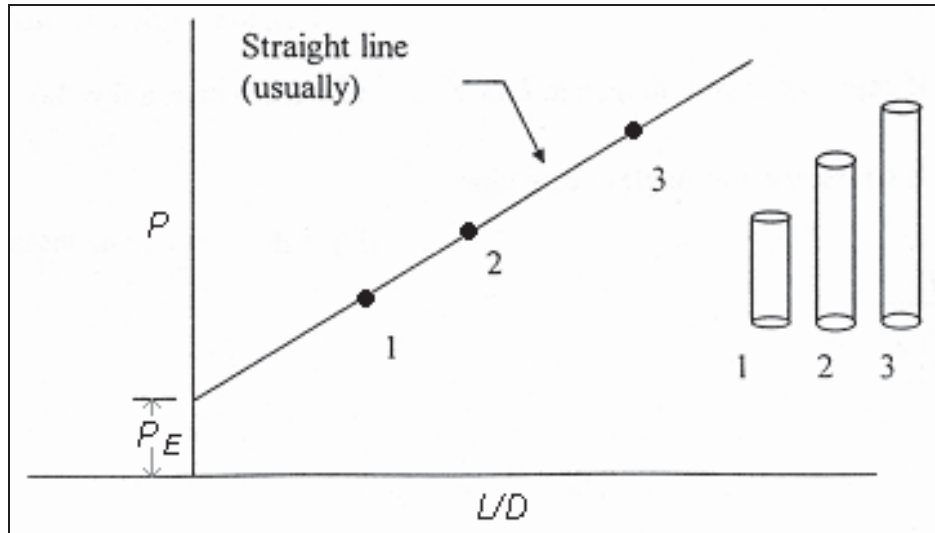


Figure 28: Bagley correction for capillary die

The extrapolation of pressure to $L/D=0$ provides the correction factor P_E , which is used for calculating the true shear stress.

$$\tau_w = \frac{(P - P_E) \cdot R}{2 \cdot L} \quad (85)$$

Where

P_E - Entrance pressure loss

To obtain the shear rate at the wall for non-Newtonian fluids Weissenberg-Rabinowitsch correction was done using the below equation:

$$\dot{\gamma}_w = \frac{\dot{\gamma}_{app}}{4} \left(2 + \frac{d \log \dot{\gamma}_{app}}{d \log \tau_{app}} \right) \quad (86)$$

Then the true viscosity was calculated.

$$\eta_w = \frac{\tau_w}{\dot{\gamma}_w} \quad (87)$$

9.3.2 Cone and Plate Rheometer

Steady shear measurements, with rate sweep from 10^{-1} to 10^2 s^{-1} , were performed with the rheometrics mechanical spectrometer RMS 800 (Figure 29), manufactured by Rheometrics Inc., Piscataway, N.J., USA. The cone and plate geometry with cone-plate diameter 25 mm and cone angle 0.1 rad was chosen. In order to avoid the oxidative degradation of the material during the measurement, the experiments were carried out in nitrogen atmosphere.

9. Experimental

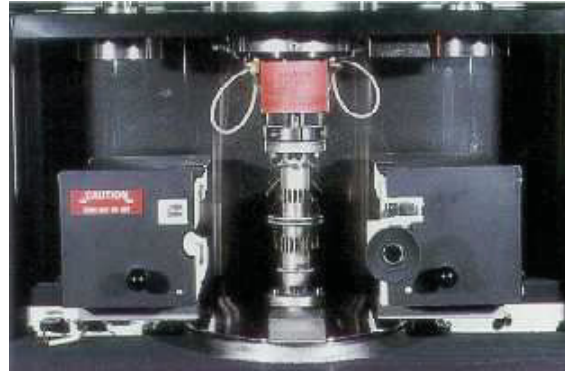


Figure 29: Rheometrics Mechanical Spectrometer (RMS 800)

The round samples (2 mm thick and 25 mm diameter) for the measurement were produced using a compression moulding machine, type P 200 PV Fabrikat Dr.Collin GmbH, Ebersberg, Germany.

The measurements were carried out at three different melt temperatures, same as high pressure capillary rheometer measurements in the frequency range between 0.1 rad/s to 80 rad/s.

9.3.3 Pressure-Volume-Temperature (pVT) Diagram

The density or its reciprocal, the specific volume, is a commonly used property for polymeric materials. The specific volume dependent on temperature and pressure, was measured using PVT 100 manufactured by the company SWO Polymertechnik GmbH, Germany (Figure 30).

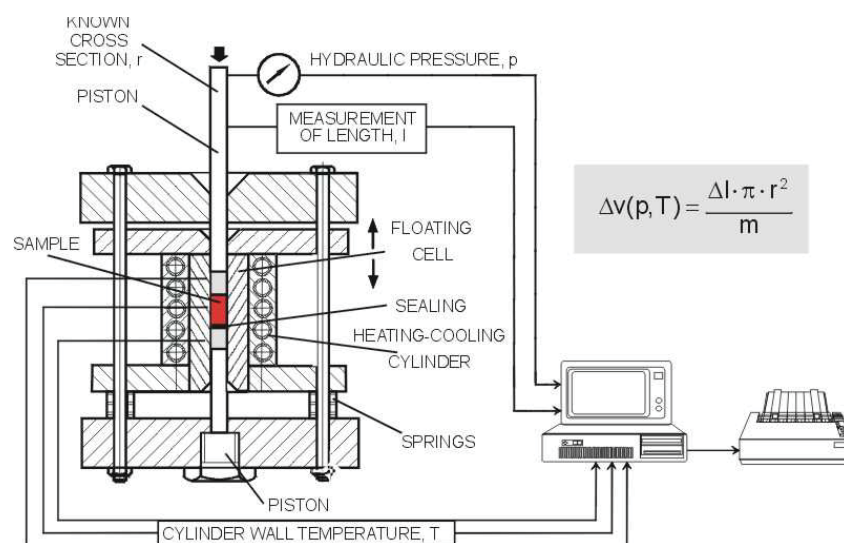


Figure 30: pVT measurement system PVT 100 Co. SWO

9. Experimental

9.3.4 Specific Heat Capacity

The specific heat c_p represents the energy required to change a unit mass of material by one degree in temperature either at constant pressure or constant volume. The specific heat capacity measurement for polypropylene was carried out using Differential Scanning Calorimeter (DSC) 200, manufactured by Netsch Gerätebau GmbH, Germany.

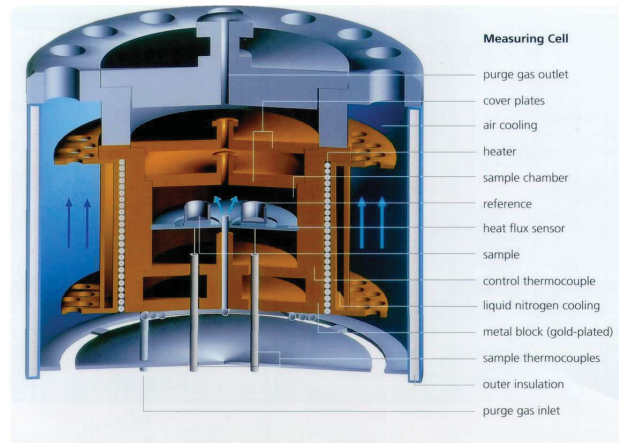


Figure 31: DSC 200

9.3.5 Thermal Conductivity

For measuring the thermal conductivity of the plastic material, the apparatus named K-System II, manufactured by Advanced CAE Technology Inc., USA, was used. The system allows quick and simple measurement of the thermal conductivity of polymers both in solid and molten state. The measurements were performed in temperature range between 50°C to 250°C.

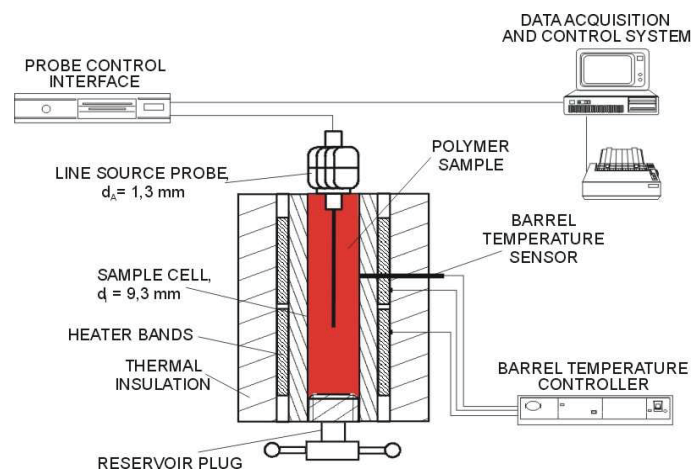


Figure 32: K-System II, apparatus for measuring thermal conductivity

9.4 Injection Moulding Machine Rheometer (IMMR)

The viscosity measurement at high volume rates were performed using an Engel injection moulding machine with a clamping force of 1300 kN, equipped with a 50 mm diameter screw, together with the newly developed rheological mould. The machine operates via a microprocessor system which allows the machine to operate automatically and adjust the different injection moulding parameters (injection rate, injection pressure, shot volume etc.). The injection screw is equipped with a back flow valve, which avoids the leakage flow of the melt towards screw channel at high shear rates.

The rheological mould with a die insert having a slit height of 1 mm was used for the entire measurements. The heating of the mould was done using four cartridge heaters and four heating plates fixed on the mould surface, which are regulated directly by the injection moulding machine. For the measurement of pressure along the flow channel, four Dynsico MDA 462-1/2 UNF flush type pressure transducers were used. All the pressure sensors were placed 20 mm apart. Since the pressure at the entrance is exposed to high pressures compared to the sensor near the exit, pressure sensors with varying measurement range were mounted. The series of pressure sensors used in this study was 1400 bar, 1400 bar, 1000 bar and 1000 bar. All the pressure transducers were calibrated using dead weight tester CPB 5000 HP by WIKA Alexander Wiegand GmbH & Co.KG, Klingenberg, Germany. Two special wall temperature measurement thermocouples, each having three K-type thermocouples, manufactured by THERMOCOAX GmbH, Germany, are placed 1 mm, 1.5 mm and 3 mm away from the wall channel. These “heat flux sensors” were used for calculating the wall temperatures near the entrance and exit of the flow channel out of measured steel temperature. The complete measurement system is shown in Figure 33.

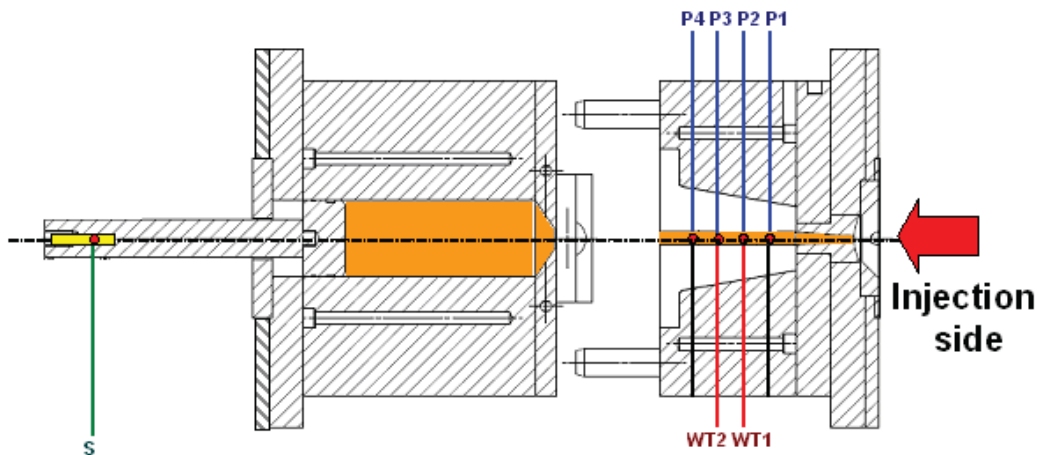


Figure 33: Injection moulding machine rheometer system [26]; S stroke sensor, P1-P4 pressure sensors and WT1 and WT2 heat flux sensors

The measurements were made at the same three different temperatures (210°C, 230°C and 250°C) as chosen for the capillary measurements. The measurements were carried out at varying flow rates between 0.3 cm³/s and 250 cm³/s. Low injection rates were used, in order to achieve low shear rates. So that the viscosity values can be compared with the conventional rheometer values. The volumetric flow rates, at which the measurements were made and their respective apparent shear rate values are given in Table 5.

Table 5: Volumetric flow rate and apparent shear rates

Volumetric flow rate cm ³ /s	Apparent shear rate 1/s	Volumetric flow rate cm ³ /s	Apparent shear rate 1/s
0.3	180	30	18000
0.5	300	50	30000
0.8	480	70	42000
1	600	90	54000
3	1800	100	60000
5	3000	120	72000
8	4800	150	90000
10	6000	200	120000
20	12000	250	150000

9. Experimental

The measurement procedure is as follows: Initially the mould and injection unit were heated to the required measurement temperature. The measurements were done once the temperature was stable. The shot volume for the first measurement was plasticized by the screw. This shot volume was changed for different flow rates. For low flow rates, less shot volume was used and for high flow rates, more shot volume was used since the measurement time was very less at high flow rates. For future measurements for each shear rate the same shot volume should be chosen due to the changing axial temperature profile in the hub volume in front of the screw. Also for each shear rate the whole hub volume should be injected. The Figure 34 shows the injection time by 250 cm³/s injection rate with a shot volume of 350 cm³ for PP HG313MO at 210°C. The total injection time was less than 2 s.

Before starting the cycle the piston inside the cylinder in the movable mould half was moved forward in such a way, that the free volume inside the cylinder was zero. The two mould halves were closed and the melt was injected into the rheological mould at the specified injection rate. The pressures, the wall temperatures and the displacement of the piston inside the cylinder were recorded during the whole injection cycle. As the melt accumulated inside the cylinder, the piston was pushed backwards. The backward motion of the piston was measured by a stroke sensor (IK4A by GEFTRAN SPA, Italy) attached to the piston. From the piston velocity and the cylinder dimensions the actual volumetric flow rate was calculated.

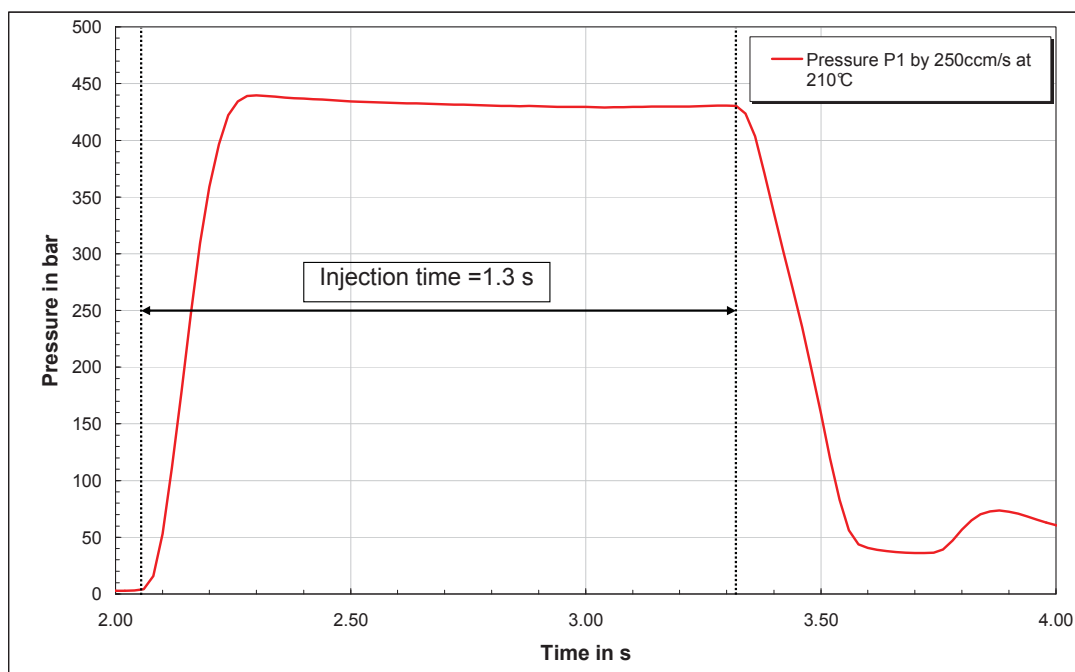


Figure 34: Injection time by high volume flow rate

9. Experimental

When the whole shot volume was injected, the plastification for the next cycle was performed. Then the mould halves were opened and the melt collected in the cylinder was pushed out from the cylinder. For this, the hydraulic system of the ejector system in the injection machine was used to move the piston forward and push the accumulated melt out of the cylinder. This process was repeated for all the flow rates. At high flow rates there was a drastic increase in the channel wall temperature. So enough time was given between each measurement, in order to have stable measurement temperature.

During each injection cycle the pressures, the temperatures and the stroke signals were sent to an A/D converter called Spider 8 by Hottwinger Baldwin Messtechnik GmbH, Germany, which converts the signals to digital format and with the help of a software called catman Easy the data were saved as Excel files. With the help of the newly developed calculation program RheoSoft V.1.0 the viscosity calculations were performed using the saved excel files.

10 Results and Discussions

10.1 Pressure – Specific Volume – Temperature

The pvT curve obtained from the measurement of Kipperer [22] is shown in Figure 35. The curve clearly shows that the material is semi-crystalline. The curves in the polymer melt range are approximated using Menges model (equation 75).

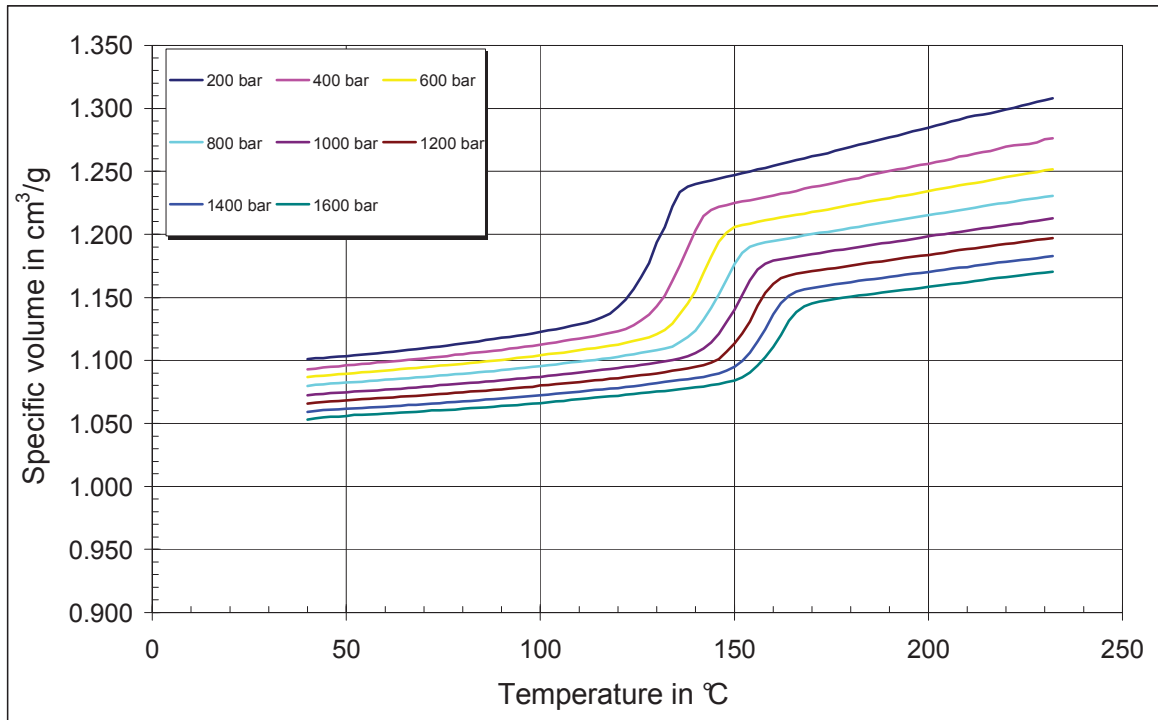


Figure 35: pvT- diagram of PP HG313MO [22]

The approximation coefficients from the Menges model (equation 75) are given in the table below. These four coefficients are further used for calculating the density of the polymer at a specified temperature and pressure, which is needed for the accurate temperature correction of viscosity.

Table 6: pvT- coefficients for PP HG313MO using Menges equation

Melting temperature range		
K1	31280	cm ³ bar/g
K2	1.3014	cm ³ bar/g°C
K3	1623.2	bar
K4	27345	bar

10. Results and Discussions

The density of the polymer melt at a particular pressure and temperature is calculated from the equation (88).

$$\rho(T,p) = \frac{1}{v(T,p)} \quad (88)$$

10.2 Thermal Conductivity

The Figure 36 shows the thermal conductivity curve measured by Kipperer [22] at different temperatures.

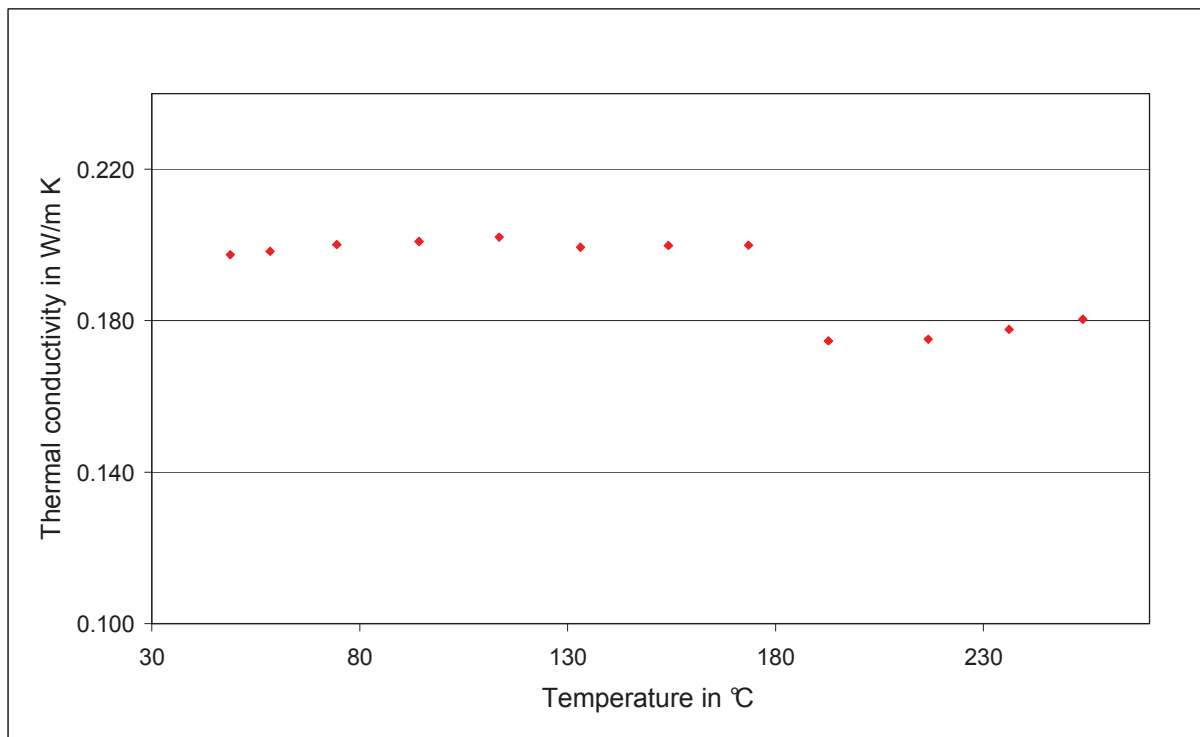


Figure 36: Thermal conductivity of PP HG313MO [22]

For the calculation of the Cameron number the thermal conductivity value in the melt temperature range is used. As shown in the graph the thermal conductivity value does not have big variations in above the transition region, so the average of the conductivity values in the melting temperature was used. For more accuracy a linear approximation was done only for the thermal conductivity values above 180°C. From the linear approximation coefficients the thermal conductivity was calculated.

$$\lambda(T) = A \cdot T + B \quad (89)$$

The approximated values are:

$$A = 9 \times 10^{-5} \text{ W/mK}^2$$

$$B = 0.1558 \text{ W/mK}$$

10.3 Specific heat capacity

The specific heat capacity measurements carried out by Kipperer [22] at a heating rate of 10 K/min and their results are shown below.

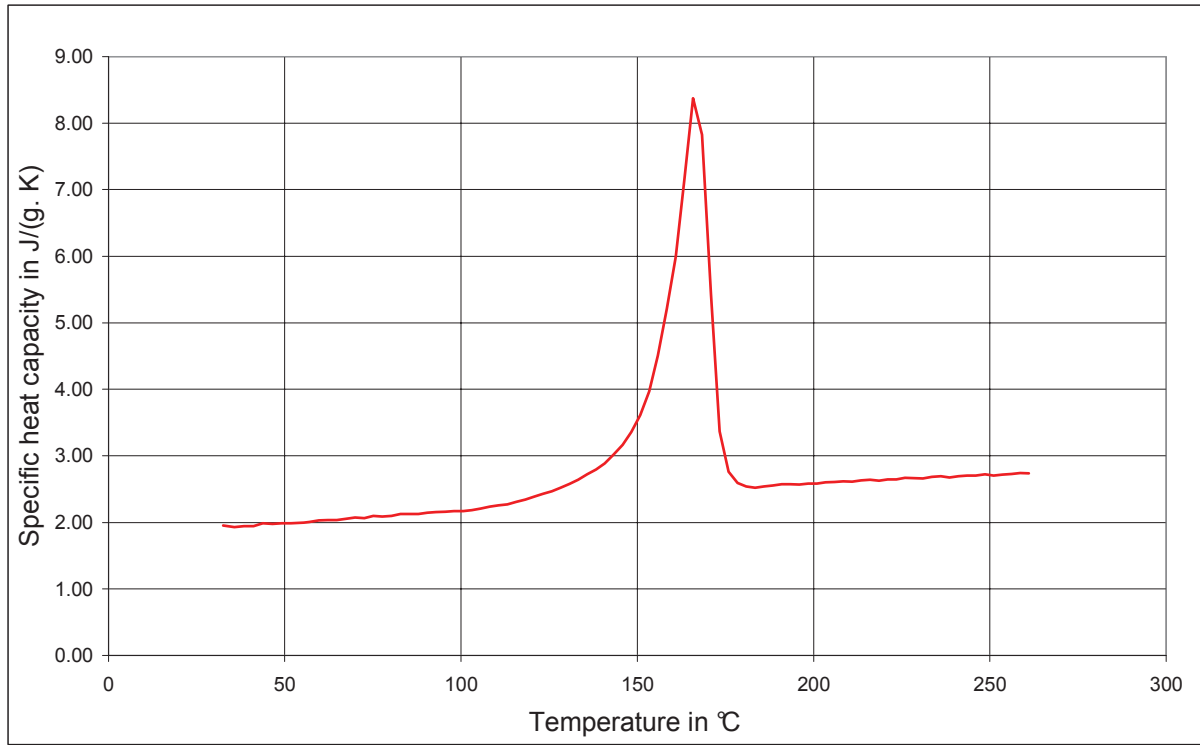


Figure 37: Specific heat capacity of PP HG313MO [22]

The specific heat capacity value in the melting temperature range is used for the calculation. This value is achieved by the linear approximation.

$$c_p = a_{c_p} \cdot T + b_{c_p} \quad (90)$$

Through approximation the constant values are as follows:

$$a_{c_p} = 0.0025 \text{ J/gK}^\circ\text{C}$$

$$b_{c_p} = 2.0959 \text{ J/gK.}$$

10.4 Viscosity

10.4.1 Conventional Rheometer Data

The viscosity curves at three different temperatures measured by Kipperer [22] using the cone and plate rheometer are shown in Figure 38. The measurements were carried under frequency sweep with frequency range from 0.1 to 80 rad/s.

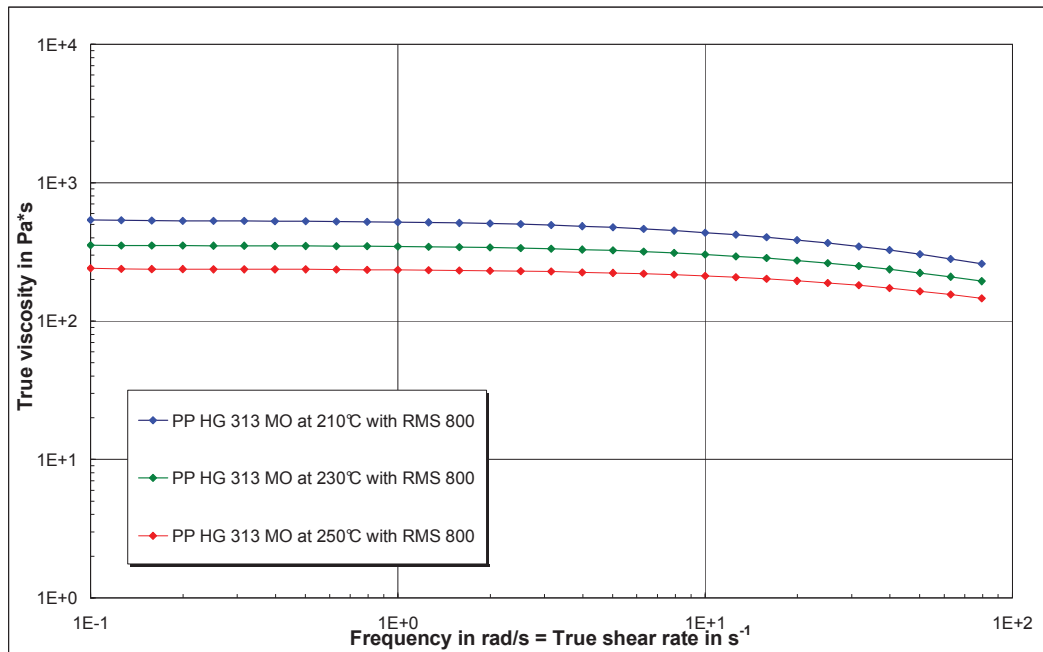


Figure 38: Zero shear viscosity curves of PP HG313MO [22]

The above viscosity plot shows the first Newtonian region of the polymer. In the shear rate range between 0.1 s^{-1} and 10 s^{-1} the viscosity is constant. This viscosity is called the zero shear viscosity.

The higher shear rate range was measured by Kipperer [22] using the high pressure capillary rheometer with round capillary die with diameter of 0.5 mm at three different temperatures. The shear rate range was covered between 100 s^{-1} and 100000 s^{-1} . The viscosity curves without temperature correction are shown in Figure 39.

10. Results and Discussions

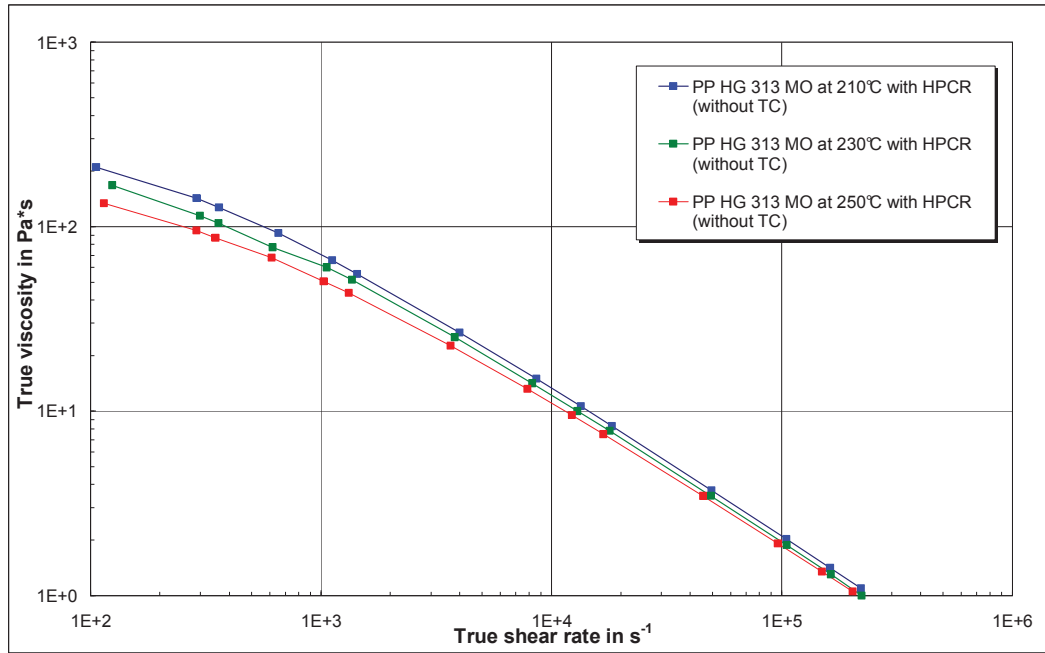


Figure 39: Viscosity curves measured with capillary die without temperature correction (without TC) [22]

At shear rates above 1000 s^{-1} there was an increase in the calculated melt temperature up to 8°C due to shear heating. This shear heating can influence the viscosity and should not be neglected. Due to this reason the temperature correction was carried out for the viscosity values.

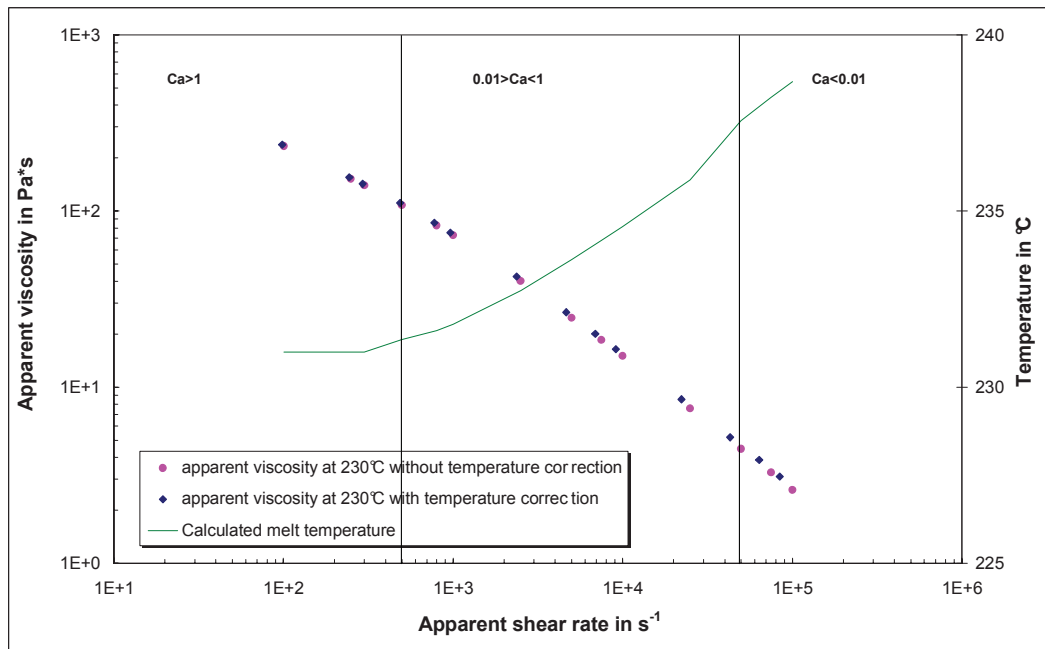


Figure 40: Apparent viscosity curves of PP HG313 MO measured using capillary die at 230°C and calculated average melt temperature using Agassant method

10. Results and Discussions

Figure 40 clearly shows that the calculated average melt temperature by Agassant method starts increasing at shear rate 500 s^{-1} . The system was no longer in an isothermal condition. The viscosity values above this shear rate has been temperature corrected. It can be clearly seen in the graph (Figure 40) that above shear rate 2000 s^{-1} the viscosity values have been temperature shifted and the temperature corrected values has higher viscosity compared to the measured values.

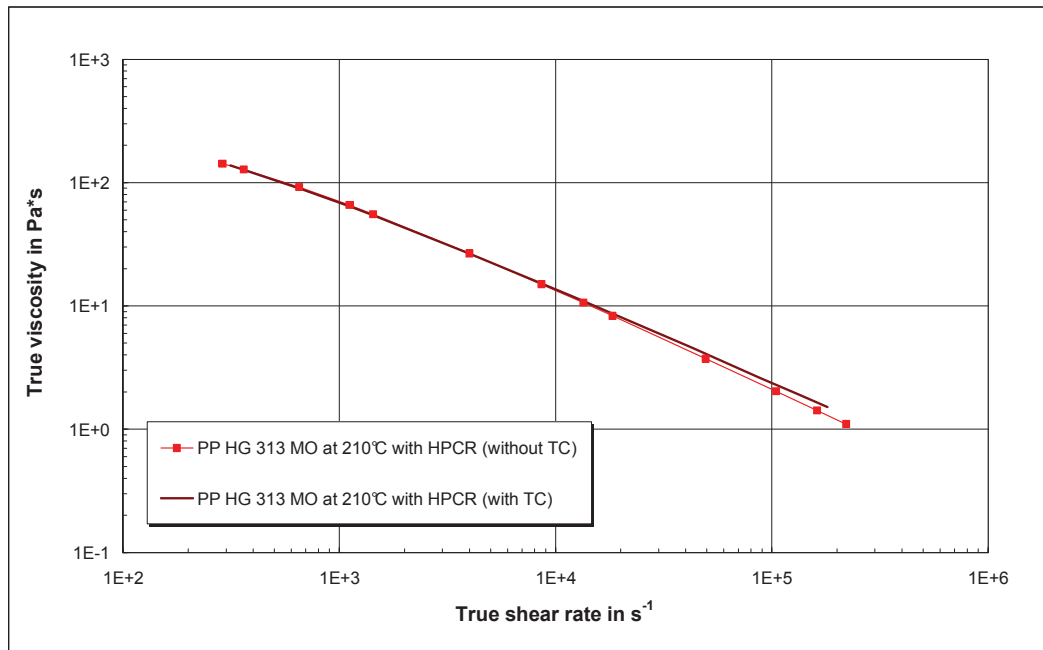


Figure 41: True viscosity curves measured on high pressure capillary rheometer (HPCR) with and without temperature correction

From the plot shown above it is clear that shear heating has high influence on the true viscosity values above 10^4 s^{-1} . Hence these uncorrected viscosities show lower values.

The Figure 42 shows the complete viscosity curves for PP HG313 MO, measured at three different temperatures using cone and plate rheometer (RMS 800) and high pressure capillary rheometer (HPCR). The viscosity values are true values with temperature correction for the capillary die measurements. The viscosity values are approximated using Cross model (equation 21) with 230°C as reference temperature. The material constants for the Cross model and the activation energy are given in Table 7.

10. Results and Discussions

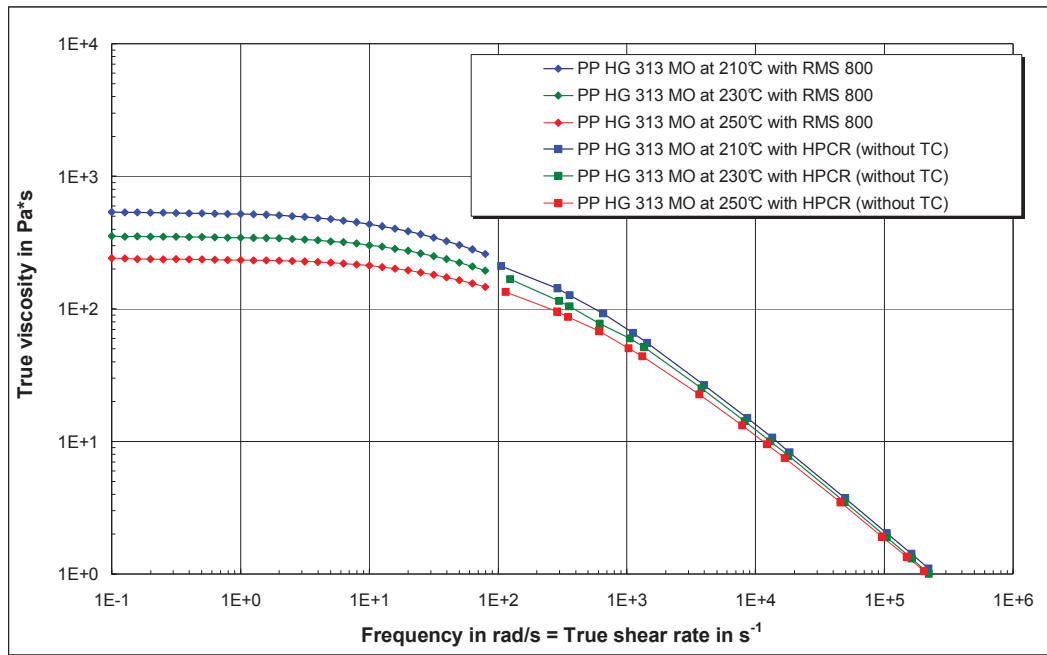


Figure 42: True viscosity at 3 temperatures [22]

Table 7: Material constants by Cross model

A	348.6708	Pas
B	0.0080	s
C	0.7691	/
E ₀	42.6171	kJ/mol
T _{reference}	230	°C

10.4.2 Injection Moulding Machine Rheometer (IMMR)

In order to study the flow behaviour of the polymer melt under the real processing conditions, rheological measurements were made directly on the injection moulding machine using the newly developed rheological mould. The results from the measurements are discussed below.

The viscosity values measured on the injection moulding machine rheometer (IMMR) without considering the heat dissipation are shown in Figure 43.

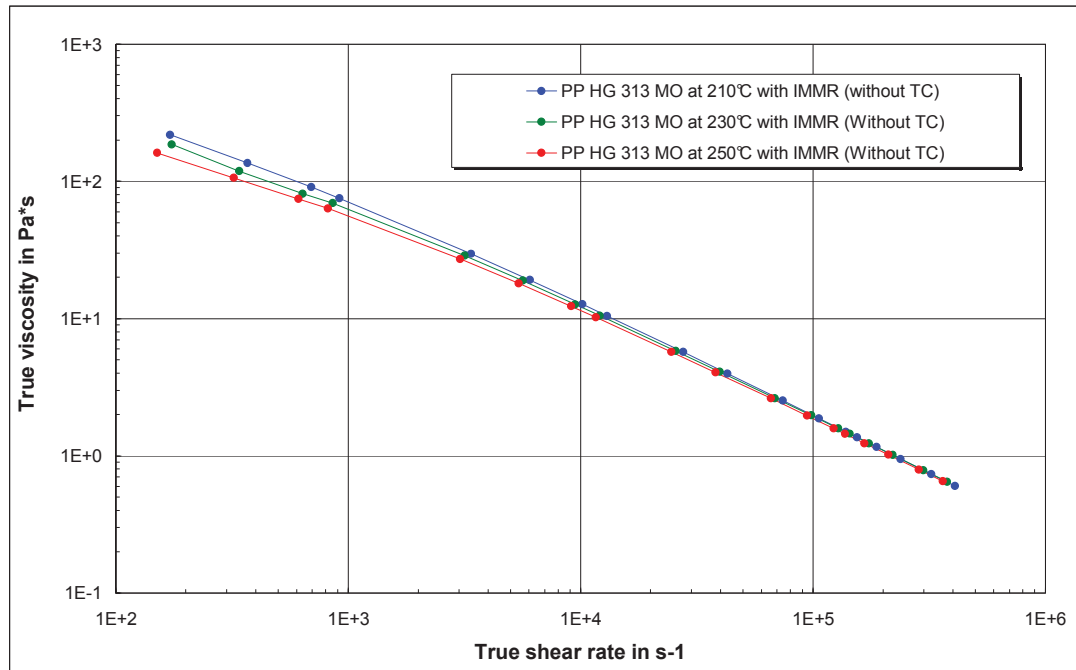


Figure 43: Viscosity curves measured with IMMR without temperature correction (without TC)

The viscosity curves clearly show the temperature dependence of viscosity of polypropylene. The increase in the channel wall temperature at high shear rates was very high and the melt temperature inside the flow channel also increases due to shear heating. Figure 44 shows the increase in the wall temperature during the injection time at flow rates of 250 cm³/s and 150 cm³/s for PP HG313MO at 250°C. The calculated wall temperature near the exit side of the die measured at the maximum flow rate (250 cm³/s) was about 150°C higher than the initial wall temperature. It shall be noted that in case of high volume flow rates the equilibrium state for the resulting wall temperature cannot be reached due to limited hub volume of the plastification unit used. The dosing stroke is limited with 3D that means 150 mm. High dosing strokes will lead to higher temperature inhomogeneity in the hub volume in front of the screw.

10. Results and Discussions

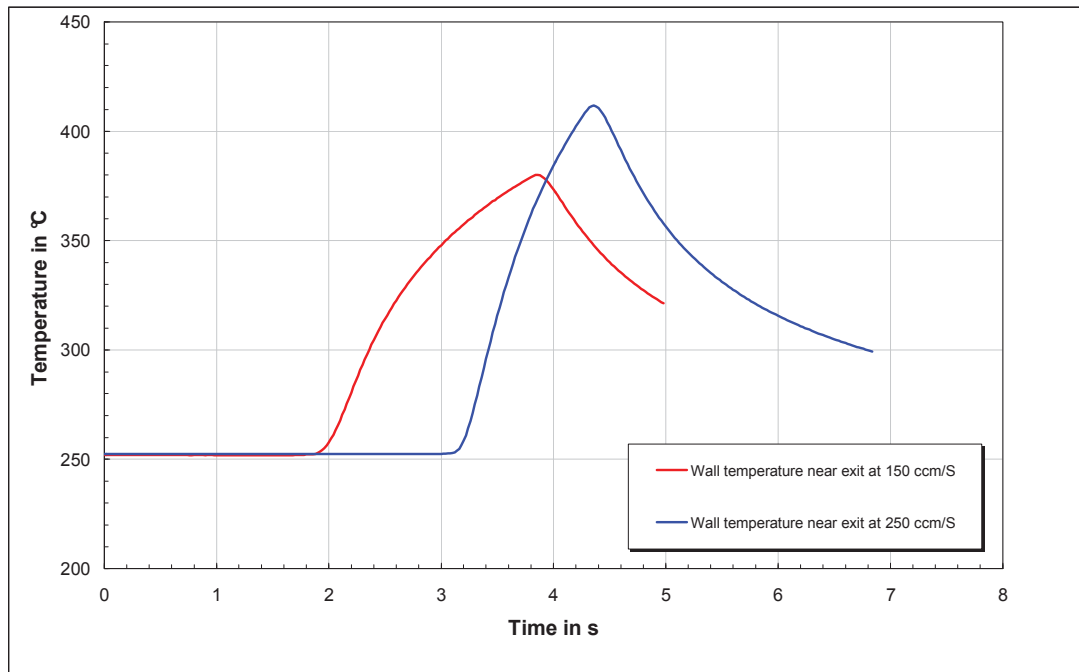


Figure 44: Increase in calculated wall temperature near the die exit for PP HG313MO at 250°C

The increase in the calculated wall temperature and the calculated mean melt temperature using the improved Agassant method [9] is shown below.

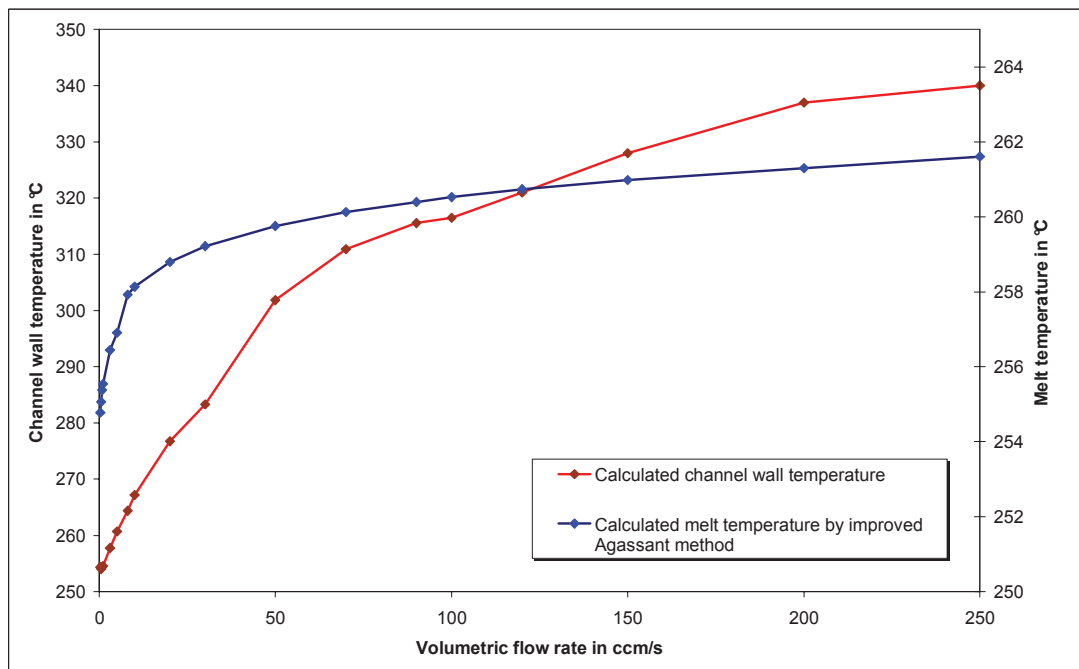


Figure 45: Increase in calculated wall temperature and calculated mean melt temperature at different flow rates for PP HG313 MO at 250°C, measured with injection moulding machine rheometer (IMMR)

10. Results and Discussions

This increase in the melt temperature has a high influence on the measured viscosity values at high shear rates, which can be clearly seen in the following figure.

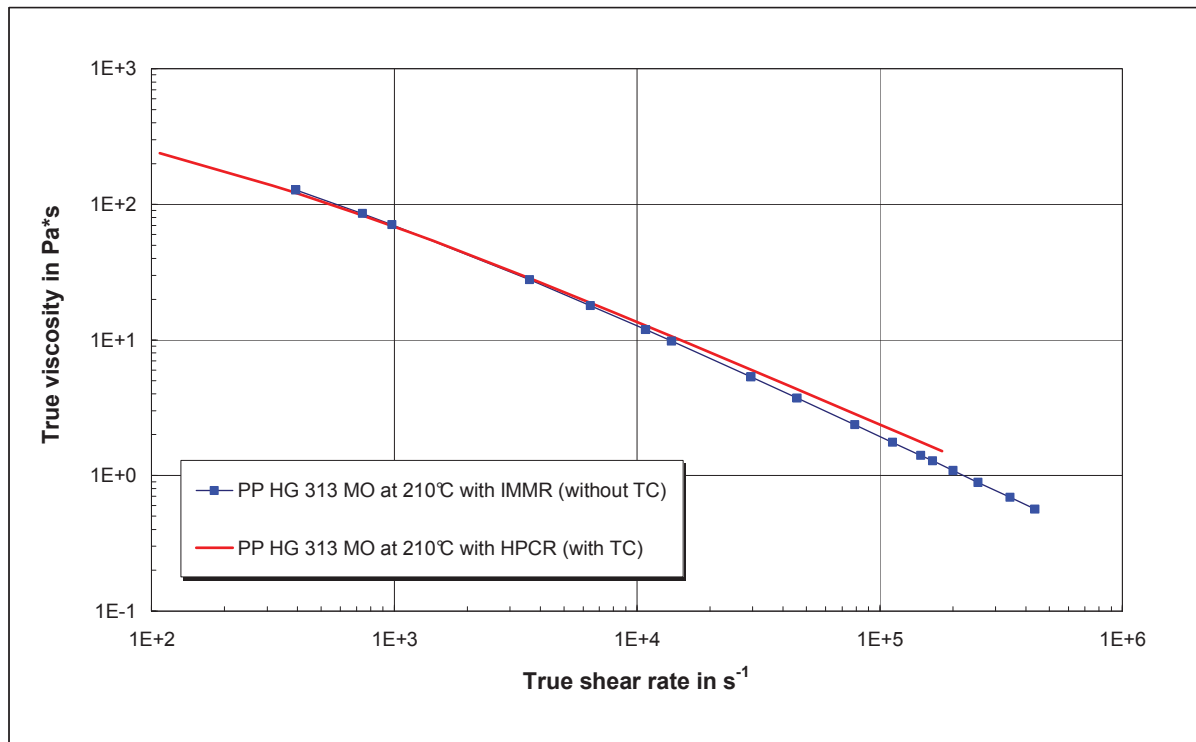


Figure 46: True viscosity values measured with injection moulding machine rheometer and capillary rheometer

In Figure 46 viscosities at shear rates less than 10^4 s^{-1} , measured with IMMR, and the temperature shifted capillary rheometer data connect smoothly with one another. In the high shear rate region above $3 \times 10^4 \text{ s}^{-1}$ the viscosity values from the IMMR are 20% lower than the capillary rheometer data. This clearly shows the influence of the melt temperature increase at high shear rates. The increase in the melt temperature due to shear heating reduces the melt viscosity. So the temperature correction was carried out. Using the improved Agassant method the average melt temperature inside the flow channel was calculated. The viscosity values were then shifted from the calculated melt temperature to the measurement temperature, by calculating the activation energy iteratively.

Figure 47 shows the comparison of the viscosity curves with and without temperature correction, in which the temperature corrected viscosity values at lower shear rates have no much change but at higher shear rate range the viscosity values have shifted to higher viscosities. There is a clear change in the viscosity values at high shear rate region.

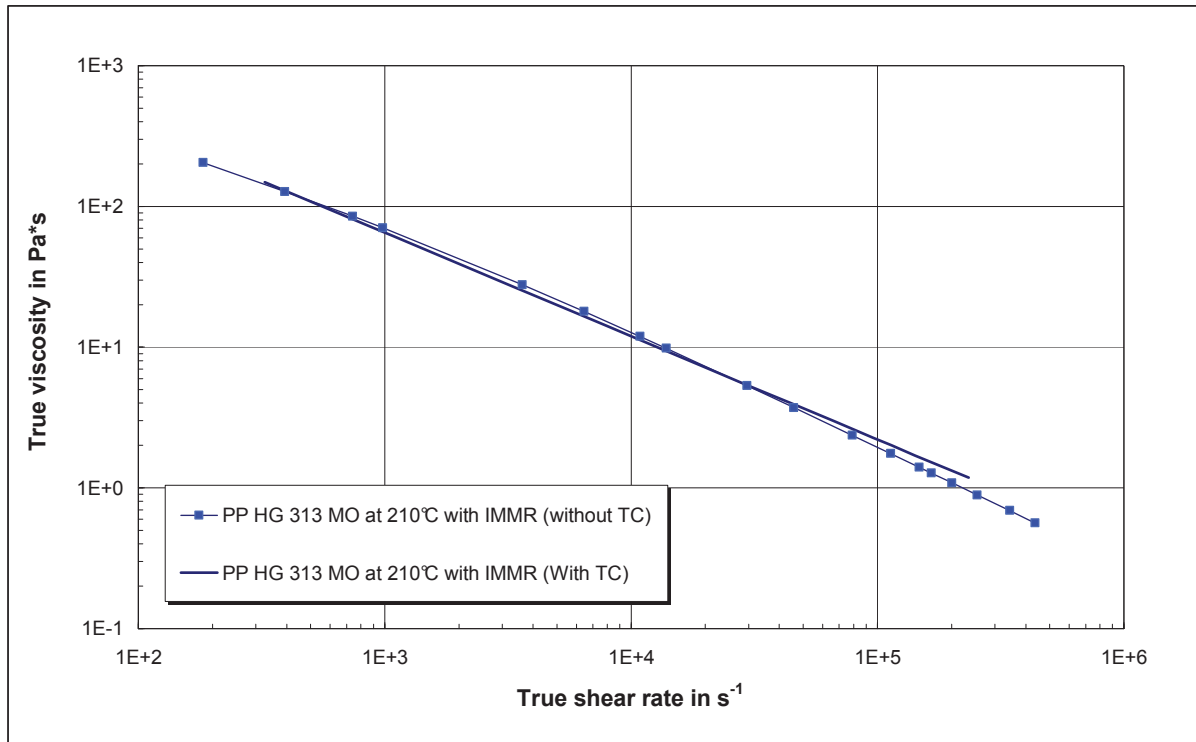


Figure 47: True viscosity values measured with injection moulding machine rheometer with and without temperature correction

10.5 Comparison between commercial rheometer and IMMR

In order to evaluate the accuracy of the new measurement technique the viscosity values measured using the injection moulding machine rheometer were compared with the measurements made on a conventional high pressure capillary rheometer. The Figure 48 below shows the true viscosity values for PP HG313MO measured at 210°C using both rheometers and for both viscosity values without temperature correction.

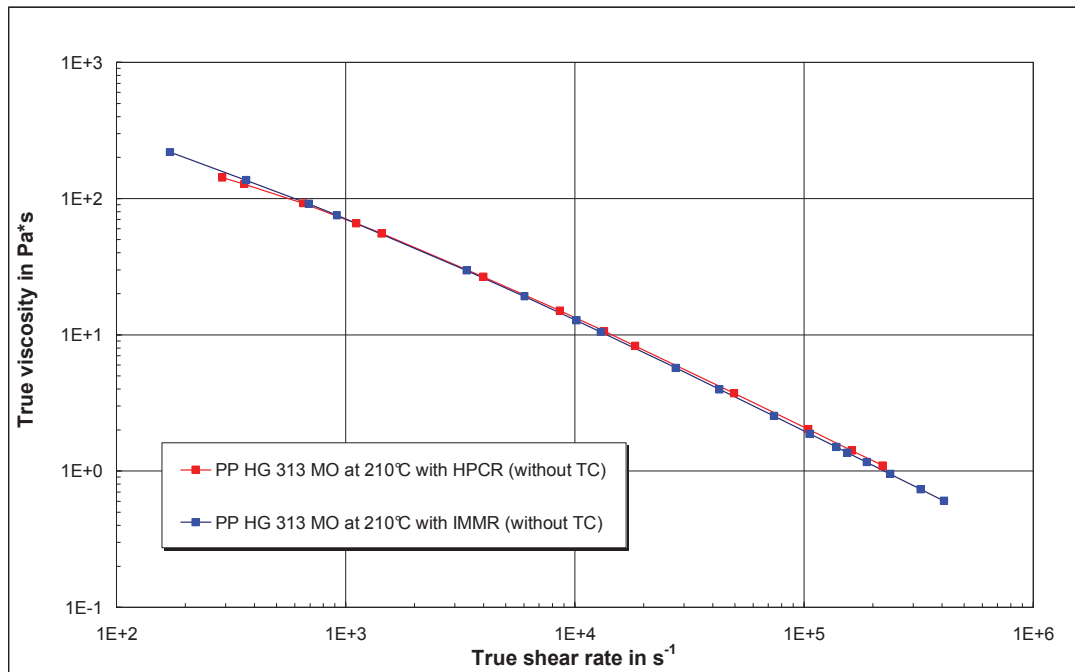


Figure 48: Comparison of viscosity values measured on HPCR and IMMR, both without temperature correction

The viscosity values measured on the injection moulding machine and on the capillary rheometer gives the similar values up to the shear rate 10000s^{-1} . For both rheometers at high shear rates an increase in the melt temperature was observed. But at high shear rates (above $4 \times 10^4 \text{ s}^{-1}$) the viscosity values measured on the IMMR lie 10% below the capillary rheometer data. One reason for this could be the pre-shearing of the polymer melt by the screw during plasticisation. Also the increase in the wall temperature due to shear heating is higher in the case of IMMR, where as in the case of the HPCR the increase in wall temperature is low. But in both cases the temperature increase was more than 2°C . This cannot be neglected and so the temperature correction was carried out for both the viscosity curves. Figure 49 shows the comparison of the viscosity values measured on IMMR and HPCR after the temperature correction. The comparison shows a better match between the two curves. In the shear rate range 10^3 s^{-1} and 10^5 s^{-1} there is a difference of 10% in the viscosity values, which is due to the different shear rate range. The HPCR values at low shear rates lie in the transition region while IMMR values lie only in the shear thinning (power law) region.

10. Results and Discussions

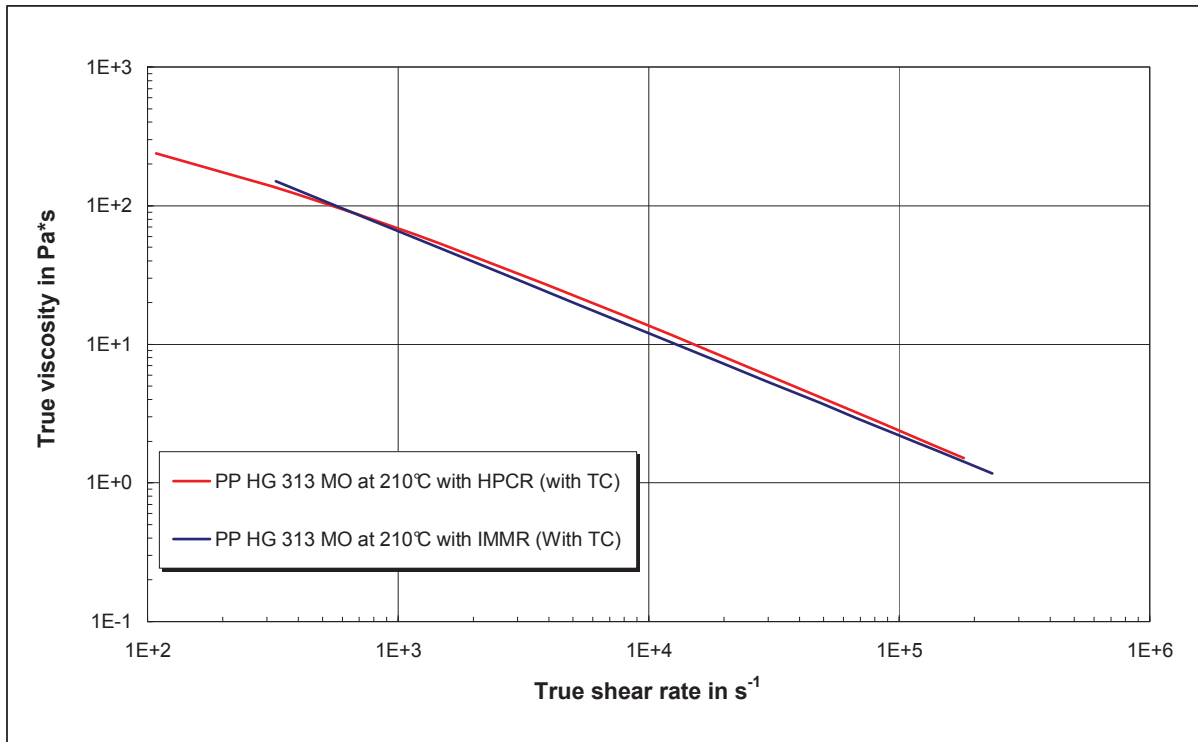


Figure 49: Comparison of the temperature corrected HPCR and IMMR true viscosity values

The complete viscosity curve for PP HG313MO measured at 210°C and approximated with Cross model is given below. It shows a very good approximation.

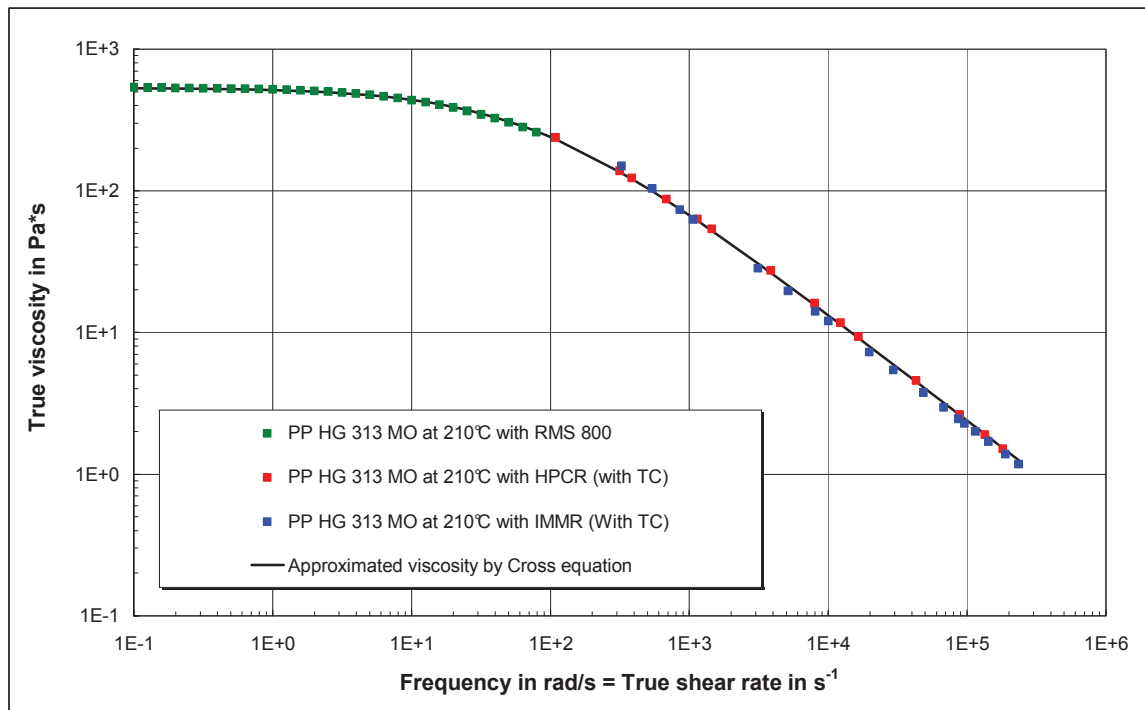


Figure 50: Viscosity curve of PP HG313MO at 210°C with Cross approximation

10. Results and Discussions

In order to know the full flow behaviour of polymer material, more experiments must be carried out over a range of temperatures and pressures, because the rheological properties are highly influenced by these parameters. The shear viscosities obtained under varying temperatures can be brought into a single master curve by time-temperature superposition principle. It also facilitates to display the complete viscosity data in a single master curve. The temperature master curve for PP HG313MO, approximated with Cross model with the reference temperature of 230 °C is shown below.

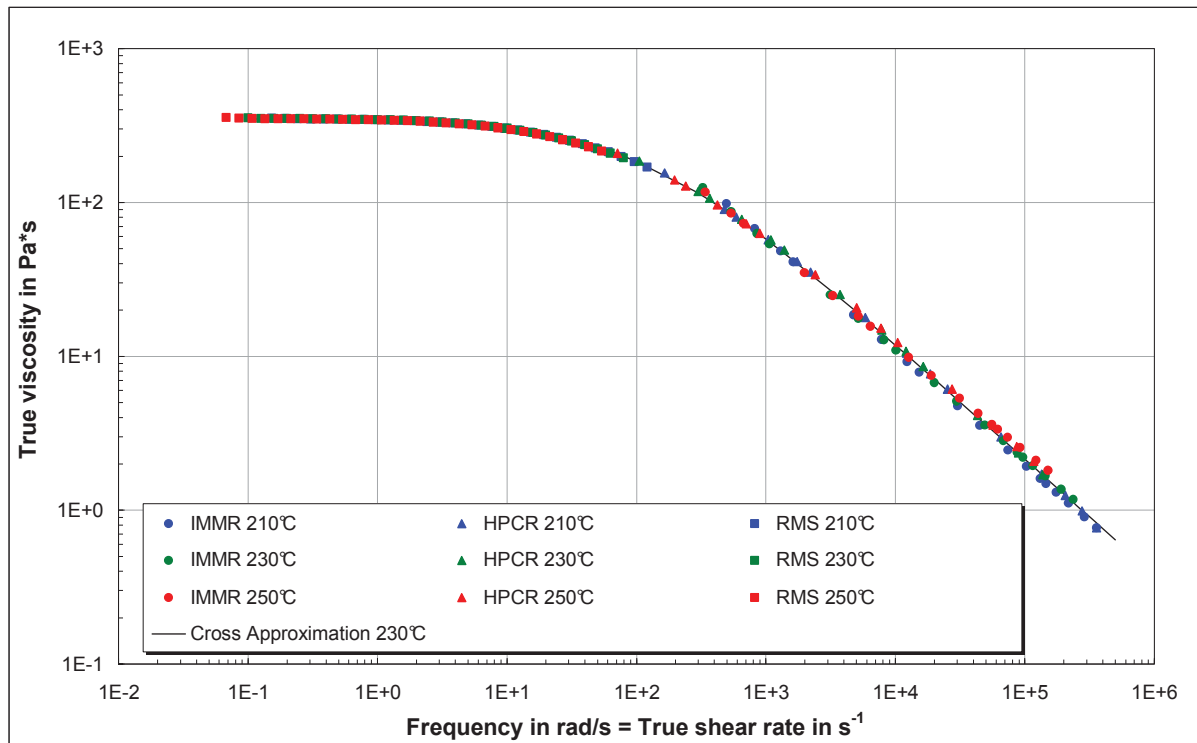


Figure 51: Temperature independent master curve of PP HG313MO

The determined material constants for PP material by Cross approximation are given in Table 8

Table 8: Material constants for PP HG313MO using Cross model

A	351.7975	Pas
B	0.0086	s
C	0.7536	/
E_0	41.6591	kJ/mol
$T_{\text{reference}}$	230	°C

11 Conclusion

Polymer melt viscosity data are the most critical of all the material properties used for the mould filling analysis. The capillary rheometers are used mainly for characterising the flow properties. In an attempt to bring the data closer to the real life scenario rheological measurements were made on an injection moulding machine.

As a part of the EU-Collective Research Projects “Pro4Plast”, a new rheological measurement technique called injection moulding machine rheometer (IMMR) was developed at the Institute of Plastics Processing in Leoben. This is an easy and fast method to measure the viscosity of the polymer melts directly on the injection moulding machine up to high shear rate range using a special rheological injection mould with slit die inserts with varying slit heights.

For making the viscosity calculations easier, in this master thesis, a calculation program (RheoSoft V.1.0) written in Visual Basic 6.0, was developed. This program can easily be installed in Excel as add-in. With help of this program the evaluations of the measurement files from the IMMR were performed as well as the temperature corrections. The rheological data, which are used for the flow simulation, were determined using different viscosity models.

The software RheoSoft V.1.0 has to be tested in practical use. Therefore in this work the rheological characterisation of semi crystalline polymer PP HG313 MO was investigated using IMMR and the results were compared with conventional high pressure capillary rheometer (HPCR) results.

The polymer melt viscosity was determined using the rheological injection mould with 1 mm slit height with 10 mm width and with a flow length of 105.5 mm at temperatures 210°C, 230°C and 250°C. Measurements were carried out at different injection rates and in a shear rate range between $2 \times 10^2 \text{ s}^{-1}$ and $3 \times 10^5 \text{ s}^{-1}$. At high shear rates a drastic increase in the wall temperatures was detected. Due to this the melt temperature also had an increase up to 7°C, which was calculated by improved Agassant method. This increase in the melt temperature was not negligible and so the temperature correction was carried out by iterative method using RheoSoft V.1.0.

Finally the comparison between the conventional rheometer data and the viscosity measured on the injection moulding machine was done. The results showed a good comparability with capillary rheometer data for the measured polypropylene.

This study showed that the injection moulding machine rheometer can produce viscosity data comparable to those of conventional rheometers. Further IMMR has

11. Conclusion

the possibility to measure viscosity at a wide shear rate range with the right shear history. So it can provide better rheological data.

An important task for future rheological measurements using an injection moulding machine is to equalize the melt temperature inhomogeneity in the hub volume in front of the screw. Therefore well known methods for combined screw speed and back pressure control can be used. In future, systematic experiments shall be performed to detect the influence of melt temperature inhomogeneity in front of screw on measured viscosity data.

12 Literature

- [1] *Takahashi H., Matsuoka T., Kurauchi T.:* Rheology of Polymer Melts at High Shear Rate, J. Applied Polymer Science, Vol. 30., 4669-4684, 1985
- [2] *Takahashi H., Matsuoka T., et. al:* Rheological Behaviour of SAN/PC Blends Under Extremely high Shear rates, J. Applied Polymer Science, Vol. 37., 1837-1853, 1989
- [3] *Crowson J., Scott J. and Saundersl W.:* Rheology of Short Glass Fiber-Reinforced Thermoplastics and its Application to Injection Molding, Polymer Engineering and Science, Vol. 21., No. 12, 785-795, August 1981
- [4] *Cox H. W. and Macosko C. W.:* Viscous Dissipation in Die Flows, J. AICHE, Vol. 20, No. 4 , 785-795, July 1974
- [5] *Haddout A., Villoutreix G.:* Polymer Melt Rheology at High Shear Rates, Intern.Polymer Processing XV, 3, 291-296, 2003
- [6] *Vlachopoulos J., Strutt D.:* The Role of Rheology in Polymer Extrusion, http://www.polydynamics.com/Role_of_Rheology_in_Extrusion.PDF [accessed July 21, 2008]
- [7] *Tadmor Z., Gogos C. G.:* Principles of Polymer Processing, John Wiley and Sons, 1979
- [8] *Friesenbichler W.:* Ermittlung von rheologischen Kenndaten für wandgleitende PVC-U Mischungen und ihren Anwendungen für Düsenberechnungen beim Extrudieren, Dissertation am Institut für Kunststoffverarbeitung, Montanuniversität Leoben, 1992
- [9] *Schuschnigg S.:* Rheologische Untersuchungen bei hohen Scher-
geschwindigkeiten mit Hilfe eines Mikrorheologie-Schlizdüsen Messsystem, Diplomarbeit am Institut für Kunststoffverarbeitung, Montanuniversität Leoben, 2004
- [10] *Rois G.:* Finite Elemente Berechnung von Extrusionswerkzeugen, Dissertation am Institute für Kunststoffverarbeitung, Montanuniversität Leoben, 1993
- [11] *Koszkul J., Nabialek J.:* Viscosity Models in Simulation of the Filling Stage of the Injection Moulding Process, Journal of Materials Processing Technology, 157–158 (2004) 183–187
- [12] *Nielsen L. E.:* Polymer rheology, Marcel Dekker INC., New York, 1977
- [13] *Agassant J.-F.(et. al.) :* Polymer Processing: Principles & Modelling, Carl Hanser Verlag, Munich, Vienna, New York, 1991
- [14] *Making Use of Models The Cross Mode:*
<http://www.rheologyschool.com/id46.html> [accessed June 10, 2008]
- [15] *The Carreau Model & Variations:*
<http://www.polytechconsultants.com/carreau.htm> [accessed June 10, 2008]
- [16] *Mathews J. H. and Fink K. K.:* Numerical Methods using Matlab, 4th edition, Prentice-Hall Inc., New Jersey, USA, 2004

12. Literature

- [17] *Petz H.*: Entwicklung eines Programm-Moduls für DATAPROC zur numerischen Auswertung rheologischen Messdaten vom Spritzgießmaschinen-rheometer, By-Pass-Extrusionsrheometer und Hochdruckkapillarrheometer, Diplomarbeit am Institut für Kunststoffverarbeitung, Montanuniversität Leoben, 1992
- [18] *Module for Nelder Mead Search for a Minimum*: http://www.scholarpedia.org/article/Nelder-Mead_algorithm [accessed June 19, 2008]
- [19] *Friesenbichler W., Langecker G. R., Duretek I., Schuschnigg S.*: Polymer Melt Rheology at High Shear Rates using a new Micro-Rheology Technique, 21st Annual Meeting of the Polymer Processing Society, Leipzig, Germany, June 19-23, 2005
- [20] *Duretek I., Friesenbichler W., Schuschnigg S., Jegadeesan R., Langecker G.R.*: Study on Rheological Behaviour of Polymer Melts at High Shear Rates Using a New Micro-Rheology Technique, Conference of the Society of Plastic and Rubber Engineers, "The Past and the Future of Polymer Engineering, Technology and Science", Zagreb, Croatia, April 27-28, 117-130, 2006
- [21] *Borealis Datasheet Polypropylene HG313MO*: <http://www.borealisgroup.com> [accessed October 29, 2007]
- [22] *Kipperer M.*: Stoffdatenmessung an drei für das Expansionsspritzgießen geeigneten Materialien ,Bachelorarbeit am Institut für Kunststoffverarbeitung, Montanuniversität Leoben, 2008
- [23] *Osswald T. A., Menges G.*: Materials Science of Polymers for Engineers, Carl Hanser Verlag, Munich, Vienna, New York, 1996
- [24] *RheoSoft V.1.0*: User Manual, Institute of Plastics Processing, University of Leoben, 2008
- [25] *Cramer A., Michaeli W., Friesenbichler W., Duretek I.*: Simulation of Injection Moulding Process for Micro-Parts, Journal of Plastics Technology 3 (2007) 1, Carl Hanser Verlag, München, 2007
- [26] *Friesenbichler W.*: Rheologische und Thermodynamische Stoffdatenbestimmung, 13 Leobner Kunststoff-Kolloquium, Institut für Kunststoffverarbeitung, Montanuniversität Leoben, 1994

13 Nomenclature

η	Viscosity of polymer melt	Pas
τ	Shear stress	Pa
$\dot{\gamma}$	Shear rate	1/s
η_{app}	Apparent viscosity	Pas
$\dot{\gamma}_{app}$	Apparent shear rate	1/s
η_w	True viscosity	Pas
τ_w	Wall shear stress	Pa
$\dot{\gamma}_w$	True shear rate	1/s
P	Pressure	bar
T	Temperature	°C
Q	Volumetric flow rate	mm ³ /s
B	Breadth of slit	mm
H	Height of slit	mm
M	Slope of the flow curve	-
\tilde{v}	Piston velocity (IMMR)	mm/s
E	Activation energy	kJ/mol
T ₀	Reference temperature	°C
η_0	Zero shear viscosity	Pas
R	Universal gas constant	kJ/mol.K
λ	Thermal conductivity	W/mK
L	Length of slit	mm
\bar{v}	Average velocity of melt flow in the slit	mm/s
ρ	Density	g/cm ³
c _p	Specific heat capacity	J/gK
k	Consistency index	Pas ⁿ
n	Power law index	-
\bar{p}	Mean pressure	bar
d _c	Diameter of piston	mm
F _p	Shape factor	-
a _T	Shift factor	-
Ca	Cameron number	-

13. Nomenclature

ΔP	Pressure difference	bar
\dot{V}	Volumetric flow rate	mm ³ /s
$T(y)$	Temperature along slit height	K
T_w	Wall temperature	K
t	Time	s
v'	Injection speed	mm/s
v_p	Piston velocity (HPCR)	mm/s
D_p	Diameter of the piston (HPCR)	mm
$C1, C2$	WLF constants	-
A, B, C, D	Material constants	-
$K1, K2, K3, K4$	Menges model coefficients	-
a_{cp}, b_{cp}	Linear approximation coefficients for c_p	-
A, B	Linear approximation coefficients for λ	-
P_E	Entrance pressure loss	bar
A_s	Cross sectional area of screw	mm ²

14 Appendix

Table 9: Injection moulding conditions

Barrel zones	Temperature in °C		
	210°C	230°C	250°C
Zone1 (Feed zone)	45	45	45
Zone 2	180	190	200
Zone 3	190	195	210
Zone 4	195	205	220
Zone 5	205	215	235
Zone 6 (Nozzle)	210	230	250

Table 10: Viscosity data, values calculated without temperature correction

Viscosity of PP HG 313 MO using IMMR with slit die 1mm					
210°C		230°C		250°C	
$\dot{\gamma}_w$ 1/s	η_w Pas	$\dot{\gamma}_w$ 1/s	η_w Pas	$\dot{\gamma}_w$ 1/s	η_w Pas
182.98	204.60	185.49	174.42	160.58	150.62
392.92	127.56	363.04	110.94	343.68	99.22
740.07	85.32	679.86	76.18	651.98	69.77
980.57	70.60	917.57	64.78	873.30	59.43
3614.21	27.78	3384.20	26.94	3236.51	25.51
6446.12	17.92	6030.26	17.72	5769.03	16.95
10864.15	11.92	10120.52	11.90	9715.17	11.54
13886.92	9.81	12918.90	9.85	12407.34	9.59
29542.52	5.34	27401.88	5.44	26275.86	5.34
45726.88	3.73	42398.56	3.84	40660.59	3.79
79038.32	2.37	73162.54	2.46	70254.60	2.45
113100.07	1.76	104832.92	1.84	100575.84	1.84
147818.93	1.40	137128.45	1.49	131231.15	1.48
165342.42	1.28	153413.64	1.36	146792.09	1.35
200538.41	1.09	186054.48	1.16	178011.70	1.16
254207.51	0.89	235332.72	0.95	225653.44	0.96
344831.16	0.69	318657.42	0.74	305068.91	0.74
436369.30	0.56	403181.34	0.61	386447.18	0.61

14. Appendix

Table 11: Viscosity data, values calculated with temperature correction

Viscosity of PP HG 313 MO using IMMR with slit die 1mm					
210°C		230°C		250°C	
$\dot{\gamma}_w$ 1/s	η_w Pas	$\dot{\gamma}_w$ 1/s	η_w Pas	$\dot{\gamma}_w$ 1/s	η_w Pas
325.58	149.97	325.46	124.79	302.28	111.67
538.36	103.53	538.95	87.31	501.22	79.08
853.91	73.69	856.20	62.91	797.40	57.61
1062.69	62.72	1066.37	53.85	993.82	49.57
3116.82	28.38	3137.94	25.07	2933.95	23.68
5138.04	19.64	5179.19	17.58	4848.91	16.81
8057.91	14.10	8131.16	12.78	7619.67	12.35
10028.84	12.00	10122.50	10.94	9488.44	10.63
19786.65	7.27	19980.86	6.76	18755.85	6.68
29462.30	5.42	29735.39	5.10	27924.72	5.09
48607.99	3.75	49081.69	3.58	46100.73	3.61
67560.35	2.94	68206.31	2.83	64112.22	2.89
86446.99	2.45	87174.75	2.38	82037.45	2.44
95830.02	2.27	96689.25	2.21	90942.81	2.27
114525.98	1.99	115568.41	1.95	108724.19	2.01
142488.53	1.70	143779.64	1.67	135332.52	1.73
188825.82	1.38	190585.37	1.37	179439.07	1.43
235118.65	1.17	236988.21	1.17	223080.17	1.23